Studies on transport of mass and energy in the vortex tubes. The significance of the secondary flow and its interaction with the tangential velocity distribution

Linderstrøm-Lang, C.U.

Publication date:
1971

Document Version
Publisher's PDF, also known as Version of record

Risø Report No. 248

Risø Report No. 248

Danish Atomic Energy Commission
Research Establishment Risø

Studies on Transport of Mass and Energy in the Vortex Tube

The Significance of the Secondary Flow and Its Interaction with the Tangential Velocity Distribution

by C. U. Linderstrøm-Lang

September, 1971

Sales distributors: Jul. Gjellerup, 87, Sölvgade, DK-1307 Copenhagen K, Denmark
Available on exchange from: Library, Danish Atomic Energy Commission
Risø, DK-4000 Roskilde, Denmark

U. D. C.
542.7:532.527

Forsvaret finder sted tirsdag den 30. november 1971 kl. 14 præcis i annexauditorium A, Studiestræde 6 o. g.

STUDIES ON TRANSPORT OF MASS AND ENERGY IN THE VORTEX TUBE. THE SIGNIFICANCE OF THE SECONDARY FLOW AND ITS INTERACTION WITH THE TANGENTIAL VELOCITY DISTRIBUTION

by

C. U. Linderstrøm-Lang

September, 1971 Risö Report No. 248

STUDIES ON TRANSPORT OF MASS AND ENERGY IN THE VORTEX TUBE. THE SIGNIFICANCE OF THE SECONDARY FLOW AND ITS INTERACTION WITH THE TANGENTIAL VELOCITY DISTRIBUTION

by

C. U. Linderstrøm-Lang

Danish Atomic Energy Commission
Research Establishment Risö
Roskilde

Denne afhandling er i forbindelse med de i forordet I-IVc nævnte tidligere offentliggjorte arbejder af det naturvidenskabelige fakultetsråd ved Københavns Universitet antaget til offentlig at forsvares for den filosofiske doktorgrad.

København, den 13. juli 1971

Morten Lange
h. a. dec.

ISBN 87 550 0101 7

CONTENTS

Page

PREFACE

The present work summarizes a number of investigations on the vortex tube carried out since 1960. All have been concerned in one way or other with diffusional processes set up by the gas rotating within the tube, and with the interaction between these processes and the secondary motion as established in the tube on passage of the gas from inlet to exits. The main findings of the work have been published in various articles and reports, as listed below. These papers will be referred to by Roman numerals, while other literature will be given by author's name and publishing year. All references are collected at the end of the review. Some considerations not reported elsewhere are included, notably in chapters 5 and 6.

I. C. U. Linderstrøm-Lang, Gas Separation in the Ranque-Hilsch Vortex Tube, Int. J. Heat Mass Transfer, 7 (1964), 1195.

II. C. U. Linderstrøm-Lang, An Experimental Study of the Tangential Velocity Profile in the Ranque-Hilsch Vortex Tube, Risö Report No. 116, 1965, 17 pp.

III. C. U. Linderstrøm-Lang, A Model of the Gas Separation in a Ranque-Hilsch Vortex Tube, Acta Polytech. Scand., Phys. Ser. No. 45, 1967.

IIIa. C. U. Linderstrøm-Lang, On Gas Separation in Ranque-Hilsch Vortex Tubes, Z. Naturforsch. 22a (1967) 835.

IIIb. C. U. Linderstrøm-Lang, Gas Separation in the Ranque-Hilsch Vortex Tube. Model Calculations Based on Flow Data, Risö Report No. 135, 1966, 30 pp.

IV. C. U. Linderstrøm-Lang, The Three-dimensional Distributions of Tangential Velocity and Total-temperature in Vortex Tubes, J. Fluid Mech. 45 (1971) 161.

IVa. C. U. Linderstrøm-Lang, Vortex Tubes with Weak Radial Flow; Part 1, Calculation of the Tangential Velocity and Its Axial Gradient, Risö Report No. 216, May 1970, 22 pp.

IVb. C. U. Linderstrøm-Lang, Vortex Tubes with Weak Radial Flow; Part 2, Calculation of the Three-dimensional Temperature Distribution, Risö Report No. 217, May 1970, 37 pp.

IVc. C. U. Linderstrøm-Lang, Vortex Tubes with Weak Radial Flow; Part 3, Calculation of the Performance and Estimation of the Turbulent Diffusivity, Risö Report No. 218, May 1970, 17 pp.

1. INTRODUCTION

The vortex tube is a device of the kind that by simplicity in construction shows immediate promise of great utility and sets the imagination working on possible uses, for sooner or later to ruin all hopes by failing through inefficiency. This applies to the expectancy first entertained by Ranque in the thirties and by Hilsch in the forties that the tube would prove an efficient cooling machine; to the possibility, investigated from the early fifties, that the tube might be useful for mass separation in gas mixtures (e. g. for isotope production); and to the studies in the sixties on the use of the tube for containment of fissile material in nuclear rockets (Bibliographies: Dobratz, 1964, Westley, 1954).

This does not mean, however, that the tube is completely useless, as special applications have in fact been found for it; thus Vortair, 1967, mentions its use for cold air breathing systems, while application to free air thermometry has also been described.

The limited usefulness of the vortex tube once admitted, the fact still remains that the functioning of the tube presents a complex and intriguing problem the solution of which may well turn out to be of a wider interest. For one thing, because the flow pattern is similar to that encountered in systems of potential practical interest such as vortex flow heat exchangers; furthermore, because the flow pattern in the tube may be used as a simple model for important phenomena such as the vortex in a tornade (Lewellen, 1964) and that on the trailing edge of delta wings (Benjamin, 1962).

The vortex tube is basically just a tube with a tangential nozzle through which the gas is set into a swirling motion which persists along the tube. One tube end is closed except for an orifice at the centre. The other end may carry a similar orifice or have some kind of valve inserted. Typical designs are shown in fig. 1.1. They each have their special applications. Long asymmetrical tubes of type (a) or (b) are best suited for the production of net temperature differences. Short tubes of the quite symmetrical type (d) with centre exits at both ends are best at gas separation, while the type (e) with many inlet nozzles spaced along the periphery and with one centre exit has formed the basis for fission rocket designs. Only the concurrent type (c) has, for reasons that will become clear later in this work, shown no special merit.

In the tube, radial and axial motion must necessarily be superimposed on the initially tangential motion from the nozzle. It is not surprising that this motion influences the tangential velocity gradients and that together

they play a deciding role for the functioning of the tube, both for the temperature and for the gas separation.

Accordingly in chapters 2, 3, and 4 the distribution of the three relevant parameters, the circulation, the concentration, and the total temperature, respectively, are studied in turn.

The three chapters all start with a discussion of two-dimensional approaches which neglect the axial gradient of circulation, of concentration and of total temperature, respectively. This constitutes a satisfactory zero-order approximation in cases where the secondary flow may be considered as purely radial. Each description provides the radial distribution of one of these three parameters, with the corresponding radial Reynolds number (based on diffusion, mostly turbulent, of angular momentum, mass, and total-enthalpy, respectively) as the governing parameter (see sections 2.1, 3.1, and 4.1); the radial Reynolds number is a measure of the relative importance of transport by radial flow (normally directed inward) and by (turbulent) diffusion (normally directed outward), and the radial distribution results as a balancing between the two transports.

In tubes with axial gradients of any one of the three parameters, where the distribution is found to be the result of an interplay between axial and radial flow, it is necessary to include terms in the equations that contain the axial flow. Chapters 2, 3 and 4 all contain sections with discussions of three-dimensional distributions of this type.

At the three-dimensional stage it is necessary to distinguish between the angular momentum case and the other two cases, since both material and total enthalpy are preserved within the tube while a considerable amount of angular momentum may be lost to the peripheral wall. The axial gradient of circulation therefore takes on a completely different shape (through the influence of eq. 2.6, a combination of the momentum equations for the radial and axial velocity components) from those of the other two (governed by material balance and total-enthalpy balance equations).

As regards the latter two distributions, it is essential to note that axial flow in the centre region tends to upset the balancing (which exists in the two-dimensional case) of the effects of radial flow and diffusion, and that the resulting net transport in the radial direction gives rise to axial gradients both in the outer annulus and in the core. The larger the axial core flow is compared to that in the outer region, the larger amounts of the quantity in question may be involved and the more important may the axial gradient of the parameter become. Expressed in another way, since the axial flow in the core region (more correct the flow through centre exits, fig. 1.1) is

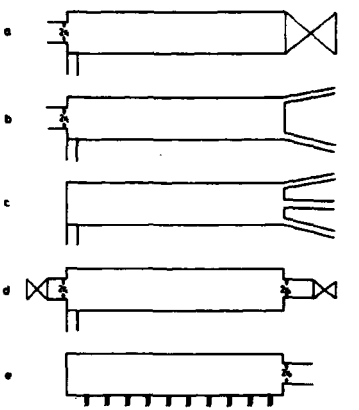

Fig. 1.1. Vortex tube designs. d and e apply both to long and to short tubes; use of type a, b, and c have so far been restricted to long tubes. The terms long and short refer to tube radius-to-length ratios less than and greater than approximately 1/10 - 1/20, respectively.

equal to the net radial flow into the core and since the latter is found to determine the radial gradient of the parameter in question (concentration or total-temperature) in such a way that this is small when the radial flow is large, it is seen that when large amounts of the quantity is transported within the core the radial gradients at the same time are small and therefore particularly suited for a large outward diffusion (which necessarily gives rise to appreciable axial gradients.)

In chapter 2 the interaction between the radial flow and the tangential velocity distribution, as indicated above, is first discussed (2.1); then in section 2.2 the influence of the end wall boundary layers is treated, while in section 2.4 its importance for a classification of vortex tubes of different types is discussed. The remainder of chapter 2 (section 2.3) is devoted to a study of the interplay between the axial flow and the axial decay of tangential velocity (ref. IV).

In chapter 3, section 3.1, studies of the radial concentration gradient

in vortex tubes, as made in connection with the fission rocket projects, are discussed in terms of the two-dimensional approximation; the results are qualitative, as the object in most cases has been restricted to showing that a heavy component has some tendency to be concentrated in a layer at a certain distance from the axis. Next (section 3.2) a short discussion of the three-dimensional theory with reference to data for low-pressure tubes is included. The main theme of chapter 3 (section 3.3), is the study of the net concentration differences that the vortex tube (at normal pressures) may produce between the two outgoing streams (ref. I), and an interpretation of the rather complex picture emerging under these conditions (ref. III).

In chapter 4 the temperature distribution within the tube is treated in some detail, made possible by a number of experimental studies that have been carried out over the past 15 years. The discussion of the three-dimensional case (section 4.2) is based on an approximate solution to the energy equation developed in ref. IV. In section 4.3 the net temperature difference between the outgoing streams is discussed on the basis of the theoretical results and a comparison with experiment.

In chapter 5 the performance of the tube both as a gas separator and as a temperature separator is considered; equations are derived in section 5.1 which describes the performance of the tube in terms of separative work (gas-separation) and availability (temperature separation). Next in section 5.2 a correlation of temperature and tangential velocity data, as described in ref. IV (with IVc) on the basis of the work treated in sections 2.3 and 4.2, is discussed. Finally (section 5.3) a comparative discussion of the mass and temperature separation effects is carried out.

In chapter 6 the performance criteria of the tube are first discussed (section 6.1) on the basis of the performance functions developed in chapter 5. In the remainder of the chapter, evaluations are made of the performance of the tube in relation to its use, on the one hand (section 6.2), for the separation of gas mixtures (isotopic) by comparison with other similar devices, such as centrifuges and nozzle separators, and on the other hand (section 6.3), for the separation of temperature by comparison with cooling machines.

It can be deduced from the discussion in chapter 6 that the tube will probably never be found useful as a separator of gas mixtures; on the other hand the possibility remains that gas separation data such as those presented in section 3.3 may, once their interpretation is clear, become useful for further study of the flow in the tubes: this also applies to such special cases as are discussed in section 5.3, where gas and temperature separation are closely correlated, and where therefore their relative magnitude provides information on the turbulence in the tubes.

2. THE TANGENTIAL VELOCITY DISTRIBUTION

The tangential velocity distribution in the vortex tube has been studied experimentally in a number of cases (Keyes 1961, Ragsdale 1961, Ross 1964b, Reynolds 1962, Bruun 1967, 1969, Hartnett and Eckert 1957, Lay 1959, Scheller and Brown 1957, Schowalter and Johnstone, 1960, Suzuki 1960, and Takahama and Kawashima 1960). It is a characteristic feature of the results that the radial distributions obtained range from anywhere near a free vortex to close to a forced vortex. This diversity of results is explained quite adequately in many cases by the two-dimensional approximation described in section 2.1.

The realization that diversion of flow into the end-wall boundary layers plays a decisive role for the secondary flow pattern has led to studies of this phenomenon and to an evaluation of its importance for the tangential velocity distribution; results of these studies are discussed in section 2.2.

In long tubes, the axial gradient of the tangential velocity is a conspicuous feature; the relation of the resultant three-dimensional pattern to the radial distribution of axial flow is discussed in section 2.3 on the basis of zero order expressions obtained by Lewellen, 1964, 1965, from an expansion of the Navier Stokes equations (ref. IVa).

In section 2.4, finally, an attempt is made to explain qualitatively the origin of the interplay between radial and axial flow and the effect of this on the tangential velocity under differing conditions as determined by the vortex tube type.

2.1. The Radial Distribution of Tangential Velocity

Einstein and Li, 1951, Pengelley, 1957, Donaldson and Sullivan, 1960, and Deissler and Perlmutter, 1960, have investigated the origin of the diversity of tangential velocity patterns encountered experimentally. Deissler and Perlmutter have employed the following simple approximation to the tangential angular momentum equation, disregarding axial gradients,

$$\rho u \partial(\bar{v}r)/\partial r = \rho\nu\,(\partial^2\bar{v}/\partial r^2 + \frac{1}{r}\partial\bar{v}/\partial r - \bar{v}/r^2); \qquad (2.1)$$

in dimensionless form this equation reads (cf. eq. 2.5)

$$\frac{\partial\phi}{\partial\xi}\frac{\partial\Gamma}{\partial\eta} = \frac{2\eta}{Re\sqrt{a}}\frac{\partial^2\Gamma}{\partial\eta^2} \qquad (2.2)$$

where $2\pi\Gamma$ is a dimensionless circulation; while $Re_r\sqrt{a} = F/\nu\ell$ is a Reynolds number, with F/ℓ the total volume flow divided by 2π into the tube per unit of tube length and ν the kinematic viscosity or the corresponding turbulent parameter (below written ϵ).

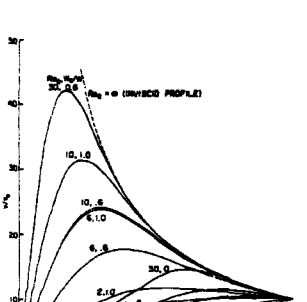

Fig. 2.1. Non-dimensional tangential velocity distribution in vortex tube. From Deissler and Perlmutter 1960; Re_o and W_c/W equivalent with $Re_r\sqrt{a}$ and $Re_r/Re_r\sqrt{a}$ in text; r_i and v_o correspond to r_o and v_{po} in text.

Typical results are shown in fig. 2.1. A simple radial flow function is employed that permits the study of the influence on the velocity pattern of the ratio of radial flow entering the core region (W_c) to total flow into the tube at the periphery (W) (tube model as in fig. 1.1b, but with nozzles spaced along the tube); W_c/W may be identified with $Re_r/Re_r\sqrt{a}$ of sections 2.3 and 2.4. The Reynolds number Re_o, used as a parameter in the figure, is based on total radial flow into the tube at the periphery per cm tube length and as such may be identified with $Re_r\sqrt{a}$ as defined above. Thus the product of the two parameters is the radial Reynolds number Re_r, based on centre-exit flow. It is seen that this radial Reynolds number, which is a measure of the relative importance of angular-momentum transport by radial flow and by viscous (or turbulent) forces in the radial direction, has a major influence on the resultant distribution in that a large influx of fluid leads to preservation of angular momentum at smaller radii, i. e. to a distribution that, in the outer part of the tube, is close to the free vortex.

The solution neglects any axial changes; it is to be expected, therefore, that the approximation works best for shorter tubes and especially for tubes of the type with nozzles along the periphery (fig. 1.1e). When the attempt is made to interpret such experimental results, the complication arises that it is necessary to postulate that the flow in the tubes is turbulent, in order to reconcile experiments with theory. On the other hand, this is a major conclusion which is fundamental to the understanding of all aspects of the tube functioning. Confirmation of the result by independent methods have been made by Kendall, 1962, and by Rosenzweig, Lewellen and Ross, 1964.

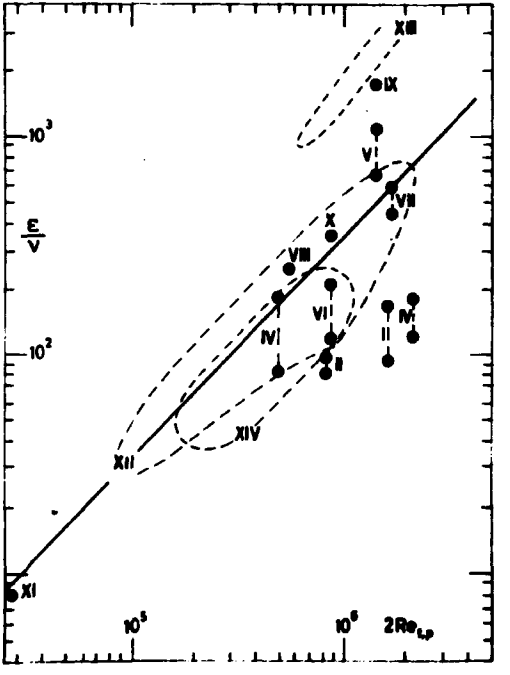

Fig. 2.2. Ratio of turbulent to laminar viscosity as a function of tangential Reynolds number (Note that abscissa is $2 \times Re_{t,p}$). Roman numerals refer to table 2.1 (p. 32).

Since the solution obtained is very sensitive to the value assumed for Re_r when this is in a suitable range, an estimation of the turbulence level in terms of turbulent diffusivity is possible by matching the theoretical curves with experimental ones, as has been done by Deissler and Perlmutter, 1960, by Keyes, 1961, and by Ragsdale, 1961. Some results of these studies are shown in outline in fig. 2.2. It is seen that the laminar tangential Reynolds number $Re_{t,p} \equiv v_{po} r_p / \nu$ has some potential as a parameter for the correlation of the results.

2.2. The Boundary Layer Interaction

Flow visualization experiments have shown that the end-wall boundary layers play an important role for the tube functioning in that a major part of the radial flow towards the centre region may be diverted into the layers owing to the fact that wall friction reduces the tangential velocity close to the wall and that this reduction tends to upset the balance between radial pressure gradient and rotation existing in the tube proper (Anderson, 1961, Rosenzweig, Ross and Lewellen, 1962, Kendall, 1962, Ross, 1964a, Lewellen, 1965, and Hornbeck, 1969).

2.1.1. The Analysis by Rosenzweig et al.

Results of a boundary layer analysis by Rosenzweig, Lewellen and Ross, 1964, are shown in figs. 2.3 and 2.4. The ordinate in fig. 2.3 measures the ratio of the circulation at the exhaust radius (fig. 1.1 type e) to that at the periphery; thus, a value of unity for this parameter indicates the presence of a free vortex in the outer region of the tube, while a low value designates approach to a forced vortex (the ratio of exhaust radius to tube radius is 1/6 in the case shown, and thus, the square of this is the ordinate that corresponds to the forced vortex). In fig. 2.4, the ordinate is that fraction of radial flow which is not diverted into the end-wall boundary layers but, according to the model, uniformly distributed along the tube.

The parameter A in figs. 2.3 and 2.4 is defined as

$$A = \frac{0.27}{(Re_{t,p})^{1/5}} \frac{\Gamma_{po} r_p}{Qt} \qquad (2.3)$$

where $Re_{t,p}$ is the (laminar) tangential Reynolds number, $2\pi\Gamma_{po}$ is the circulation at the periphery and $2\pi Q$ the flow into the tube (and, since there is no peripheral exit, also the flow into the core) per cm tube length. The

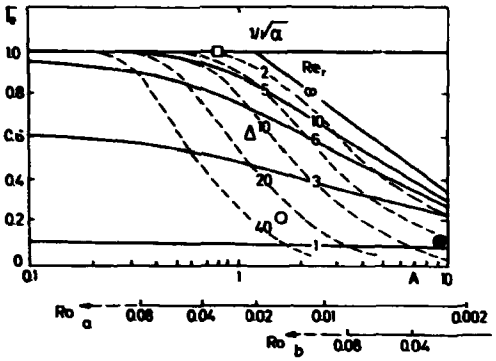

Fig. 2.3. Circulation at edge of exhaust hole as a function of A (Eq. (2.3)); solid curves (from Rosenzweig, Lewellen and Ross, 1964), radial Reynolds number Re_r held constant.

Dashed curves, based on eq. (2.16) with tube radius-to-length ratio $\sqrt{\alpha}$ held constant. Ro-abscissa (with $(Re_{t,p})^{1/5} = 10$) valid for core flow fraction $Re_r/Re\sqrt{\alpha}$ = (a) 1, (b) 0.1.

Experimental points; data from ref. 11 ($Re_r/Re\sqrt{\alpha} = 1$), □ $\sqrt{\alpha} = 1/2$, Δ $\sqrt{\alpha} = 1/15$, ○ $\sqrt{\alpha} = 1/30$; data from Mürtz and Möller, 1961, ($Re_r/Re\sqrt{\alpha} \ll 1$), ● $\sqrt{\alpha} = 1/7$.

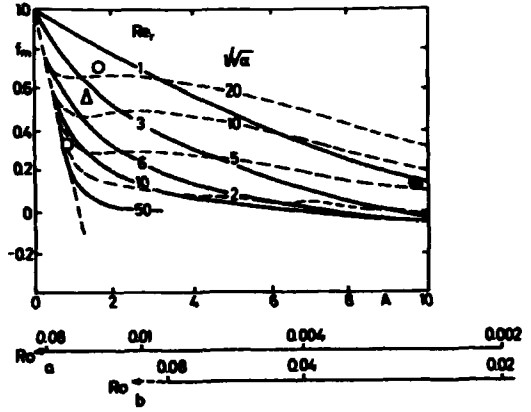

Fig. 2.4. Minimum mass flow, f_m, in body of tube as a function of A; see legend to fig. 2.3.

turbulent radial Reynolds number is defined (as in section 2.1) as

$$Re_r = Q/\epsilon \qquad (2.4)$$

A is essentially a swirl parameter inversely proportional to a radial Rossby number, $Ro_r = (Q\ell)/(\Gamma_{po} r_p)$, similar to that defined by Lewellen (1962 and 1964) (see section 2.3). A is important in this context, because it is a measure of the fraction of the flow that must be accelerated towards the centre region in the end-wall boundary layer in order to make up for the excessive radial pressure gradient there, while Re_r is important because it influences the shape of the radial distribution of tangential velocity which again determines the shape of the radial pressure gradient (a free vortex has a much steeper pressure gradient at intermediate radii than that of a forced vortex with the same tangential velocity at the periphery).

It was found in the study that A-values in the experimentally interesting range (see section 2.4) do not have a large effect on the radial change of the circulation even though a substantial part of the flow is diverted into the end-wall layers; in agreement with this conclusion the data obtained in the study (XIV) agree quite well with those of Keyes (XII) in fig. 2.2, where A has been of the order of 0.5 - 2 (cf. figs. 2.3, 2.4). The reason for this is that the boundary flow is rejected axially from the boundary layers at intermediate radii without having experienced excessive loss of circulation in the layers.

The analysis is valid only for conditions in tubes of type d and e, which have exits at the centre exclusively. Thus, in these cases the very simple picture presented by Einstein and Li and Deissler and Perlmutter still holds true.

2.2.2. Some Experimental Results

In ref. II an investigation was carried out of the tangential velocity distribution in the vortex tubes (type d fig. 1.1) that were employed for the gas separation experiments described in chapter 3.3 (ref. I). The diameter of these tubes was rather small so that extensive measurements could not be made (probes necessarily alter the flow pattern inside a narrow tube). Thus the data were restricted to wall pressure measurements along the periphery, at the end walls and in the exit ducts, from which approximate tangential velocity distributions were deduced on the assumption that the tangential velocity is proportional to the radius raised to a fixed power, n, i.e. $v \propto r^n$, in the outer part of the tube, with n the parameter to be deter-

mined by fitting to experiment. n-values between -1 and +1 (in certain cases somewhat higher than one) can be expected, corresponding to distributions between the free and the forced vortex (in certain cases, an angular velocity increasing with radius). It was assumed that the flow in the whole of the core region forms a forced vortex, and that the transition between the two regions is sharp (similar assumptions have been made previously by other workers (Kerrebrock and Keyes, 1959)).

In the experiments, the inlet nozzle geometry and the gauge pressure of the supply gas was kept constant with the result that the total flow through the tube was quite constant (though somewhat dependent on orifice diameters), see section 3.3 and ref. 11. n-values close to -1 were found in the very short tubes that had the strongest radial flow, while positive n-values appeared in tubes above a certain length, both results in agreement with the positions of the corresponding points in fig. 2.3. In the longest tubes tested it was furthermore found that the tangential velocity decreased markedly along the tube, a situation typical of the long tubes with weak radial flow to be treated in the next section.

2.3. The Three-dimensional Distribution of Tangential Velocity

A theoretical investigation of the tangential velocity distribution in the vortex tube that takes into account that axial gradients may exist has been carried out by Lewellen, 1962. From the continuity equation and the Navier Stokes equations for the velocity components in cylindrical coordinates, Lewellen eliminated the pressure, introduced the circulation $2\pi\Gamma \equiv 2\pi vr$ and the axi-symmetric stream function

$$\partial\Psi/\partial z \equiv ur \quad \text{and} \quad \partial\Psi/\partial r \equiv -wr$$

and obtained the following two equations, where all quantities are dimensionless

$$\frac{\partial\psi}{\partial\xi}\frac{\partial\Gamma}{\partial\eta} - \frac{\partial\psi}{\partial\eta}\frac{\partial\Gamma}{\partial\xi} = \frac{2\eta}{Re}\frac{\partial^2\Gamma}{\partial\eta^2} + \frac{a}{2Re}\frac{\partial^2\Gamma}{\partial\xi^2} \tag{2.5}$$

$$\Gamma\frac{\partial\Gamma}{\partial\xi} = Re^2\left\{4\eta^2\left[\frac{\partial\psi}{\partial\xi}\frac{\partial^3\psi}{\partial\eta^3} - \frac{\partial\psi}{\partial\xi}\frac{\partial^3\psi}{\partial\xi\partial\eta^2} - \frac{2}{Re}\left(2\frac{\partial^3\psi}{\partial\eta^3} + \eta\frac{\partial^4\psi}{\partial\eta^4}\right)\right]\right.$$

$$\left. + a\left[-\frac{\partial\psi}{\partial\xi}\frac{\partial^2\psi}{\partial\xi^2} + \eta\frac{\partial\psi}{\partial\xi}\frac{\partial^3\psi}{\partial\eta\partial\xi^2} - \eta\frac{\partial\psi}{\partial\eta}\frac{\partial^3\psi}{\partial\xi^3} - \frac{1}{Re}\left(4\eta^2\frac{\partial^4\psi}{\partial\eta^2\partial\xi^2} + \frac{a}{2}\eta\frac{\partial^4\psi}{\partial\xi^4}\right)\right]\right\} \tag{2.6}$$

Here $\Gamma \equiv \tilde{\Gamma}/\Gamma_s$ and $\psi \equiv \tilde{\psi}/\psi_s$ are normalised circulation and stream functions respectively; $\zeta \equiv z/z_s$ is a normalised axial position; $\eta \equiv (r/r_s)^2$ measures the radial position as the square of a normalised radius; and $\alpha \equiv (r_s/z_s)^2$ is the square of a ratio of characteristic lengths. Furthermore $Ro \equiv \psi_s/(\Gamma_s r_s)$ and $Re \equiv \psi_s/(\nu_s z_s)$ are Rossby and Reynolds numbers, respectively. ν is the kinematic viscosity. The above equations are, strictly speaking, derived for laminar flow; in ref. IV it was, however, assumed (see e.g. Deissler and Perlmutter, 1960) that they may be applied unaltered to the turbulent case with Re interpreted as a constant turbulent Reynolds number. ψ_s is a suitable standard flow rate.

Eq. 2.5 equates the transport of angular momentum out of a volume element by secondary flow (left side) to that by turbulent diffusion into the volume element (right side). Eq. 2.6 describes the fact that the gradients of radial and axial velocity necessarily must be related through the mixed second order derivative of the pressure; i.e. that the radial pressure gradient which appears in the radial momentum equation and the axial gradient which appears in the axial momentum equation may be eliminated by suitable differentiation followed by combination of the two equations.

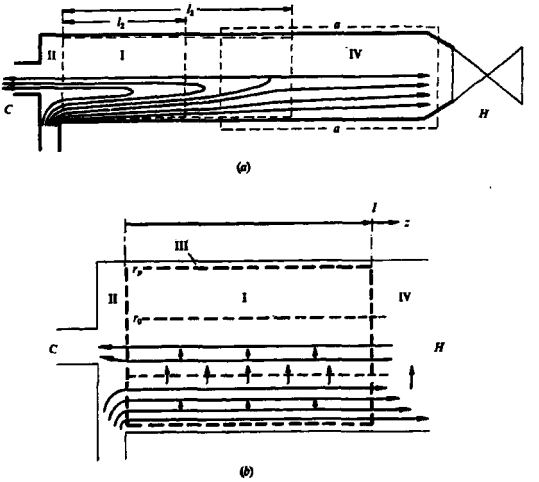

Fig. 2.5. a. Vortex tube with schematic stream line pattern and boundary of region I (two examples shown). b. Diagram of region I; arrows indicate axial and radial flow components.

2.3.1. The Analysis by Lewellen for $u \ll w$

Lewellen selected the quantity $Q\ell$ for ψ_s, where $2\pi Q\ell$ is the total radial volume flow at r_o, i.e. at the radius where the axial velocity changes sign (see fig. 2.5). In most cases of interest the resultant $Ro_r \ll 1$, and thus, the form of eq. (2.6) suggests a series expansion of Γ and ψ in Ro_r as described by Lewellen, 1962, writing

$$\Gamma = \sum_{0}^{\infty} \Gamma_n(\eta,\xi) Ro_r^{2n} \tag{2.7}$$

$$\psi = \sum_{0}^{\infty} \psi_n(\eta,\xi) Ro_r^{2n} \tag{2.8}$$

By inserting these expressions into 2.5 and 2.6, and collecting terms of the same power in Ro^2, it was found that the zero order expression of eq. (2.5) may be written

$$2\eta\, \Gamma_o'' - Re_r \Gamma_o' \partial\psi_o/\partial\xi = 0 \tag{2.9}$$

with Γ_o independent of the axial coordinate. The corresponding zero-order stream function, written as a polynomial in ξ, was found to take the form

$$\psi_o = f_{oo}(\eta) + \xi f_{o1}(\eta) \tag{2.10}$$

Thus eq. (2.9) may be written

$$2\eta\, \Gamma_o'' - Re_r f_{o1} \Gamma_o' = 0 \tag{2.11}$$

It follows that the radial flow alone governs the radial distribution of the circulation; eq. (2.11) can be shown to be identical with the simple equation (2.2), which has been found useful in two-dimensional studies.

2.3.2. The Theory for $u \ll w$

Lewellen proceeded to discuss the first order set of equations and the convergence of the series. Implicit in the treatment is that both f_{oo}' ($\equiv \partial f_{oo}/\partial\eta$) and f_{o1} are of order one. If, however, $\partial\psi/\partial\eta \gg \partial\psi/\partial\xi$, as may well be the case, then $\partial\psi/\partial\xi \times \partial\Gamma/\partial\eta$ and $\partial\psi/\partial\eta \times \partial\Gamma/\partial\xi$ in eq. (2.5) may be of the same order of magnitude. This case was treated by Lewellen,

1964, on the basis of an expansion of Γ and ψ in terms of Ro_r, rather than Ro_r^2. The resultant zero-order expressions of (2.5) and (2.6) describe conditions in long vortex tubes with weak radial flow quite well, as was shown in ref. IV. As shown in ref. IVa, it is advantageous to transform the original zero order equations (Lewellen, 1964) and express them in terms of experimentally available parameters. This was done on the basis of the following set of reference parameters (cf. fig. 2.5):

$$r_s \equiv r_p, \quad z \equiv \ell, \quad \Gamma_s \equiv \Gamma_{po} \equiv v_{po} r_p, \quad \text{and} \quad \psi_s \equiv F, \tag{2.12}$$

where r_p is the tube radius, ℓ the length of region I, $2\pi\Gamma_{po}$ the circulation at the periphery near the nozzle (and v_{po} the corresponding tangential velocity) and $2\pi F$ the total volume flow through the tube. The resulting equations read

$$\frac{2\eta}{Re}\,\frac{1}{\sqrt{a}}\,\Gamma_o'' + f_{oo}'\Gamma_{11} - \frac{Re_r}{Re\sqrt{a}}\,f_{11}\,\Gamma_o' = 0 \tag{2.13}$$

$$\Gamma_o\Gamma_{11} = 4\eta^2 Ro^2 \left[f_{oo}''' \frac{Re_r}{Re\sqrt{a}} f_{11} - f_{oo}' \frac{Re_r}{Re\sqrt{a}} f_{11}'' - \frac{2}{Re}\,\frac{1}{\sqrt{a}}\,(2f_{oo}''' + \eta f_{oo}'''') \right] \tag{2.14}$$

Here $Ro \equiv F/(\Gamma_{po} r_p)$, $Re\sqrt{a} \equiv F/(\varepsilon \ell) = F/(\varepsilon r_p) \times \sqrt{a}$, while $a \equiv (r_p/\ell)^2$, $\eta \equiv (r/r_p)^2$ and $\xi \equiv z/\ell$; furthermore, in (2.13) and (2.14) Γ and ψ are approximated by

$$\Gamma = \Gamma_o + \Gamma_{11}\,\xi$$

$$\psi = f_{oo} + \frac{Re_r}{Re\sqrt{a}}\,f_{11}\,\xi \tag{2.15}$$

where Γ_o, Γ_{11}, f_{oo}, and f_{11} are all functions of η, only. Re_r is the radial Reynolds number so chosen that $Re_r/(Re\sqrt{a})$ is equal to $Q\ell/F$, the ratio of the total radial flow of region I (fig. 2.5) at r_o (the radius at which the axial velocity changes sign) to the total flow through the tube.

The validity of (2.13) and (2.14) is restricted to $\Gamma_{11} \ll 1$ and $Re_r/Re\sqrt{a} \times f_{11} \ll 1$ (see Lewellen 1964). This may be achieved in the experimental cases considered by restricting attention to short tube lengths, i.e. by choosing $\sqrt{a}$ large enough; that Γ_{11} is reduced by this choice as well

may be deduced from the fact that $\sqrt{a}\Gamma_{11}$ in eqs. (2.13) and (2.14) is invariant to changes in $\sqrt{a}$.

Equations equivalent to (2.13) and (2.14) may be derived, as mentioned in ref. IVa, directly from (2.5) and (2.6) on the basis of (2.15) and with the assumption that $\sqrt{a} \ll 1$. The same restriction as above that only short tube lengths are to be considered has to be made, here expressed by the demand that ξ has to be kept small compared to unity.

2.3.3. Comparison with Experiment and Interpretation of the Results

The connection between the secondary flow and the circulation, established through eqs. (2.13) and (2.14), was investigated in ref. IV (in detail in IVa). For this purpose the equations were solved with respect to the circulation Γ_0 and its axial gradient Γ_{11} on the basis of prescribed secondary flow functions. The radial flow was found to have essentially the same effect on Γ_0 as represented by eq. (2.2) of previous two-dimensional investigations (compare fig. 2.6b and fig. 2.1), and to have very little influence on Γ_{11} (fig. 2.6d). The inclusion of the additional term containing Γ_{11} in (2.13) as compared with eq. (2.2) was found to have an effect on the radial distribution of Γ_0 somewhat akin to the effect of the radial flow term; its physical relevance is therefore somewhat difficult to assess (fig. 2.6a).

It was furthermore found in ref. IV (with IVa) that the axial gradient of the circulation, $2\pi\Gamma_{11}$, is linked in a unique way to the axial velocity and its radial gradients through eq. (2.14). That is to say that, although eq. (2.14) contains higher order derivatives of f_{00} that cannot be derived directly from experiment (since this would demand excessive accuracy), there appears to be essentially only one single f_{00}-function for each case (distinguished primarily by the ratio of the flow in the outer annulus to that in the core, i.e. the cold flow fraction) that satisfies the requirements of the experimental axial velocity distribution, and, at the same time, provides a physically relevant axial gradient of circulation Γ_{11}. Comparison with experiment shows the latter conditions to cause the tangential velocity distribution to have Γ_{11} negative (i.e. Γ decreasing with z) within an annulus bounded approximately by $\eta = \eta_0$ and the periphery, while it shall be positive in the core (see fig. 2.6c and d; and e.g. Bruun, 1967, 1969 or Hartnett and Eckert, 1957).

The effect on the circulation of a radial flow that increases with axial position, as is often found experimentally (see section 2.4), is not taken into account in the present approximation, which is limited to linear ψ-gradients in the ξ-direction. It is possible, as discussed in ref. IVa, that

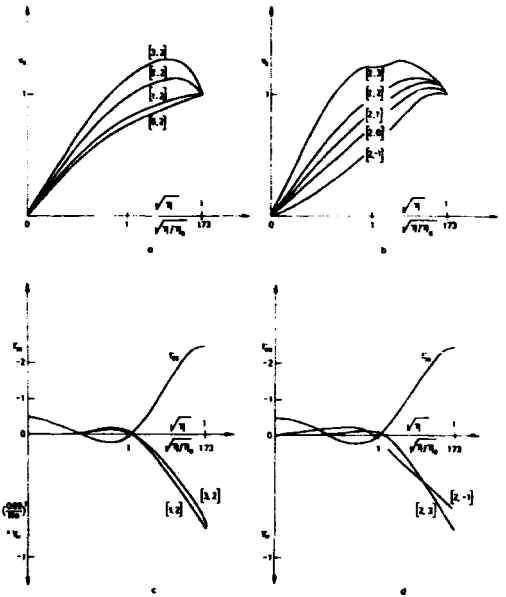

Fig. 2.6. $\Gamma_o/\sqrt{\eta} = v_o (= \bar{v}/v_{po}$ at $z = 0)$; and c, d, $\Gamma_{11}/\sqrt{\eta} = v_{11} (= \frac{\partial v}{\partial z}\frac{\ell}{v_{po}}$; as functions of $\sqrt{\eta}$. Also shown, corresponding secondary flow functions, $\partial\psi/\partial\eta$, at $\xi = 0$ and $\xi = 1$ (i.e. $w_p^2/(2F)$ at $z = 0$ and $z = \ell$). $\sqrt{a}Re = 15$, $\mu = 0.01$, $1/\eta_o = 3$.

a and c: $Re_p/Re\sqrt{a} = 0.055$; Ro = 0 | 0.040 | 0.090 | 0.124

curve: [0, 2] | [1, 2] | [2, 2] | [3, 2]

b and d: Ro = 0.090; $Re_p/Re\sqrt{a}$ = -0.055 | 0 | 0.0275 | 0.055 | 0.110

curve: [2, -1] | [2, 0] | [2, 1] | [2, 2] | [2, 3]

the large positive axial gradient of circulation found typically at small radii in part has its origin in such an effect as this gradient is not well reproduced within the present approximation. At larger radii where the axial reduction of circulation takes place, such radial flow-increase with axial position cannot be invoked as the cause of the reduction, since in the work by Bruun, 1967, 1969, where radial data are available, it is found that the axial gradient of circulation maintains its typical trend in tube sections, where the

radial velocity is constant or even has a tendency to decrease (see discussion in ref. IVa).

The calculations in ref. IV showed that Γ_{11} is almost proportional to Ro^2/Re (fig. 2.6c and eq. (2.14)). This means that the axial gradient of circulation in the outer part of the tube is larger the smaller the peripheral circulation and the larger the axial volume flow. According to the model, this implies that the axial gradient of the centripetal acceleration, $\partial(\tilde{v}^2/r)/\partial z$, is related, through the axial variation of the radial pressure gradient, to turbulent stress created by the radial gradient of the axial velocity.

When the theory is applied to experimental cases, turbulent Reynolds numbers can be obtained by adjusting the calculated Γ_{11}-curve until an optimum fit with experiment is obtained. Results of this procedure are shown in fig. 2.2 for a number of cases from the literature all involving long asymmetric tubes of type a or b (fig. 1.1) with weak radial flow. The inconsistency that the theory is developed for incompressible flow while the experiments considered are compressible cases is discusssed in ref. IV (IVa).

The flow in the tube need not be turbulent; thus in Suzuki's case (fig. 2.2, point XI) conditions are close to being laminar because the tangential velocity is comparatively low. Small tangential Reynolds numbers may also be obtained by reducing the pressure level sufficiently, as was done by Mürtz and Nöller, 1961, in their investigation of the mass separation potential of vortex tubes of type c (fig. 1.1). Fig. 2.2 predicts, on the basis of their tangential Reynolds number, that laminar conditions are just reached by the pressure level chosen.

It is seen from fig. 2.2 that the turbulent diffusivities obtained in the present cases are of the same order of magnitude as those of previous (quasi-)two-dimensional studies.

A procedure somewhat similar to that described here has been adopted by Wolf, Lavan and Fejer, 1968.

2.4. The Connection between Secondary Flow and Tangential Velocity

The treatment in section 2.3 does not provide any explanation of why the axial and radial flows are distributed as they are, i.e. it is taken for granted that the axial flow emerges from the end-wall boundary layer in such a way and provides such a radial flow that the experimental tangential velocity distribution results. Some insight into this problem may be achieved on the basis of the treatment in section 2.2. The theory there

does not include long asymmetric tubes, but one may argue that the tube region removed some distance from the nozzle (say, region IV of figure 2.5) in a way behaves like an extended boundary layer of the short tube type.

2.4.1. Further Discussion of the Boundary Layer Analysis in 2.2.1

The treatment in section 2.2 employs Re_r and A as independent parameters; however, the results of section 2.1 - 2.3 indicate that the turbulent to laminar viscosity ratio is related to the tangential Reynolds number $Re_{t,p}$, so that with some justification we may assume

$$\varepsilon/\nu = C\, Re_{t,p} \tag{2.16}$$

where 1/C, according to fig. 2.2, is about $2.5\ 10^3$. Furthermore, $Re_{t,p}$ may be written, in accordance with the definitions in section 2.3,

$$Re_{t,p} = \frac{\varepsilon}{\nu}\frac{Re}{Ro} = \frac{\varepsilon}{\nu}\frac{Re_r}{Ro}\frac{1}{\sqrt{a}}\frac{1}{Re_r/(Re\sqrt{a})} \tag{2.17}$$

so that from eq. (2.16)

$$Re_r = \frac{1}{C}\, Ro(Re_r/Re\sqrt{a})\sqrt{a} \tag{2.18}$$

(where Ro is the Rossby number). $Re_r/(\sqrt{a}Re)$ is here taken to mean the ratio of the net radial flow into the core region, as measured by the flow through the exits in the centre, to the total flow through the tube; this means that region I (Fig. 2.5) is taken to cover the whole tube with ℓ equal to the tube length. It is clear that $Re_r/Re\sqrt{a}$ in all cases must be less than or equal to one. Since A may be written (eq. (2.3))

$$A = 0.27\,\frac{1}{(Re_{t,p})^{1/5}}\;\frac{1}{Ro(Re_r/Re\sqrt{a}}\,, \tag{2.19}$$

the governing parameters of figs. 2.3 and 2.4 are now $Ro(Re_r/Re\sqrt{a})$, the radial Rossby number, and $\sqrt{a}$, the ratio of radius to length of tube, with $Re_{t,p}$, the laminar tangential Reynolds number, a third parameter of less importance. Experiments set limits to the values of these parameters with the result that only the regions covered by the dashed curves in figs. 2.3 and 2.4 (see below) are of interest.

All factors in (2.18) and (2.19), the reference tangential velocity, v_{po}, being the only exception, contain easily accessible external parameters. Without actually measuring it, a prediction of v_{po} is possible on the fol-

lowing evidence. In most experiments, conditions with sonic velocity in the nozzle(s) have been sought; it is generally found that v_{po} almost reaches this limit in long asymmetric tubes, while in shorter tubes of the more symmetric type (d or e in fig. 1.1) a considerable reduction in velocity takes place when the gas enters the tube (down to 20% or less of the velocity in the nozzle). This incidentally has been a major obstacle to the practical use of the vortex tube for containment in nuclear fission rockets. Rosenzweig, Lewellen and Kerrebrock, 1961, discuss this velocity reduction on the basis of a torque-balance analysis by Rosenzweig, 1961, for laminar flow. They find that the radial turbulent Reynolds number and the ratio of injection radius to tube radius (or rather its deviation from unity) are the two parameters that govern the reduction. Their results are difficult to use in most cases of interest because the ratio in question does not have a well-defined value, as it usually covers the range from one to 3/4 or less. Furthermore they predict better velocity recovery with increasing radial Reynolds number for the tubes under consideration (of type e), while the opposite seems to apply, as described above, for the transition from long tubes with weak radial flow to short tubes with strong flow.

The total range of Ro spanned by experiment is no more than a factor of about 50 (from 0.002 to 0.08), and different types of vortex tube tend to cover the same range; the reason for this is basically that the interest over the years has been centred on obtaining maximum flow rates ($2\pi F$) through the tubes under the given conditions. These, in tubes with centre outlets, are rather restrictive on F (if the radial pressure gradient is not to be ruined), while at the same time in the usually short tubes of this type, v_{po} tends to be rather small, as mentioned above. Conversely, in long vortex tubes with peripheral outlet, the hot exit normally can carry a larger amount of gas, but v_{po} tends to be larger too. Thus the ratio of the two quantities (appearing in Ro) remains within the same range of values.

2.4.2. Classification of Vortex Tubes according to Flow Type

On the basis of the above considerations, it is now possible to relate the secondary flow pattern and resultant radial distribution of tangential velocity to external tube parameters and thereby explain in qualitative terms the dependence of the patterns on tube type, as found experimentally.

1. The forced vortex type flow with mainly axial flow in tubes of the long asymmetric type is found from eqs. (2.18) and (2.19) to arise, on the one hand because $\sqrt{a} = r_p/\ell$ is small, on the other hand because the radial flow fraction $(Re_r/Re\sqrt{a})$ in many of the experimental cases recorded has

been small (cf. table 2.1). Both effects tend to make Re_r (eq. 2.18) small while the latter one tends to increase A (eq. 2.19). Since this implies that the tubes considered are represented by points in fig. 2.3 towards the right and in the lower part of the figure where F_e is small, the presence of the forced vortex is strongly indicated. Furthermore, fig. 2.4 shows the axial diversion in long tubes with Re_r small and with A sufficiently large (i.e. $Re_r/Re\sqrt{a}$ sufficiently small) to be large; this means that the smaller the percentage of net radial flow, the larger is the tendency for all of it to be diverted along the tube.

The interpretation of these results is as follows. The radial flow is diverted because the radial pressure gradient is reduced along the tube (the tangential velocity level decreases), so that an axial pressure gradient builds up that is larger than necessary for the axial flow moving towards the peripheral hot exit; somewhere in region IV the extra axial flow induced by this pressure gradient changes to radial and then to axial flow towards the cold exit. Part of this flow may even be recirculated to the periphery at the nozzle as in the work by Bruun, 1967, 1969. Because of the small level of actual radial flow, the radial transport of angular momentum is small and the forced vortex results. Furthermore the relatively high axial flow rate tends to transport angular momentum far down the tube.

2. Long tubes with outlets at the centre only (type d) or tubes of types a and b with the cold flow fraction $\mu \to 1$ stand a somewhat better chance than the above type of having a free vortex in the outer part of the tube, because $Re_r/Re\sqrt{a} = 1$ (fig. 2.3). However, $2\pi F$ is rather limited in magnitude, as mentioned above, while v_{po} may still be large; Ro is therefore likely to be on the low side, and the possibility of finding a forced vortex rather than a semifree in the tube is enhanced (as in the experiments of ref. 11, cf. point corresponding to long tube in fig. 2.3). As seen from fig. 2.4, part of the radial flow in tubes of this type is distributed along the tube, but a substantial part is still diverted.

The origin of these effects is in general terms as follows. The axial pressure gradient created by the decrease in axial velocity along the tube is still appreciable compared to case 1 above, and the major part of the radial flow enters the core region away from the nozzle end; that part which is reversed towards the cold exit may have sufficient angular momentum left to impart a deviation from the forced vortex; furthermore a sufficient amount of radial flow is left to provide a substantial, uniformly distributed radial flow which carries additional angular momentum into the core. Thus

with the change from $\mu = 0$ (case 1) to $\mu = 1$ (case 2), some approach towards the free vortex may be seen provided, as mentioned above, that the limited capacity of centre exits in general does not reduce the total amount of gas through the tube.

In long symmetric tubes (of type e) the situation is similar to the case considered above (for type d) except that the increased radial flow takes place in the two end-wall boundary layers rather than along the tube in region IV.

3. In short tubes of type d or e, the free or semifree vortex appears, on the one hand because the radial flow fraction $Re_r/Re\sqrt{a}$ is equal to one, on the other hand because $\sqrt{a} = r_p/t$ is comparatively large; factors that tend to make Re_r large and A small (cf. points referring to results from ref. 11, in fig. 2.3). The resultant tendency to form the free vortex is directly deducible from fig. 2.3 (see also section 2.2). At the same time the axial diversion of the flow to the end-wall boundary layers has a tendency to become complete (fig. 2.4). An excess, even, of flow in the boundary layers appears possible in practice with the surplus recirculated to the periphery in the main part of the tube (i.e. $f_m < 0$ in figure 2.4; according to Rosenzweig, Lewellen and Ross, 1964, this may be an additional effect of the centre exit discontinuity, which they allow for by the use of an extra parameter (not included in figs. 2.3 and 2.4)).

These results may be interpreted as follows. The diversion of the flow into the boundary layers is complete, because a large radial pressure drop at intermediate radii (and the presence of the exit) tend to draw a substantial axial flow into the tube proper from the end-wall layers; these have to be fed from the periphery and thus the diversion takes place. The large pressure drop at intermediate radii takes place because the free or semifree vortex is obtained in the outer annulus, and this in its part is caused by the large radial flow (or rather Re_r), which, although it may all be diverted into the end-wall boundary layers, may preserve sufficient angular momentum to create the free vortex.

In conclusion it may be appropriate to quote Lewellen, 1965 (who referred to tubes of type e, but as discussed above the statement may be generally valid): "... the fluid will gravitate to ... regions of lower centrifugal force that provide a path of least radial resistance. Combined with this fact, is the fact that the radial velocity supports the swirl by convection of angular momentum. Thus, the radial velocity always distributes itself in a way that tends to make the tangential velocity two-dimensional as far as is possible".

Table 2.1

	No.	μ	r_p cm	Approx. $1/\eta_o$	F cm^3/sec	v_{po} cm/sec	Ro = $F/(v_{po} r_p^2)$	$\frac{1}{v_{po}} \frac{\partial \check{v}}{\partial (z/r_p)}$ at $r=r_p$, $z=0$
Hartnett and Eckert	I	0	3.8	2.5	$2.9\ 10^4$	$2.4\ 10^4$	0.08	0.027
Lay, 10psig	II	0	2.5	3	$1.0\ 10^4$	$2.1\ 10^4$	0.08	0.030
Lay, 30psig	III	0	2.5	3	$1.7\ 10^4$	$2.9\ 10^4$	0.09	0.024
Schowalter and Johnston	IV	0	10	2.5	$2.5\ 10^4$	$3.4\ 10^3$	0.07	0.054
Takahama	V	0	3.9	3	$6.5\ 10^3$	$2.1\ 10^4$	0.02	0.051
Takahama	VI	0	2.64	3.5	$6.5\ 10^3$	$1.7\ 10^4$	0.05	0.045
Bruun	VII	0.23	4.7	2	$1.2\ 10^4$	$1.8\ 10^4$	0.03	0.048
Scheller and Brown	VIII	0.5	1.25	3	$1.5\ 10^3$	$2.2\ 10^4$	0.04	0.048
Takahama	IX	0.5	3.9	2.5	$6.5\ 10^3$	$2.1\ 10^4$	0.02	0.051
Takahama	X	0.5	2.64	3	$6.5\ 10^3$	$1.7\ 10^4$	0.05	0.060
Suzuki	XI	1	1.4	3	110	$1.3\ 10^3$	0.05	0.12

Keyes XII, Ragsdale XIII, Rosenzweig, Lewellen and Ross XIV.

3. THE CONCENTRATION DISTRIBUTION AND THE GAS SEPARATION

A number of papers on the stationary concentration distribution in the vortex tube of binary gas mixtures has appeared in connection with the development of gaseous nuclear rockets, as carried out by various groups in the USA (Kerrebrock and Meghreblian, 1958, Kerrebrock and Lafyatis, 1958, Rosenzweig, Lewellen and Kerrebrock, 1961, Keyes, 1961, Ragsdale, 1960, Pivirotto, 1966, Kendall, Mensing and Johnson, 1967); these studies will be briefly described in section 3.1 within the two-dimensional approximation.

The possibility that the vortex tube may act as a separator of gas mixtures appears to have been first realized by H. R. von Traubenberg during World War Two, according to an obituary in Zeitschrift für Naturforschung 1 (1946) p. 420. A number of papers on this subject has since appeared that has treated the problem experimentally (Stone and Love, 1950, Elser and Hoch, 1951, Baker and Rothkamp, 1954, Tcrocheshnikov and Koval, 1958, Nöller and Mürtz 1958, Bornkessel and Pilot, 1962, and ref. I) and in some cases theoretically (Mürtz and Nöller, 1961, Strnad, Dimic and Kuscer, 1961, and ref. III).

Experimental investigations of the concentration gradients within the tube in connection with these studies have been made in only one case (Mürtz and Nöller, 1961) and then at pressures far below atmospheric. These results will be discussed briefly in section 3.2 together with a presentation of equations that describe the three-dimensional distribution of concentration in the tube.

At pressures above atmospheric it has proven difficult to obtain reproducible gas separation results, because the effects that can be obtained are very small; however, well-defined effects do exist, as was shown by the use of a suitable analytical method in ref. I; the interpretation of the results obtained in that study will be discussed in section 3.3.

3.1. The Radial Distribution of Concentration

The nuclear rocket concept has been investigated on the assumption that it might be possible to keep a heavy gaseous nuclear fuel contained in a vortex chamber (of type e, fig. 1.1) through which a light propellant is passed. The idea has been that the centrifugation of the gas should prevent the heavy fuel component from being carried with the light gas to the centre region. Thus the propellant should pass through the fuel zone and thereby be heated

by the fission processes for finally to pass axially out of the tube through a Laval type nozzle at supersonic velocity.

So far the idea has not met with success. This does not mean that the containment effect does not exist, in fact it has been demonstrated in a number of cases, but simply that it has not been of sufficient magnitude to be of practical use. The reason for this is know to be the comparatively high degree of turbulence in the tube, the presence of which has three undesirable consequences for the tube performance. For one thing, the turbulence makes it impossible, as mentioned in section 2.4, to obtain at the same time a high peripheral tangential velocity and a free vortex with a further velocity increase towards the centre; thus, although close-to-a-free-vortex may be formed in the outer annulus, the benefit is limited owing to the appreciable velocity reduction that takes place when the gas enters the tube. Furthermore, with turbulence in the tube, a prohibitively high radial inflow (see below) may be required in order to get close enough to the free vortex (to make Re_r in eq. (2.11) or (2.2) (fig. 2.1) sufficiently large). Finally, turbulence in the tube reduces the attainable height of the concentration peak.

The distribution problem has been approached theoretically by Ragsdale, 1960, and by Rosenzweig, Lewellen and Kerrebrock, 1961, on the basis of the two-dimensional approximation, which is quite adequate for the outer annulus of type e tubes (fig. 1.1). The treatment thus neglects the effect of the diversion of flow into the end-wall boundary layers; however, it is possible to argue, as was done in the case of angular momentum (section 2.2), that the combined effects of boundary layer flow plus axial redistribution may not be essentially different from the results of the purely two-dimensional approach.

The treatments by Rosenzweig et al. and by Ragsdale do not differ much in their basic assumptions; both write the diffusion equation as an integrated version of the following equation

$$\rho u r \frac{\partial N}{\partial r} = \frac{\partial}{\partial r}\left[\rho \varepsilon_n \left(r \frac{\partial N}{\partial r} + \frac{\rho D}{\rho \varepsilon_n} \frac{M_2 - M_1}{R\bar{t}} \bar{v}^2 N(1-N)\right)\right] \qquad (3.1)$$

where $M_2 - M_1$ is the molecular weight difference, N the mole fraction of the heavy component and ε_n the turbulent mass diffusivity. Eq. (3.1) reads in non-dimensional form (cf. eq. (4.2)).

$$\frac{\partial \psi}{\partial \xi} \frac{\partial N}{\partial \eta} = \frac{\partial}{\partial \eta}\left[\frac{2\eta}{Re_n \sqrt{a}} \left(\frac{\partial N}{\partial \eta} - \frac{Co}{t} N(1-N)\, \omega^2\right)\right], \qquad (3.2)$$

where

$$Co/t \equiv \frac{M_2 - M_1}{\rho \varepsilon_n / \rho D} \frac{v_{po}^2}{2RT_\infty} \tag{3.3}$$

(with t being of order one and $0 < N < 1$); thus Co/t is a measure of the diffusional force divided by the effect of the turbulence, while taken as a whole it is a measure of the attainable concentration gradient at equilibrium (Co may be considered as referring to K. Cohen, who has contributed much to the theory of mass separation in the gas centrifuge; it should not be confused with the Co designating the Cowling number of magneto-hydrodynamics).

$$Re_n \equiv F/(r_p \rho \varepsilon_n) \tag{3.4}$$

is a Reynolds number based on turbulent mass diffusion; it is related to the corresponding Reynolds number Re, for turbulent momentum transport, through the turbulent Schmidt number

$$Sc \equiv \rho \varepsilon_n / \rho \varepsilon = Re/Re_n \tag{3.5}$$

In both of the above treatments, Sc is assumed to be equal to 1; the selection of a proper value is a somewhat ambiguous process, as is the choice of a turbulent Prandtl number in chapter 4 (see ref. IV), since the concept of turbulent diffusivities as such has a rather weak theoretical foundation.

It is noted that, in eq. (3.2) (compare (3.1)), the usual molecular diffusion term has been replaced by the turbulent diffusion term $2\eta/Re_n\sqrt{a} \times \partial N/\partial\eta$, while the pressure diffusion term $2\eta Co/(Re_n\sqrt{a}t) \times N(1-N)\omega^2$ is assumed to retain its laminar form. These adaptations to the turbulent case appear reasonable, granted that an approximation has to be made; however, there is no good reason, as discussed in the work by Rosenzweig et al., why the relation should be quite as simple as that.

Eq. 3.2 is valid in the outer part of the tube, where axial transport of mass may be neglected; it equates the net transport by radial flow out of the volume element (left side) with the net diffusion, also in the radial direction, into the element (right side).

Diffusion acts towards the building-up of an equilibrium concentration gradient $Co/t \times N(1-N)\omega^2$; thus the diffusion current is outward (when N is the concentration of the heavy component) and tends to make $\partial N/\partial\eta$ positive. The radial inflow counteracts this diffusion; in chapter 4 the same takes

place with the total enthalpy; here, however, the transport by flow more than outweighs the diffusion in the outer region, but because the tangential velocity increases towards the centre (Re_r large in fig. 2.1) a reverse concentration gradient with $\partial N/\partial \eta < 0$ builds up with the result that a concentration maximum appears at intermediate radii (see fig. 3.1). The steeper the equilibrium gradient is, the higher the concentration peak and the less important the loss of heavy gas to the exhaust. It is seen that turbulence in this connection is harmful because it reduces the value of Co.

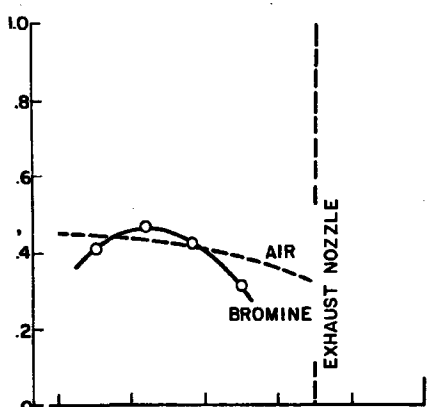

Fig. 3.1. Experimental bromine density as a function of non-dimensional radius $\sqrt{\eta}$. From Ragsdale, 1960. Estimated turbulent radial Reynolds number 2.1; peripheral tangential velocity $v_p = 1.4\ 10^4$ cm/sec; mole fraction of bromine $N_o = 3.7\ 10^{-3}$. The bromine density data would lie on the dashed line, were there no separation effect.

The position of the concentration peak is independent of the turbulence level, since it is determined by setting $\partial N/\partial \eta = 0$ in eq. (3.2), a condition which makes $\rho\varepsilon_n/(\rho D)$ disappear from the equation; however, the peak position is still a function of the laminar Reynolds number, so that, above a certain radial flow, the peak will be swept far enough towards the centre axis to be caught by the axial flow. This limit happens to be so low that the

tangential velocity profile, owing to the turbulence (low turbulent Reynolds number Re_r), cannot be brought close to the desired free vortex.

3.2. The Three-dimensional Distribution of Concentration

Eq. (3.2) in section 3.1 does not necessarily apply to the core region where the axial flow is strong; the reason is that the axial flow term neglected in (3.2) may be of greater importance than the radial term and thus the balance between transport by radial diffusion and by radial flow may be upset. In tubes with a peripheral exit this situation may apply to the whole of the tube as in the total-temperature case to be described in section 4.2. An equation analogous to eq. (4.3) that takes this possibility into account reads (Cohen, 1951) in non-dimensional form

$$\frac{\partial \psi}{\partial \xi}\frac{\partial N}{\partial \eta} - \frac{\partial \psi}{\partial \eta}\frac{\partial N}{\partial \xi} = \frac{\partial}{\partial \eta}\left[\frac{2\eta}{Re_n\sqrt{a}}\left(\frac{\partial N}{\partial \eta} - \frac{Co}{t}N(1-N)\omega^2\right)\right] + \frac{\partial}{\partial \xi}\left(\frac{\sqrt{a}}{2Re_n}\frac{\partial N}{\partial \xi}\right); \tag{3.6}$$

this expression equates the net transport by secondary flow of heavy component out of a volume element (left side) with the net accumulation in the volume element of the same component from radial and axial turbulent diffusion (the latter contribution will normally be of minor importance in vortex tubes).

In most cases, it is possible to treat $N(1-N)/t$ as a constant with the result that the partial differential equation (3.6) takes identically the form of the energy equation (4.3). It might therefore be solved by the methods of section 4.2 and the results would be qualitatively as in that work for a given secondary flow and tangential velocity distribution. There are, however, too few data of this kind for a test to be worth-while; instead, the conclusions drawn in section 4.2 may serve as a guide for the further discussion in this chapter.

The only results available are those of the low-pressure experiments by Mürtz and Nöller, 1961. These authors used a tube of the concurrent type (fig. 1.1c) with the flow left to distribute itself between centre exit and peripheral exit; the major part of the gas therefore leaves the tube through the latter (owing to the pressure gradient) and the tube thus belongs to the "weak-radial-flow" type. The pressure level in the tube was much reduced in order to make the flow laminar (see section 2.3). The pressure distribution shown in the paper indicates a forced vortex at all radii in

agreement with the tube's position, as calculated and shown in the diagram of fig. 2.3.

The authors assume in their calculations that radial equilibrium is attained in the tube, i.e. that

$$\partial N/\partial \eta = Co/t \times N(1-N)\,\omega^2 , \qquad (3.7)$$

and they proceed to discuss their data in terms of this equation. As shown in section 4.2 (for $\mu \ll 1$, a range which in view of the above data is the relevant one for the comparison), this is a correct procedure provided the radial flow is strictly zero. On the other hand, even a very small radial flow is able to level-off the distribution considerably (fig. 4.6) (see also the discussion in chapter 1); the comparison of the theory with experiment, made in the paper, shows quite clearly this effect at work, see fig. 3.2 where some of the data are reproduced.

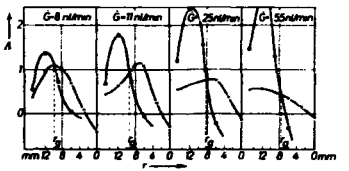

Fig. 3.2. Concentration gradients $A = \frac{1}{N(1-N)}\,dN/dr$ as a function of radius. From Mürtz and Nöller, 1961. Gas mixture $H_2/CO_2 = 1/3$. G, in litres at 1 atm. and 0°C, corresponds to $2\pi F$ in text. —x— experimental data and —o— calculated equilibrium gradients.

Mürtz and Nöller also studied the effect of the centre exit size. The flow in the tube does not have to change when this is changed, because the flow configuration is of the concurrent type; thus the concentration gradient may not be affected either. In agreement with this conclusion, the effect on the separation of varying the exit radius was found to be that which arose because smaller or larger core fractions were cut from the main stream.

As regards the effect of tube length on the gas separation, Mürtz and Nöller found a maximum at a certain length ($\eta_a = 0.15$, with $Ro \simeq 0.06$), which they attributed to the decay of tangential velocity. It is quite reasonable that this is the case in the concurrent tube used in the experiments; on

the other hand, a change in the secondary flow pattern may also be responsible, as it would be in tubes with counter-current flow (see section 5.3). The above effect of the axial gradient of tangential velocity was included in the treatment by Strnad, Dimic and Kuscer, 1961, through introduction of an exponential decay of tangential velocity along the tube; any close agreement between theory and their experiments (conducted at low pressure) was not to be expected, since, as also stated by the authors, the radial flow had been neglected.

3.3. The Over-all Gas Separation

Difficulties with the reproducibility of the separation results prompted Mürtz and Nöller (section 3.2) to reduce the pressure and thereby obtain laminar conditions. Other authors have had similar difficulties. In ref. I it was, however, shown that it is possible to obtain small well-defined gas separation effects in tubes at or above atmospheric pressure.

3.3.1. Experimental Results at Atmospheric Pressure

Most of these experiments were carried out with air, and oxygen concentrations were determined. The evidence that some separation does occur was first produced with a sensitive differential analyser working on chemical principles (Linderstrøm-Lang, 1960). Later a sensitive Beckman Oxygen Analyzer was utilized. This meter records changes in magnetic susceptibility with changing oxygen concentration. Differences in mole fraction of oxygen as small as 10^{-5} in the range from 0.209 to 0.210 can be detected; that is to say a difference in oxygen concentration of two flows measured within 3-5 minutes are reproducible to that extent. Typically, the concentration differences detected were $10\text{-}30 \times 10^{-5}$.

Vortex tubes of different designs were tested, including traditional Hilsch tubes (type a, fig. 1.1), but most experiments were conducted with type d tubes which had the additional feature (ref. I fig. 1) that peripheral exits at both tube ends (normally covered up) could be used if desired.

A number of design parameters were found to influence the net separation detected. In addition, the hot flow fraction θ ($= 1 - \mu$ with μ the cold flow fraction) had a decisive effect. Typical examples are shown in fig. 3.3.

The most conspicuous feature of the results of ref. I is that positive as well as negative separation effects with well-defined peaks are created in many cases (where a positive effect is characterized by a heavy "hot" exit stream (fig. 1.1d) i.e. a hot stream containing comparatively more of the heavy component than the light). Furthermore, when a vortex tube with a

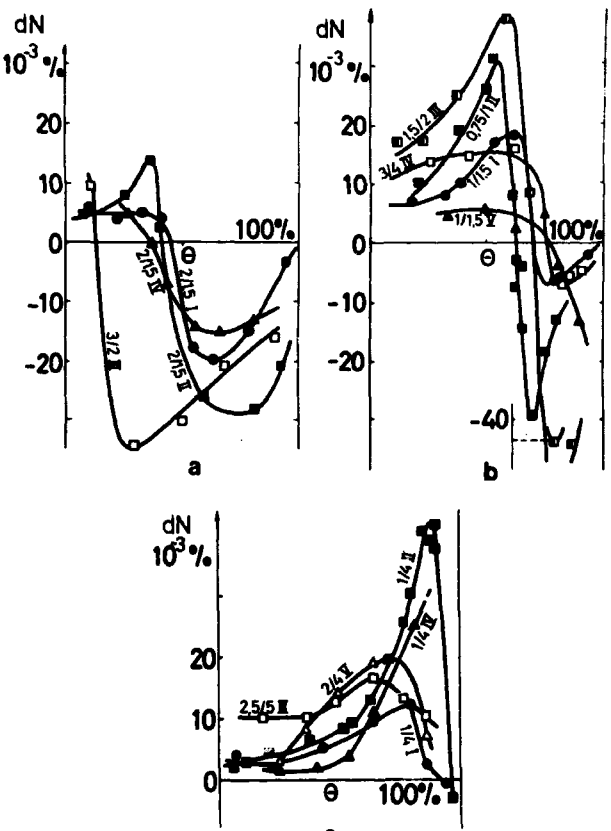

Fig. 3.3. Gas separation effect (in per cent) $dN = N_h - N_c$ as a function of "hot" flow fraction θ. From ref. 1, (cf. fig. 1.1d). Ratios indicate r_c/r_h (mm/mm). Circles $\overline{a}$ (based on tube length) = 1/2; squares $\overline{a}$ = 1/12; triangles $\overline{a}$ = 1/27. r_p = 0.5 cm; N(1-N) = 0.16.

certain set of design parameters produces effects of both signs, the positive effect always appears at low hot-flow fraction and the negative at high hot-flow fraction. The parameters that determine the shape of the curves such as those in figs. 3.3 were found to be 1) the ratio of the diameters of the two orifices, 2) the absolute sizes of the orifices compared to the tube diameter, 3) the length of the tube and 4) the throughput of gas, i.e. the size of the inlet nozzle diameter. The first three parameters will be discussed below, the fourth one in chapter 5.

The first parameter, the ratio of the orifice diameters, is of special interest, as a close correspondence between the deviation of this from unity and the asymmetry of the curves is found. Thus a large cold to hot orifice ratio extends the negative effect range, while a small cold to hot orifice ratio favours the range with positive effects. When the orifices are of the same size, the curve is fairly symmetrical about the point $\theta = 1/2$ and zero effect. In ref. I (fig. 6) this correspondence was shown to originate in the further feature that the point of effect cross-over (the point of zero effect) is closely correlated with the ratio of the flow capacities of the two exit ducts (as determined by their dimensions and by the conditions in the tube, notably the pressure gradient) when the valves at both ends are open. Since the closing of one or the other valve, i.e. departure from this intermediate state, necessarily leads to axial pressure gradients in the core region and therefore to changes in the axial flow pattern, it seems obvious that these changes are responsible in some way for the appearance of the complex effect curves.

The symmetry displayed by the results provides a strong case for the conclusion that the nozzle position is of only secondary influence and with this that the outer part of the tube contributes little to the gas separation effect. This conclusion is further supported by results obtained with the peripheral annular exits of the tube open (ref. I fig. 1) and a limited amount of gas withdrawn at the two ends of the tube in addition to the streams through the centre exits (see ref. I fig. 7). The concentration in the peripheral streams did not follow the typical pattern, and thus the characteristic effect curve is obviously a feature originating in the central part of the tube.

It is important to note, before an interpretation of these results is attempted, that two or more independent driving forces behind the separation could never lead to symmetries and correlations as described above and in ref. I; furthermore, that the separation takes place in a region removed from all walls, so that centrifugation (pressure diffusion) is the only cause of any probability, as has also been assumed in previous sections of this

chapter. Strong support for this conclusion is found in ref. 1, table 1, where good agreement is shown to exist between the tube separation potentials (see chapter 5) obtained with three gas mixtures of different chemical compositions.

3.3.2. The Flow Dynamic Basis

In search for a more detailed explanation, it was noted in ref. 111 that the diversion of flow into end-wall boundary layers, as described in chapter 2, leads to strong axial currents at intermediate radii where this flow is discharged into the tube. It was furthermore clear from the discussion by Rosenzweig, Lewellen and Ross, 1964, that discontinuities in the end-walls, especially that at the edge of the exit, increase the axial flow discharge from the boundary layer into the tube. Finally, it was shown by flow visualization experiments (Kendall, 1962, Rosenzweig, Ross and Lewellen, 1962, Ross, 1964a) that the axial flow moves in annular layers with a high degree of mixing within the layers but with little between them. On this evidence, it was concluded in ref. 111 that the basic secondary flow pattern in the vortex tubes considered, could be depicted as in fig. 3.4, for the case with both valves open. (It should be added that the model is not valid for tubes with large orifices where the centre flow is into rather than out of the tube.) It is readily seen that, according to this flow picture, radial mass diffusion between the streams does result in concentration changes ultimately detected as a net separation effect between the hot and cold streams.

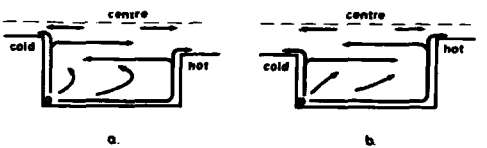

Fig. 3.4. Secondary flow patterns with axial flow at intermediate radii.

It should be noted that the explanation offered in ref. I differs somewhat from that of ref. III; the most important change is that originally concurrent systems were considered (see ref. I, fig. 11), while in the later paper the counter-current viewpoint was adopted. The main distinction is, in cases such as considered here, whether it is possible to identify an inner layer against an outer in a given stream and trace the layers separately past the point where they separate; if that is the case, it is the diffusion across the two layers in the stream that matters, and the concurrent viewpoint should be taken. If this is not possible, it is the diffusion across the boundary between streams that contributes most to the separation and the counter-current concept is the one to apply. In the present case the axial streams appear to be well-mixed, so that the latter point of view is the correct one to take (see fig. 3.5).

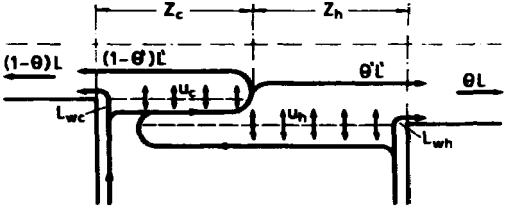

Fig. 3.5. Schematic representation of regions with separation, when both valves downstream of exit ducts are open ($\theta = \theta_o$). a. $r_c < r_h$; b. $r_c > r_h$.

The flow pattern in fig. 3.4 gives some indication of why the outer region of the tube is secondary as regards gas separation, since it seems quite likely that a large part of the separation there will be lost again by mixing on approaching the core region. However, this cannot be entirely true, as experiments where temperature effects were measured along with gas separation showed no close correlation. Thus, no temperature effect reversal (except in the shortest tubes) took place along with the gas separation reversal (see section 5.3 for a further discussion of these results), and yet the equations governing the two separation processes have almost the same form (compare eqs. (3.6) and (4.3); see also chapter 1). The only probable explanation is, on the one hand, that the direct flow into the exits

(fig. 3.4) must play some important part and, on the other hand, that conditions for temperature separation are better in the outer region than in the core of the tube. The latter conclusion entails that the effective turbulence level must be higher at the periphery than in the core; as discussed in section 5.3 this may be a reasonable proposition.

However, if this picture is to be correct and if the assumption below holds true that all concentration gradients are small enough to be independent of the turbulence level (see eq. (3.8)), the low efficiency of the outer region as regards gas separation can be understood only, if the results of chapter 2 are taken into account as well, i.e. that the tangential velocity, in the tubes of interest, increases towards the centre with a maximum close to the exit radius, so that also the driving force of the diffusion (eq. 3.6) is largest there (see section 5.3).

Eq. (3.6) might in principle, as discussed in section 3.2, be used for a calculation of the concentration gradients encountered, provided experimental secondary flow patterns were available. Although it might be possible to devise a reasonable flow pattern in the case shown in fig. 3.4, f. ex. on the basis of the data in Reynolds, 1962, this would not be sufficient, since these only apply to the case where both valves of the tube are open, while the object of a theoretical study of the effect curves (fig. 3.3) must include the changes in the axial flow caused by the closing of the valves.

3.3.3. The Approximate Diffusion Equation

Because of these difficulties, a much cruder approach was adopted in ref. III. The secondary flow was represented by systems of counter-current units such as shown in fig. 3.5; it was assumed that the radial flow between two counter-flowing streams is zero, and that the flow rate in all streams is so large that appreciable radial concentration gradients nowhere are able to develop (and that axial diffusion gives a negligible contribution). With these approximations eq. 3.6 is reduced to

$$-\partial\psi/\partial\eta \quad \partial N/\partial\xi = \frac{\partial}{\partial\eta}\left[\frac{2\eta}{Re_n\sqrt{a}}\ \frac{Co}{t}N(1-N)\omega^2\right]; \qquad (3.8)$$

this may be quite a reasonable approximation provided the flow rates in all streams are high, since then (as discussed in section 4.2 and ref. IV for large cold flow fraction; see also chapter 1) radial gradients are likely to be small (this also implies that a small radial flow does not disturb the separation process appreciably).

Eq. (3.8) may be integrated with respect to η (after introduction of the continuity equation, which here reads $\partial^2\psi/\partial\xi\partial\eta = 0$) to give

$$\partial(\bar{N}\Delta\psi_{12})/\partial\xi \left(\equiv \partial\left[\int_1^2 N\partial\psi/\partial\eta d\eta\right]/\partial\xi\right) = -\frac{2}{\sqrt{a}}\frac{Co}{Re_n^t} N(1-N)\left[(\eta\omega^2)_2-(\eta\omega^2)_1\right] \tag{3.9}$$

$\bar{N}$ is the average mole fraction of the heavy component in the stream and $\Delta\psi_{12}$ the flow rate (non-dimensional), while $\eta\omega^2$ with subscripts 1 and 2 are the tangential velocities at the two radial boundaries; $N(1-N)/t$ is considered as constant. Co/Re_n, which does not contain the turbulent diffusivity (cf. eq. 3.1), may be calculated from a knowledge of the diffusion coefficient. The tangential velocity is assumed to be independent of the axial position; thus integration of eq. (3.9) with respect to ξ gives

$$\Delta\bar{N}\Delta\omega_{12} = -2\frac{Co}{Re_n^t} N(1-N)\frac{\Delta\xi}{\sqrt{a}}\left[(\eta\omega^2)_2 - (\eta\omega^2)_1\right] , \tag{3.10}$$

an equation which relates the mean concentration change ΔN of the heavy component of the stream over the tube length $\Delta\xi$ to the radial diffusion of the component through the radial boundaries of the stream over the same length.

3.3.4. The Flow Dynamic Model

In order to proceed with the calculation, material balance equations for each component must be introduced; for that purpose it is necessary, as was done in ref. III, to specify the secondary flow pattern under various conditions. This remains a somewhat arbitrary process, though a certain number of criteria have to be met before any choice can claim to be physically relevant. Some experimental tests are also possible: Thus if the pattern in fig. 3.5, which depicts conditions with both valves open, is to be correct there must be competition between the two regions with separation and, dependent on the relation between the lengths of the two zones and that between the tangential velocities at the separating boundaries, either stream may become enriched in, say, the heavy component; end-wall conditions will therefore determine the sign of the effect found, in such a way that increase in the axial flow from an end-wall boundary layer will tend to increase the length of the nearby zone. Experimentally such an increase was established in two ways, either by placing steps on the end wall at intermediate radii in the form of lumps of glue (see ref. III, fig. 4) or by

replacing the end wall orifice by a coaxial tube, of the same diameter as the exit, reaching into the tube (ref. I, fig. 8); this tube is likely to promote an axial flow along it's outer surface. In all cases (where the flow pattern as such did not change radically by the modification, i. e. in cases where the orifices were comparatively narrow) the expected change (see above) in the separation effect occurred. Thus, to this point the model is probably quite realistic.

When one valve is partly closed, a pressure increase in the corresponding exit duct results; this must be felt more strongly at the centre than at the periphery of the exit duct. Indeed the flow will be quite easily stopped and reversed near the centre before any large change in the flow fraction has taken place; this will lead to a shift of the stagnation point on the axis towards, and perhaps into, the partly closed exit duct, as indicated in fig. 3.6. The flow reversal at some distance from the axis may not be much affected, and thus a third counter-current system may appear as indicated in the figure. This idea was developed in ref. III on the basis of various assumptions which, necessarily in a crude fashion, were brought into relation with accessible tube parameters. The main purpose was not to give an accurate description of the processes occurring, but rather to enable a discussion on a reasonably realistic basis of the origin of the complex experimental results. That this goal was in fact achieved, is indicated

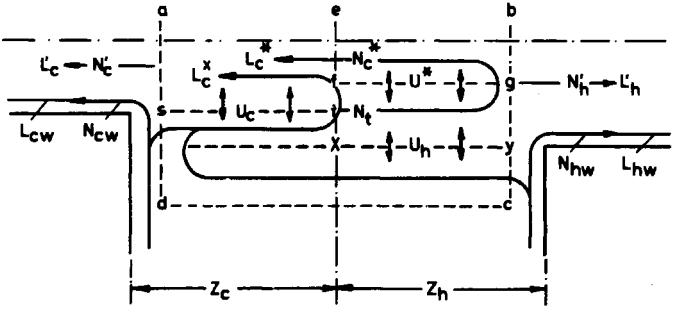

Fig. 3.6. Schematic representation of region with separation when valve downstream of "hot" exit duct is partly closed ($0 < \theta_o$). Lettering a, b, c, ... defines the control volumes used in appendix.

by the fact that the theory both reproduced qualitatively, as described below, all pertinent features and gave results of the experimental order of magnitude (with the use of available experimental data) (ref. III).

The derivation of the pertinent equations has not been given in detail before; it is therefore included as an appendix in order to facilitate the understanding of the model.

3.3.5. Comparison with Experiment and Interpretation of the Results

The results of the parameter study carried out in ref. III are shown in figs. 3.7, 3.8, 3.9. In fig. 3.7 the effect of varying the ratio of the orifice diameters is studied. A comparison with fig. 3.3 shows that all essential features of the curves are well reproduced. These results may therefore be interpreted with some confidence in terms of the model. For that purpose it is essential to note that the capacity of the exits is proportional to

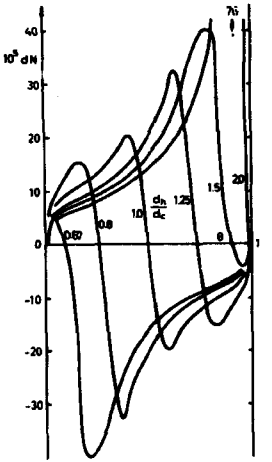

Fig. 3.7. Calculated gas separation, $dN = N_h - N_c$ as a function of "hot" flow fraction θ. Influence of ratio of "cold" to "hot" orifice diameters, d_c/d_h. From ref. IIIb. $\bar{a}$ (based on tube length) = 1/12; $(r_c + r_h)/r_p$ approx. 0.4; r_p = 0.5 cm; n (in $v \propto r^n$) = -0.5; m (in $\theta_o/(1-\theta_o) = (r_h/r_c)^m$) = 4; $N(1-N) = 0.16$.

the radius raised to a power, m, that is considerably greater than one (due to the presence of the radial pressure gradient); this is evident from the finding that the hot flow fraction with open valves is a very sensitive function of the orifice diameter ratio. Furthermore, that axial momentum considerations indicate that the intensity of the outflow at a given radius in an exit is proportional to r to the same power (in fig. 3.3 the exponent m is set equal to 4). This means that the third separating surface $r = r^{*}$, referred to in the discussion of fig. 3.6, moves quickly away from the centre axis when minor deviations occur from the hot flow fraction ϑ_o where both valves are open. Since the changing of ϑ in one or the other direction from ϑ_o means the appearance of opposite axial pressure gradients and, accordingly, oppositely directed third separating zones, it is clear why the experimental effect curve, when ϑ is made to increase from below ϑ_o to above this value, passes quickly from a large positive to a numerically large negative value. The return to zero or small effects at low and high ϑ is, according to the model, caused by the contributions from the end-wall flows which gain in importance in these cases. Experimental support for the latter conclusion is found in the experiments with peripheral exits, referred to earlier in this chapter (ref. I, fig. 7), where the concentrations of the "hot" centre and peripheral streams were found to be almost identical when the hot flow fraction approached zero, while the same tendency was at work for the cold stream at hot flow fractions close to one.

The shift of the cross-over point with orifice diameter ratio is, according to the model, related to the fact that this point must, in view of the rapid reversal of the axial flow represented by the widening of the r^{*} surface, remain close to ϑ_o, the value where both valves are open. Furthermore, since ϑ_o is a very sensitive function of the orifice diameter ratio, so is the cross-over point. The concomitant shift in the relative magnitude of the maximum and minimum reflects the facts that the displacement of the cross-over point away from the midpoint ($\vartheta_o = 1/2$), say, towards $\vartheta_o \simeq 1$ prevents the negative effect from developing owing to the increased influence of the cold-end boundary-layer contribution, and enhances the maximum, which then occurs at ϑ close to one (but nevertheless at $\vartheta < \vartheta_o$), because diffusion into a stream is felt more strongly when this, the cold stream in this case, is small.

Fig. 3.8 shows the effect of the width of the orifices compared to the tube diameter on the separation curves; it was found in ref. I that the numerical values of both the maximum and minimum increase with decreasing

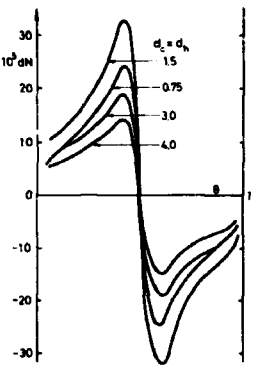

Fig. 3.8. Influence of ratio of exit radii to tube radius. Calculated gas separation dN as a function of "hot" flow fraction θ. $r_c/r_p = r_h/r_p$ varied from 1.5/10 to 4/10. Other data as in fig. 3.7.

orifice diameters until a certain point below which the trend is reversed. The interpretation, based on the results of ref. III, is that the maximum tangential velocity, located close to the exit radius (see above), moves in with decreasing exit diameter, while at the same time its absolute value increases until the orifices are so narrow that their flow capacity becomes the limiting factor for the throughput; this leads to a drop in inlet nozzle velocity below sonic and then to a drop in tangential velocity level in all parts of the tube.

Fig. 3.9 reproduces the result reported in ref. I that the tube length has a profound effect on the separation curve. The most efficient separation is found in comparatively short tubes. This is, according to the model, to be attributed to the change in velocity profile mentioned in section 2.2, i.e. to an increase of n, where $v \propto r^n$, with increasing tube length, a change that eventually leads to a considerable drop in the tangential velocity at intermediate radii. In long tubes the typical effect curve pattern disappears; in fig. 3.9 this change is brought into relation with the concomitant reduction of the pressure-gradient at intermediate radii (towards that corresponding to the forced vortex) through a suitable reduction of the exponent m,

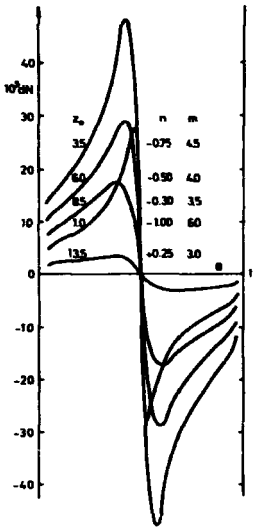

Fig. 3.9. Influence of ratio ($\sqrt{a}$) of tube radius to tube length. Calculated gas separation dN as a function of "hot" flow fraction θ. $\sqrt{a}$ (= r_p/z_o) varied from 1/7 to 1/27. $r_c/r_p = r_h/r_p = 1/10$; $r_p = 0.5$ cm.

on the ground that a low radial pressure gradient tends to produce an outflow that is uniformly distributed across the exits; the evidence in the figure for this interpretation is, however, inconclusive. It seems more likely, as discussed in section 5.3, that the axial flow pattern changes and becomes much more diffuse when the tube becomes long enough.

A quantitative test of the present theory is described in ref. III.

4. THE TOTAL TEMPERATURE DISTRIBUTION AND THE ENERGY SEPARATION

Numerous investigations of the vortex tube as a temperature separator has been published over the years; a detailed account of the early history has been given by Fulton, 1950, while the two bibliographies, Westley, 1954, and Dobratz, 1964, cover the period up to 1963; later references are given below and in section 6.3.

The widespread interest in the tube has prompted several detailed experimental investigations of the temperature distribution within the tube, as well as a number of theoretical treatments.

It was early recognized that both transport of heat by conduction and transport of kinetic energy by friction might contribute to the energy separation represented by the net temperature difference detected between the outgoing streams. It was also early recognized that without turbulence in the tube there would not be sufficient time for any appreciable separation to take place. The turbulent energy equation should therefore form the basis for discussion and calculations. In order to make the problems in connection with the solution of this equation tractable it has been necessary to reduce its complexity. This has been done either on the basis of analogies to the laminar case, replacing laminar by turbulent parameters, or (Reynolds, 1961, and Bruun, 1967, 1969) through an order of magnitude analysis of the different turbulent terms. In the latter case, to make the equation amenable to calculations, it has been necessary to interpret the remaining turbulent contributions in terms of turbulent viscosity and turbulent thermal diffusivity. The results of the two approaches may therefore be closely related, as is true of the Deissler and Perlmutter equation in section 4.1 and the energy equation in 4.2.

The interpretation of the remaining turbulent contributions is not unambiguous. Kassner and Knoernschild, 1948, were the first to discuss these problems in connection with the vortex tube. The most important questions to settle are the shapes taken by the radial equilibrium gradients of tangential velocity and of static temperature in a turbulent tube. As regards the first problem, it has been generally accepted (and was tacitly so in chapter 2) that the turbulent transport of momentum, i.e. transport through the motion of fluid lumps in the velocity field, is sufficiently akin to the molecular process in the laminar case that the same equilibrium gradient, i.e. a forced vortex (with $v \propto r$), is approached in both cases; experimental vortex tube results, as discussed in the various parts of the present

work, certainly all point in that direction. The problem in case of the turbulent transport of thermal energy is not so clear, because pressure changes in a gas are necessarily accompanied by temperature changes. Kassner and Knoernschild, 1948, appear to have been the first to argue that the radial equilibrium gradient of static temperature in the turbulent case is the adiabatic gradient and not the isothermal gradient found in the laminar case. This point of view finds support in meteorological observations of large-scale turbulence in air. The evidence in case of the vortex tube cannot be said to be conclusive, though in the calculations to be described in section 4.2 (ref. IV), it was found difficult to reconcile experiment and calculated results with the use of an isothermal equilibrium condition; however, the accuracy obtained was limited, owing to the influence of the badly determined radial flow.

Previous treatments have focussed on different aspects of the development of the temperature separation. The purely two-dimensional approach, analogous to the treatments in sections 2.1 and 3.1, is here represented by the work by Deissler and Perlmutter, 1960; it will be described briefly in 4.1. Most other studies have attempted to account for the axial development (presumed to exist or measured) in one of two ways: 1) Either by viewing the tube as a concurrent system in which it is possible to trace the path of the air stream filling the space between centre and periphery, and moving in a spiral away from the nozzle region. The point of view is Lagrangian, and the methods known from channel flow may be applied (Kassner and Knoernschild, 1948, Fulton, 1950, Hartnett and Eckert, 1957, Lay, 1959, Sibulkin, 1962, Takahama, 1965). 2) Or, by viewing the vortex tube as a counter-current system akin to a heat exchanger (Gulyaev, 1966, Scheper, 1951, Suzuki, 1960, and ref. IV).

The Lagrangian point of view has severe limitations owing to the existence of a significant counter flow in the core region in all cases; the same difficulty arises in the mass separation case discussed in section 3.3. The counter-current concept has a better prospect of success, the more so as concurrent phenomena may be included simply by changing the sign of certain parameters. The subsequent discussion will therefore be based on this concept.

It is clear from what was said above that any treatment, in order to be successful, must take into account the transport of both heat and kinetic energy. Some of the previous counter-current descriptions have been incomplete in this respect. Furthermore, some have failed to recognize that the equilibrium condition is not total-temperature equality between the two streams.

In order to reduce the complexity of the computations, some kind of integral procedure is desirable. This has been set up in some cases by ascribing to each stream a mean total temperature (or, less satisfactorily, just a mean static temperature) and by making estimates of or assumptions on the rate of heat (and kinetic energy) transfer across the boundary between the streams. In this way the mathematical treatment becomes identical to that valid for a heat exchanger or rather, in the correct approach, a chemical column system such as a distillation column (see fig. 4.3). This method as applied to mass separation was used in ref. III (see chapter 3.3).

In ref. IV an integral equation of a different kind was obtained. It is based on an approximate solution to the energy equation that eliminates the radial coordinate according to a procedure previously employed for mass separation in two-component gas mixtures in rotating flow (Cohen, 1951). The resultant equation is a first order differential equation in the axial coordinate with the total-temperature as the dependent variable; the form of the equation is found to be identical to that of the governing equation for a distillation column (and equivalent to the corresponding equation for a heat exchanger), but the parameters in it have a more complex meaning. The advantage of the method, as it is developed in ref. IV, is that sufficient information is embodied in the first order differential equation so that an approximation not only to the axial but also to the radial total-temperature gradients is obtained as a result of the calculations. A discussion of the solution with interpretations of experimental results on temperature distributions will be carried out in section 4.2.

The possibility of predicting the net temperature effects measured between the outgoing streams on the basis of the model in section 4.2 will be briefly treated in section 4.3.

4.1. The Radial Distribution of Total Temperature

Deissler and Perlmutter have based their two-dimensional treatment of the temperature separation on their study of the tangential velocity distribution described in section 2.1, with the use of the same simple radial flow function as was employed there. Their energy equation reads

$$\rho u r \frac{d\tilde{T}}{dr} + \rho u r \frac{1}{2c_p}\frac{d\tilde{v}^2}{dr} = \frac{d}{dr}\left[r\rho\varepsilon_h\left(\frac{d\tilde{T}}{dr} - \frac{1}{c_p}\frac{\tilde{v}^2}{r}\right) + r\rho\varepsilon\,\frac{v}{c_p}\left(\frac{d\tilde{v}}{dr} - \frac{\tilde{v}}{r}\right)\right] \quad (4.1)$$

where $\tilde{T}$ is the static temperature, and ε_h and ε are turbulent diffusivities. This in non-dimensional form becomes

$$\frac{\partial t}{\partial \bar{z}} + \frac{Ec}{2}\frac{\partial v^2}{\partial \bar{z}} = \frac{\partial}{\partial \eta}\left[\frac{2\eta}{Re_h\sqrt{a}}\left(\frac{\partial t}{\partial \eta} - \frac{Ec}{2}\frac{v^2}{\eta}\right) + \frac{2\eta}{Re\sqrt{a}}\left(\frac{Ec}{2}\frac{\partial v^2}{\partial \eta} - \frac{Ec}{2}\frac{v^2}{\eta}\right)\right] \qquad (4.2)$$

The notation of chapter 2 has been used with the addition that $t \equiv \vartheta/T_\infty$, where T_∞ is the temperature (total temperature) of the supply gas before expansion and acceleration. $Re_h\sqrt{a} = F/(\varepsilon_h i) = F/(\mu r_p)\sqrt{a}$ (where F here is based on mass flow, rather than on volume flow as in chapter 2; $\bar{z}$ is changed accordingly) is the thermal Reynolds number (Peclé number). $Ec = v_{po}^2/(c_p T_\infty)$ is an Eckert number, which is a measure of the fraction of internal energy converted into kinetic energy.

The calculations provide radial distribution curves of total-temperature which are the results of a balancing between transport of total enthalpy by radial inflow and by outward turbulent diffusion. Deissler and Perlmutter tested their theory on the data of Hartnett and Eckert and found it satisfactory. The fitting provided a most-probable value for the thermal Reynolds number, which was compared with the value of the corresponding Reynolds number obtained by fitting the authors' theoretical tangential velocity profile to Hartnett and Eckert's experimental data (see chapter 2.1). The same procedure was used in ref. 1Vc on the same data, and with an equally reasonable result. Admittedly, the discrepancies found in the two cases went in opposite directions, although the treatments, at the cold flow fraction in question, are not much different; the use of different radial flow functions (zero core flow in Deissler and Perlmutter's case) have undoubtedly caused this disagreement.

4.2. The Three-dimensional Distribution of Total Temperature

It is a general feature of the total-temperature distributions obtained experimentally by various authors that they can be represented by a series of smooth radial curves shifting in a uniform manner along the tube (see figs. 4.1b and 4.2b). It is furthermore a characteristic feature that the cold flow fraction to a large extent determines the pattern, so that curves with steep radial gradients and little axial variation in the outer part of the tube appear when μ is small, while rather level curves with an appreciable axial shift are produced when the cold flow fraction is increased sufficiently ($\mu > 0.5$). The origin of this effect has already been mentioned in the introduction (chapter 1); in the present section it will be discussed in more detail.

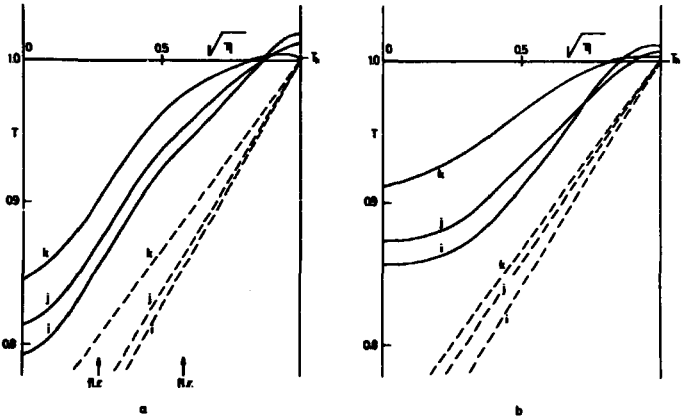

Fig. 4.1. Total temperature T as a function of radius ($\sqrt{\eta} = r/r_p$). Comparison of calculated and experimental distributions at cold flow fraction $\mu \simeq 0$, for $\zeta = 0.06$(i), $\zeta = 0.34$(j), and $\zeta = 1.0$(k). From ref. IV (fig. 9). $Ec_{calc.}$ chosen to give same mean equilibrium total-temperature gradients gradients (dashed lines) in figure a and b. Pr = 1. Ratio of tube radius to length of region I, $\sqrt{a} = 1/12$ (cf. fig. 2.5).

a. Calc. case 382; $\mu = 0.02$.
Reynolds number $Re_h\sqrt{a} = 20$; ratio of radial flow within region I (at s_o-surface) to total flow $Re_{hr}/Re_h\sqrt{a} = 0.12$; $\sqrt{\bar{r}_b} = 0.58$.

b. Exp. case I, Hartnett and Eckert, 1957; data as in table 2.1, with $2\pi F = 336$ g/sec and Ec = 0.20.

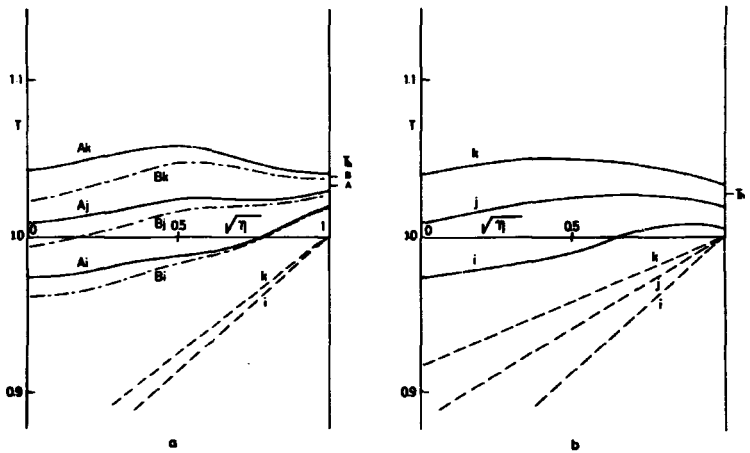

Fig. 4.2. Comparison of calculated and experimental distributions at $\mu = 0.49$ for $\xi = 0.17$(i), $\xi = 0.59$(j), and $\xi = 1.0$(k). Dashed lines indicate mean equilibrium total-temperature gradients (adjusted as in fig. 4.1). From ref. IV (fig. 11). $\sqrt{a} = 1/14.5$, $Pr = 0.7$.

a. Calc. case 480, $\Delta T_h (= T_p(1) - T_h) =$ (A-curves) 0.01, = (B-curves) 0. $Re_h\sqrt{a} = 3.5$; $Re_{hr}/Re_h\sqrt{a} = 0.16$, $\sqrt{\eta_0} = 0.63$.

b. Exp. case VIII, Scheller and Brown, 1957; data as in table 2.1, (p. 32) with $2\mu F = 14\,g/sec$ and $Ec = 0.15$.

4.2.1. The Approximate Energy Equation

It is clear from the above introductory remarks on the experiments that the two-dimensional theory of the previous section does not suffice when μ is large and appreciable axial gradients exist. It then becomes necessary to include axial flow terms in the energy equation. This was done in ref. IV on the basis of the turbulent energy equation and by use of the results of Reynolds, 1961, and Bruun, 1967, 1969, who has investigated the relative importance of the various terms in that equation under specified conditions; the resultant equation reads (in non-dimensional form)

$$\frac{\partial\psi}{\partial\xi}\frac{\partial T}{\partial\eta} - \frac{\partial\psi}{\partial\eta}\frac{\partial T}{\partial\xi} = \frac{\partial}{\partial\eta}\left[\frac{2}{Re_h\sqrt{a}}\eta\left(\partial T/\partial\eta - \partial T_{eq}/\partial\eta\right)\right] \qquad (4.3)$$

where

$$\partial T_{eq}/\partial\eta = Ec\left[\omega^2 + ((1-Pr)/2)\times\eta\partial\omega^2/\partial\eta\right]. \qquad (4.4)$$

Here ω is the non-dimensional angular velocity based on $\omega_{po} = v_{\mu o}/r_p$. Pr is the turbulent Prandtl number. T is the non-dimensional total temperature $T \equiv \tilde{T}/T_\infty$ which on the right side of eq. (4.3) is approximated by

$$T = \tilde{T}/T_\infty + Ec/2\times(\tilde{v}/v_{po})^2 , \qquad (4.5)$$

an approximation, which amounts to neglecting in T both the kinetic energy of the secondary motion and that in the turbulent modes. The error may become serious, close to the axis when the cold flow fraction, μ, is large, otherwise it should be at most a few per cent.

Eq. 4.3 could also have been obtained in way similar to that employed by Deissler and Perlmutter for the derivation of eq. (4.2) in section 4.1.

Eq. (4.3) equates the net transport of total-enthalpy carried into a volume element by the secondary flow with the net accumulation of total enthalpy in the element due to radial turbulent diffusion. Axial diffusion terms are neglected because they are found to be of minor importance, even in cases with appreciable axial gradients.

The second term on the right side of eq. (4.3) is written $\partial T_{eq}/\partial\eta$ to denote that this term determines the equilibrium total-temperature gradient, i.e. the gradient in the (hypothetical) case that the secondary flow has no influence on the total-enthalpy transport.

A test of the energy equation (4. 3) is possible when all terms are known from experiment. Such tests were carried out in connection with the work presented in ref. IVc, for selected tube cross-sections, of which one example is shown in the report. The fit is by no means perfect, but this is not surprising in view of the serious approximations made. Two errors may, as discussed in ref. IVc, cause the discrepancy: 1) the radial diffusion term on the right side of (4. 3) does not cover all total-enthalpy transport by turbulent diffusion near the centre, and 2) the turbulent transport of fluid in the radial direction is not wholly adiabatic, but some exchange of heat takes place during the turbulent displacement of a fluid lump. The test when applied to the data of Bruun, 1967, in a cross-section near the nozzle, was even less satisfactory than the above-mentioned example; however, conditions there were peculiar for other reasons also, as mentioned in the discussion of fig. 1 in ref. IVc.

4. 2. 2. The Method of Solving the Equation

In order to proceed with the calculation, the fact that the total enthalpy is preserved within the tube must be introduced; this was done in ref. IV through the following energy balance equation (in non-dimensional form)

$$\int_0^1 \psi \partial T/\partial \eta d\eta - \int_0^1 \frac{\sqrt{a}}{2Re_h} \partial T/\partial \xi d\eta = \psi_h (T_p - T_h), \qquad (4.6)$$

ψ_h is the hot flow fraction; T_p is the total temperature at the periphery of the cross-section; and T_h is the total temperature of the hot gas. It has been assumed in eq. (4. 6) that diffusion through the peripheral boundary of the region considered (region 1, fig. 2. 5) can be neglected. The equation expresses the fact that the total enthalpy is preserved within the cylinder a-a (fig. 2. 5) limited by an arbitrary tube cross-section, the periphery, and the hot end of the tube.

The second term on the left of (4. 6) is the contribution from axial diffusion of total enthalpy through the cross-section; this is of minor importance and is included only in order to enable a discussion later of certain limiting cases (a possible deviation of Pr from one has been neglected in this term).

In solving equations (4. 3) and (4. 6), it was assumed in ref. IV that the secondary flow functions and the tangential velocity distribution were known as functions of η and ξ. In the computations the distributions devised and calculated in ref. IV (see chapter 2. 3) were used. The exact form chosen

for these functions is found not to be very important in the present context, since the solution obtained does not contain higher than first order derivatives. Thus, the fact that the calculations in section 2.3 refer to incompressible flow while the present study necessarily involves compressibility effects is not of primary importance here.

The energy equation, with the secondary flow and tangential velocity functions introduced and ξ kept constant, may be written as a first order differential equation in $\eta\partial T/\partial\eta$, which has the following formal solution

$$\eta\frac{\partial T}{\partial\eta} = \Phi(\eta)\left[\int_0^{\eta}\frac{1}{\Phi(\eta')}\left(-1/2\,\mathrm{Re}_h\,\alpha\,\frac{\partial\psi}{\partial\eta'}\frac{\partial T}{\partial\xi} + \frac{\partial}{\partial\eta'}\left(\eta'\frac{\partial T_{eq}}{\partial\eta'}\right)\right)d\eta'\right] \quad (4.7)$$

where

$$\Phi(\eta) \equiv \exp\left\{\int_0^{\eta}\mathrm{Re}_h\,\alpha/(2\eta')\times\partial\psi\,\beta\xi\,d\eta'\right\} \quad (4.8)$$

and where the boundary condition $(\eta\partial T/\partial\eta)_{\eta=0} = 0$ has been introduced This solution may be used to eliminate $\partial T/\partial\eta$ in (4.6). In the resultant equation only $\partial T/\partial\xi$ and T_p remain undetermined.

As a next step in the procedure a reasonable assumption about the radial dependence of $\partial T/\partial\xi$ has to be made, so that, with this introduced, integration with respect to the radial coordinate can be carried out; Cohen, 1951, in the mass separation case, took $\partial N/\partial\xi$ to be independent of η, here a linear relationship is assumed, i.e.

$$\partial T/\partial\xi = [1 + E(1-\eta)]\,dT_p/d\xi \quad (4.9)$$

where $dT_p/d\xi$ is the axial gradient of total temperature at the periphery. E is a constant, which has to be determined by some averaging procedure. Reference to experiment, which generally shows $\partial T/\partial\xi$ to depend on η in quite a regular and uniform manner, shows expression (4.9) to be a promising one from the physical point of view. As the computations show (see ref. IVb, fig. 1), the expression is quite satisfactory from the mathematical point of view as well, i.e. the inconsistency introduced by assumption (4.9) is quite small in many cases.

Introduction of (4.9) into the above mentioned combination of 4.8 and 4.6 leads to a first order differential equation in T_p with ξ as the independent variable, as follows

$$d(T_p-T_h)/d\xi = -\frac{\phi_h}{c_5}(T_p-T_h) + \frac{c_1}{c_5} \quad (4.10)$$

where c_5 and c_1 are functions of ξ only (see ref. IV, eqs. (26), (27), and (28)); in the special case that both ψ and ω are independent of ξ, i.e. that the radial flow and the axial tangential velocity gradient are both negligible, c_1 and c_5 are constants, as follows (with Pr = 1)

$$c_1 = Ec \times \int_0^1 \psi\omega^2 \, d\eta \tag{4.11}$$

$$c_5 = \frac{Re_h r_a}{2} \int_0^1 \frac{\psi}{\eta} \left[\int_0^\eta \frac{\partial \psi}{\partial \eta'^2} (1 + E(1 - \eta')) \, d\eta' \right] d\eta + \frac{r_a}{2Re_h} \int_0^1 (1 + E(1 - \eta)) d\eta \tag{4.12}$$

In this simple case, the solution of (4.10) is straight forward, leading to

$$T_p - T_h = \left[1 - \exp \left\{ (1 - \xi)\psi_h / c_5 \right\} \right] c_1 / \psi_h \tag{4.13}$$

where, as an example, the boundary condition $T_p(1) - T_h = 0$ has been introduced. Any value selected for $T_p(1)$ is in fact acceptable from the mathematical point of view, so that $T_p(1) - T_h$ may be used as an adjustable parameter to make theory fit with experiment.

Provided an acceptable value for E can be found, equation (4.13) (or the complete version in ref. IV) is seen to render possible a calculation of the peripheral total temperature along the tube. On the same condition and by means of the expression for $\eta \, \partial T / \partial \eta$, T in any part of the tube may be determined. Thus, if the mathematical solution is to be acceptable, it is necessary that the axial total-temperature gradients found in this way match "reasonably" well those determined by (4.9); in ref. IV it was argued that this correspondence may be ensured by setting

$$\bar{E} = - \frac{\int_0^1 \left[\left(\frac{\partial T}{\partial \eta} \right)_{\xi=1} - \left(\frac{\partial T}{\partial \eta} \right)_{\xi=0} \right] d\eta}{T_p(1) - T_p(0)} \tag{4.14}$$

It should be noted that even when this approximation is successful from the mathematical point of view, there is still no guarantee that the solution will also be of physical interest; the reason is that the method leaves no possibility of specifying the radial temperature distribution at the axial

boundaries in any detail nor the temperature gradient at the peripherey. However, it was generally found in the computations of ref. IV that the resultant boundary functions are quite closely related to experiment. Furthermore, that a meaningful comparison may be made, even though the set of boundary conditions derived in the calculations does not exactly match those of the experiments.

Analytic details are presented in ref. IVb.

4.2.3. The Distillation Column Analogy

It is helpful for the understanding of the functioning of the vortex tube, as already mentioned in the beginning of the present chapter, to recognize that the tube may be viewed as a generalized type of heat exchanger with total enthalpy transported and conserved. A special feature of the transport is, as also mentioned, that equilibrium between the two streams does not imply temperature equality but a total temperature difference determined by the pressure gradient (the tangential velocity). The system therefore resembles chemical separation units such as distillation columns (see fig. 4.3). This fact is emphasized in the solution represented by eq. (4.10) which has the same form as the corresponding differential equation for a distillation column. In ref. IV it was shown that the column parameters equivalent to c_1 and c_5 read (see fig. 4.3 for the meaning of the symbols)

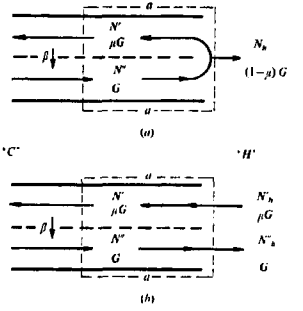

Fig. 4.3. Diagrams of counter-current systems. a. Distillation column; b. heat exchanger or extraction column.

$$c_1^{\mathbb{K}} \equiv \mu\beta \tag{4.15}$$

$$c_5^{\mathbb{K}} \equiv \mu G/K \tag{4.16}$$

β is a measure of the equilibrium condition, $(N' - N'')_{eq} = \beta$, and G/K measures the ratio of flow rate to specific rate of transverse diffusion.

Thus, using the analogy with the vortex system, we may write for the cases shown in fig. 4.3 (compare eq. 4.13)

$$N'' - \bar{N}_h = \left[\exp\left\{(z-z_o)\frac{K}{G}\frac{1-\mu}{\mu}\right\} - 1\right]\frac{\mu}{1-\mu}\beta \tag{4.17}$$

This equation could have been derived (as shown in ref. IV) from the following two equations, corresponding to (4.3) and (4.6), respectively

$$G\frac{dN''}{dz} = -K\left[(N'' - N') - \beta\right], \tag{4.18}$$

and

$$N'' = N'\mu + (1-\mu)\bar{N}_h \tag{4.19}$$

Furthermore, either of these equations, together with (4.17), may be used to obtain N' as follows

$$N' - \bar{N}_h = \left[\exp\left\{(z-z_o)\frac{K}{G}\frac{1-\mu}{\mu}\right\} - 1\right]\frac{1}{1-\mu}\beta \tag{4.20}$$

The last step corresponds closely to that made in the vortex tube case, when the radial distribution of total temperature is calculated on the basis of (4.7) and (4.13).

4.2.4. Discussion of the Calculations

With the equivalence between the two systems established, conditions in the vortex tube, as determined by various pertinent parameters, may be discussed in terms of the corresponding column parameters.

As regards $c_1^{\mathbb{K}} \equiv \mu\beta$ (equivalent to c_1, eq. (4.11)) it is immediately clear by inspection of eqs. (4.17) and (4.18) that both the transverse N-difference and the longitudinal gradient of N are proportional to $c_1^{\mathbb{K}}$ (and to β). This implies that all gradients vanish when β is zero; conversely, that the concentration jump β ($\neq 0$) across the boundary between the two streams at equilibrium is a necessary condition if separation is to take place. The same is true of the total-enthalpy separation in the vortex tube

as regards Ec, to the extent that centrifugation is the cause of all separation. On the other hand, the total-temperature gradients in the tube do not have to be proportional to Ec (as erroneously stated in ref. IV), the reason being that the proportionality in the distillation case results because the boundary condition used in (4.17), $N''(1)-N_h = 0$, is a necessary choice for a single distillation column, while the difference between $T_p(1)$ and T_h in case of the vortex tube is an adjustable parameter, which can be used to take into account any further separative treatment the gas may undergo outside the region under consideration.

Nevertheless it is to a large extent true that c_1 (Ec multiplied by an integral which takes into account the effect of the interplay between axial flow and tangential velocity distribution on the peripheral total-temperature change) governs the absolute level of the total-temperature separation potential of the tube, so that the value of Ec has little qualitative influence on the results.

$c_5^{\varkappa} = G/K$ in the distillation case determines the rate of transverse transport compared with the longitudinal flow rate, and, as such, governs the concentration change along the column (eq. (4.17)). In the vortex tube case, c_5 is in principle as stated, through the influence of Re_h (see eq. (4.12)), but at the same time it is a complex function of φ that takes into account the influence of the shape (but not the absolute magnitude) of the radial and axial total-temperature gradients throughout the tube on the total-temperature change at the periphery.

In the limit, in eqs. (4.17) and (4.20) when $G/K \to 0$, the exponential goes to zero and $N''-N' = \beta$ obtains except at $z = z_0$ (axial diffusion is neglected). In the equivalent vortex tube case with $Re_h \to 0$ because the secondary flow (in the general case both axial and radial) decreases relative to the turbulent diffusion, the equilibrium distribution T_{eq}/T_0 is approached everywhere except at $\xi = 1$ (eq. (4.4)), as far as permitted by the axial diffusion represented by the second term in (4.12).

Conversely when $G/K \to \infty$ in the distillation column, both $N''-N_h$ and $N'-N_h$ go to zero. Exactly the same happens in the vortex tube when Re_h goes to infinity and the secondary flow becomes of dominating influence, so that finally there is hardly any total-temperature change in the tube.

With G/K of intermediate magnitude, the "cold" flow fraction μ becomes a governing parameter in eq. (4.17) through the factor $\frac{\mu}{1-\mu}\frac{G}{K}$ in the exponent. Similarly, in the vortex tube case, with Re_h in the experimentally interesting range, the total-temperature distribution becomes strongly influenced by the value taken by μ.

Thus, it is seen that with $\xi \to 0$, the exponentials in eqs. (4.17) and (4.20) for the distillation case go to zero except at $z = z_o$ (the "hot" end); the over-all axial changes approach the limits $N''(0)-N_h = 0$ and $N'(0)-N_h = -\beta$, while $N''-N' \to \beta$ at all z except close to z_o where $N' = N'' = N_h$. In the vortex tube case when the flow in the core towards the cold exit is small compared to that in the outer annulus, this means that even a large total-temperature change with ξ in the core involves only a small amount of (net) total-enthalpy transport across the boundary $\eta = \eta_o$ and therefore only little change at the periphery, see fig. 4.1. Furthermore, with $\xi \to 0$, a total-temperature distribution close to what may be termed the pseudo-equilibrium distribution, as determined by the radial flow (see below for a definition of this term), can be easily established and maintained along the tube. The steep axial gradient seen in the distillation case in the "cold" stream as $z \to z_o$ may or may not have its counterpart in the vortex tube case, since in eq. (4.20) it is caused by the strict boundary condition $N(1)-N_h = 0$.

An increase in μ will, in the distillation case, have the following three effects: 1) It will make the two axial gradients approach one another by gradual increase of the gradient in the outer stream and decrease in the inner stream; 2) cause a decrease of $N''-N'$, i. e. a departure from the equilibrium condition; 3), depending on the value of G/K, make the axial gradients independent of z. In the vortex tube case this means that with increasing μ, 1) an increasing amount of total enthalpy has to diffuse from the core stream to the annular stream in order to change the temperature of the former; 2) non-equilibrium conditions with the radial temperature gradient rather small at intermediate η-values and even at low ξ, become more probable, with the result that a substantial amount of total-enthalpy passes the boundary between the two streams at all η (fig. 4.2); 3) as a direct result of this diffusion the axial gradients tend to be large and, depending on the value of Re_h (fig. 4.5, see also ref. 1V p. 178), independent of axial position.

In the limiting case, in the distillation column (eqs. (4.17) and (4.20)) when ξ goes to one, the axial change in both streams become linear in z, while $N''-N' \to 0$ at all values of z; the amount of "hot" gas goes to zero while the limiting value for the over-all axial change,

$$N''(0) - N_h \to - z_o \frac{K}{G} \beta = - z_o c_1^{\varkappa}/c_5^{\varkappa}, \qquad (4.21)$$

is approached. In the vortex tube case this means that, when $\mu \to 1$, the amount of total enthalpy transferred may well continue to increase but, as

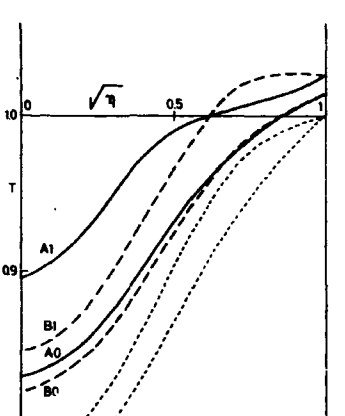

Fig. 4.4. Total temperature T as a function of radius ($\sqrt{\eta} = r/r_p$) (A-curves); with pseudo-equilibrium distribution, referred to peripheral total temperature T_p (B-curves); and equilibrium distribution, $\int_1^{\eta} (\partial T_{eq}/\partial \eta')d\eta'$, referred to unity at the periphery (C-curves); at axial positions $\zeta (= z/z) = 0$ and 1. From ref. IV (fig. 5).
Case 495, cold flow fraction $\mu = 0.23$, Reynolds number $Re_h\sqrt{\alpha} = 6.2$; ratio of radial flow within region I (η_o-surface) to total flow $Re_{hr}/Re_h\sqrt{\alpha} = 0.16$; $\sqrt{\eta_o} = 0.63$; $Ec = 0.11$.

most of the gas is returned in the core, the net amount goes to zero. At the same time the axial temperature change approaches a maximum, determined by c_1/c_5.

The radial flow has no counterpart in the distillation column analogy. It acts through the term $(\partial\psi/\partial\xi)(\partial T/\partial\eta)$ in eq. (4.3) as a kind of net diffusion term, which counteracts, in case of inflow, the effect of the pressure gradient (the tangential velocity), with the result that the apparent equilibrium gradient on the average is smaller than the equilibrium gradient $\partial T_{eq}/\partial\eta$ (see fig. 4.4). In agreement with this interpretation it is found (fig. 4.6) that radial flow reduces both the radial and the axial total-temperature gradients. It is clear that the effect of the radial flow must be felt strongest at small μ, where a balancing with the diffusion is easily established.

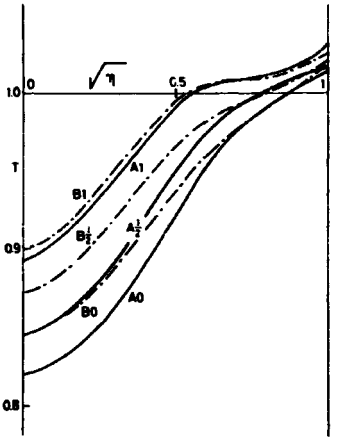

Fig. 4.5. Influence of Reynolds number. Total temperature as a function of radius at ξ = 0, 1/2 and 1. From ref. IV (fig. 7). Case 495; A-curves $Re_h\sqrt{a} = 3.1$, B-curves $Re_h\sqrt{a} = 9.3$; other data as in fig. 4.4.

The direct influence of the radial flow at higher cold flow fraction is correspondingly less. However, it should not be forgotten that the total radial flow into the core necessarily is equal to the total axial flow through the cold exit; furthermore, that the fairly level radial total-temperature distributions formed at higher ξ result from the convective redistribution of total enthalpy (caused by diversion of the flow (section 2.4) along the tube coupled with counter flow in the core) and thus may be said to be the effect of a strong mean radial flow in the sense this term is used in section 2.4. On the other hand it should be noted that this, essentially two-dimensional, point of view is not sufficient for the description of the separation process as it does not give credit to the fact that a well-developed axial counterflow system is favorable for the creation of a large axial total-temperature gradient and thereby of a large net temperature effect (similar arguments apply to the mass-separation case in section 3.3).

The presence of an axial total-temperature gradient at low ξ, which above was ascribed to the nature of the axial boundary condition at ξ = 1, may also be the effect of the tangential velocity decay along the tube. This

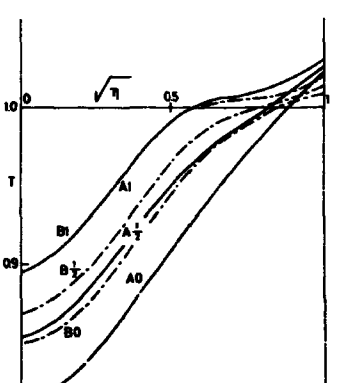

Fig. 4.6. Influence of radial flow. Total temperature as a function of radius at ξ = 0, 1/2 and 1. From ref. IV (fig. 8). Case 496; $Re_{hr}/Re_h^{1/6}$ (A-curves) = 0, (B-curves) = 0.32; other data as in fig. 4.4.

decay leads to a decrease in the radial equilibrium gradient of total temperature with axial position, with the result that non-equilibrium at low ξ is established followed by an increased outward radial diffusion of total enthalpy and therefore an enhanced axial gradient (see fig. 4.7).

Two factors besides those discussed above influence the total-temperature distribution. The most important is the shape of the radial tangential velocity distribution since ω^2 enters into the expression for the equilibrium gradient. It might be expected from an inspection of eqs. (4.13) and (4.11) that a velocity distribution as close as possible ω the free vortex in the outer part of the tube would be highly desirable; however, this necessarily would mean an increase of Re_h (see section 2.4), so that the end result would not be obvious. These problems will be discussed in section 6.1.

The other factor of some interest is the turbulent Prandtl number Pr, since this has a modifying influence on the radial tota--temperature gradients through the term $\partial\omega^2/\partial\eta$ in eq. (4.4). The influence is most pronounced near the periphery (ref. IV, fig. 10), where $\partial\omega^2/\partial\eta$ normally is numerically large and negative, but even there the effect is not decisive. This is fortu-

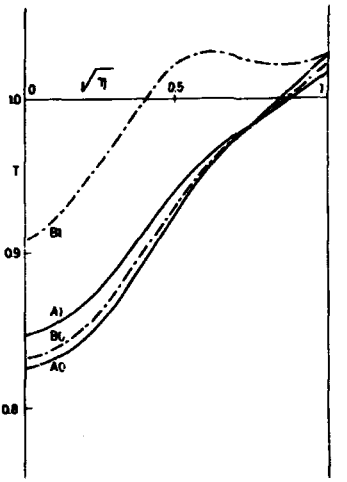

Fig. 4.7. Influence of axial gradient of angular velocity or circulation (Γ_{11}). Total temperature as a function of radius at $\xi = 0$ and $\xi = 1$. From ref. IV (fig. 6.). Case 495; A-curves $\Gamma_{11} = 0$; B-curves, $(\Gamma_{11})_{\eta=1} = 0.76$; other data as in fig. 4.4.

nate, because, as mentioned also in section 3.1, the concept as such has a weak theoretical foundation. Values of either 0.7 or unity was used in ref. IV in accordance with the experimental evidence avialable.

4.2.5. Comparison with Experiment

A comparison of computed curves with experiment was carried out in ref. IV from which examples are shown in figs. 4.1 and 4.2. Essential features were reproduced in all cases, as might be anticipated since the general description of experimental results given at the beginning of this section agrees with the above discussion of the model.

Most experiments pertain to cases where the cold flow fraction has been zero. As explained above, the distribution is likely, under these conditions, to be the essentially two-dimensional distribution described in section 4.1, with any axial gradient of total temperature caused at least in part by the axial decay of the tangential velocity. Fig. 4.1a is an attempt to reproduce

the experimental distributions shown in fig. 4.1b; the overall equilibrium total-temperature difference, $\int_0^1 T_{eq}/\, d\eta$ is derived from experiment, while the Re_h-value and the level of radial inflow are derived from the study of tangential velocity decay, described in section 2.3. The axial flow function employed has two points of flow reversal (see fig. 4.1a); thus the centre flow is directed towards the hot exit, as is often found experimentally.

One interesting feature, which is well-reproduced in the calculated curves, is the negative axial total-temperature gradient at the periphery. The reason for this cross-over phenomenon is, according to the model, that the outer part of the tube acts as a concurrent system in which the axial gradient at intermediate radii (but still at $\eta > \eta_0$) and the gradient near the periphery have opposite directions, as the two streams in a concurrent distillation system must have; this situation is made possible by the presence of the radial total-temperature gradient. Mathematically it is expressed by c_1 becoming negative, as would c_1^* (eq. (4.15)) in a concurrent distillation column, where μ is negative (fig. 4.3).

The fit of the calculated curves to the experimental results in fig. 4.1 is by no means perfect at low η, especially close to $\xi = 1$. The reason may be partly that the axial boundary conditons at $\xi = 1$ are not identical in the two cases, while at low ξ-values quick adjustment to quasi-equilibrium leads to better agreement. Partly that the radial inflow increases with axial position (a possibility excluded in the present model), so that, in agreement with the two-dimensional discussion in section 4.1, the quasi-equilibrium gradient tends to become less step with ξ.

At $\mu = 0.5$, conditions are entirely different as shown in fig. 4.2. As expected, the radial gradients have become small and the axial gradient at all η appreciable. At the same time the magnitude of the axial gradients has become sensitive to the value of Re_h (see ref. IV, fig. 12). It is therefore worth noting that the value used for the curve system in fig. 4.2a is close to both that to be derived in section 5.2 and to the Re-value found in ref. IVa (section 2.3). This quantitative agreement, as well as the qualitative correspondence between experiment and calculations, are very satisfactory, the more so as the agreement extends to the values of the boundary parameter, $T_p(1)-T_h$) (a point that is further discussed in ref. IV).

The relative significance of the turbulent transport of heat and of kinetic energy has been discussed in the literature on several occasions. The results in ref. IV (fig. 13) throw some light on the problem. It is concluded there that the kinetic energy diffusion contributes most to the total-temperature separation at radii close to the periphery, while heat diffusion dominates

near the centre axis, a conclusion also reached by Reynolds, 1961, in his analysis.

4.3. The Over-all Temperature Separation

The over-all temperature separation as calculated from the above examples and its variation with the cold flow fraction are of interest since this is the effect which is most important for the practical utilization of the tube. Results of this type, as calculated on the basis of a set of consistent parameters, are shown in fig. 4.8 together with an experimental curve from Hilsch, 1946.

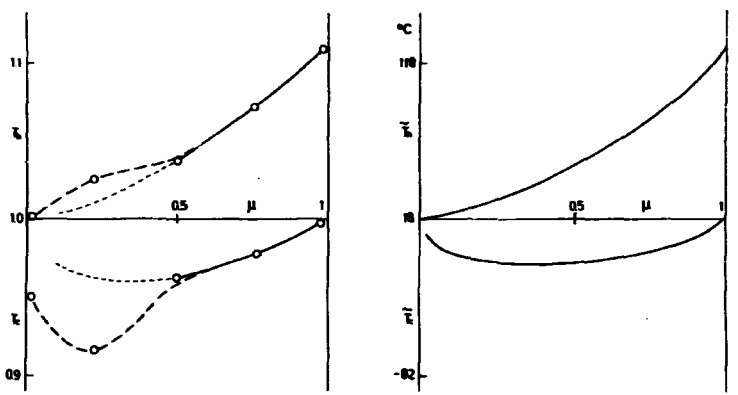

Fig. 4.8. Temperature separation as a function of cold flow fraction μ. From ref. IV (fig. 14).
a. Calculated curve.
b. Data from Hilsch, 1946.

At high cold flow fraction, the trend is, as might be expected, quite realistic; the upward concave tendency of the curves is readily explained by the theory as being the feature common to all counter-flow systems of the distillation column type that maximum separation occurs when the "reflux ratio" goes to one (i.e. . - 1).

A close fit at low μ is not found nor expected in view of the lack of agreement discussed in section 4.2 between the calculated and experimental distributions. Only the typical, reduced performance of the tube as μ approaches zero is reproduced quite well. This is achieved by permitting a central flow into the tube proper through the cold end orifice (fig. 4.1a). Such reversed flow on the axis is known to exist under these conditions; if it is strong enough compared to the net flow out of the cold exit, the cold stream temperature will rise close to the inlet temperature, because the air drawn-in will have a higher temperature than the outward flow, so that a counter-flow system with heat diffusion towards the periphery of the duct takes place. The influence of the rotation may be felt as well, though it will probably be small at the down-flow end of the duct.

5. THE SEPARATIVE WORK AND THE AVAILABILITY

The separative work concept, first described by Cohen, 1951, has been found most useful in connection with gas centrifuge development. In view of the close similarity between the mass separation processes in the centrifuge and the vortex tube, it is not surprising that the concept applies equally well to the performance of the tube, as was shown to be the case, in the work by Mürtz and Nöller, 1961, and in ref. I.

An equivalent concept applicable to the total-enthalpy separation in the tube was developed in ref. IV (with IVc) and shown to be an approximate availability function, as is in use for the description of the cooling efficiency of refrigeration machines.

In section 5.1 the separative work function will be derived by the method used in ref. IV for the approximate availability, and the relation between the two concepts will be discussed.

As briefly described in ref. IV (and in more detail in ref. IVc) the availability function may provide the turbulent diffusivity in the vortex tubes to which it is applied, through estimation of the turbulent thermal Reynolds number (the turbulent Peclé number) Re_h. The magnitude of this parameter cannot be obtained with any accuracy directly from a fitting of calculated total-temperature curves to experiment, especially not when μ is small (section 4.2). The availability method was therefore adopted in ref. IVc, and the thermal Reynolds number obtained in some cases for which the corresponding Reynolds number, Re, as derived from the axial decay of tangential momentum (section 2.3), was available. These results will be discussed in section 5.2.

As previously noted, the models employed in case of total-enthalpy separation (section 4.2) and mass separation (section 3.2) lead to expressions in total temperature and concentration, respectively, that are almost identical in form (compare eq. (3.6) and eq. (4.3)). The analogy even applies to the driving forces or, what amounts to the same, the equilibrium gradients in the two cases, which have essentially the same functional dependence on the velocity field of the tube (near-proportionality to the angular velocity squared, ω^2). In the approximation that the turbulent Prandtl number Pr is unity and on the assumption that the quantity $N(1-N)/t$ is constant within the tube(simplifications that have little effect on the resultant distributions) the two expressions become identical in form except for the dependence of Co in eq. (3.3) on the turbulence level. In view of this close analogy it is of considerable interest to compare the available mass and

temperature separation data and to test how well the correlation between separative work and availability exposed in section 5.1 fits into the experimental picture; this problem will be treated in section 5.3.

The use of the two functions for the determination of separation performances of the vortex tube will be treated in chapter 6.

5.1. The Derivation of the Functions

The separative work concept was developed in the 1940's in order to facilitate the design of separation plants for stable isotopes. In case of plants based on the gas centrifuge, the introduction of the separative work function provides in a simple way the minimum number of centrifuges that has to be placed in parallel and in series for given production rates of (partially) separated material. The treatment necessarily includes an assessment of the value of a single centrifuge in the plant - a parameter called, among other things, the separative work capacity or potential of the centrifuge. It is established by attaching to any stream of gas a value U that is the product of a specific value-function V_n and the amount of gas G in the stream, where V_n is a function of the mole fraction of the stream.

5.1.1. The Value Concept

The value of a centrifuge, ΔU, may then be expressed as the value increase experienced by the gas streams passing through the centrifuge, as follows

$$\Delta U \equiv \mu G V_n(N') + (1-\mu) G V_n(N'') - G V_n(N_o) \qquad (5.1)$$

Here, G denotes the total mass flow rate through the centrifuge, while μ and $(1-\mu)$ denote the two fractions into which the gas mixture is divided. N', N'', and N_o are the mole fractions of the two products and the feed, respectively.

V_n is so specified that the value increase per centrifuge becomes independent of position in the separation plant; this definition is chosen in order to ensure that the value increase has a unique relation to the economic parameters of a given type of centrifuge.

In the vortex tube, when it is used as a mass separator (e.g. of isotopes), the problem is exactly the same and equation (5.1) applies, as follows

$$\Delta U/2\pi F = \mu V_n(N_c) + (1-\mu) V_n(N_h) - V_n(N_o) \qquad (5.2)$$

The approximate availability concept, developed in ref. IV for the total-temperature separation in the tube, can also be derived on the basis of economic criteria as the above and by the same method; thus, it is not surprising that an economically interesting function results from the seemingly ad hoc mathematical procedure adopted in ref. IV.

Conversely, the method in ref. IV may equally well be applied to the derivation of the separative work concept. Since this leads directly to the expression of interest here, a short account of the procedure will be presented below.

5.1.2. The Value Increase across a Tube Region (the Separative Work Potential and the Availability)

The value increase for mass separation across an arbitrary volume within the tube is, according to the definition of the value function (compare ref. IV eq. (46)),

$$\Delta U \equiv \int_\sigma V_n(N)\vec{G} \cdot d\vec{\sigma} = \int\int\int \mathrm{div}(V_n\vec{G})d\tau, \qquad (5.3)$$

where the first integration is carried out over the surface of the volume, with $\vec{G} \cdot d\vec{\sigma}$ the mass flow normal to and through the surface element $d\sigma$; while the second set of integrations is the corresponding volume integral. Since the flow is stationary,

$$\mathrm{div}\vec{G} = 0 \qquad (5.4)$$

For comparison with ref. IV eq. 48 we can write

$$dU \equiv \mathrm{div}(V_n\vec{G})d\tau, \text{ so that } \Delta U = \int\int\int dU \qquad (5.5)$$

When the whole tube is considered, (5.3) or (5.5) becomes identical with (5.2).

It follows from (5.4) that

$$\mathrm{div}(V_n\vec{G}) = (\vec{G} \cdot \mathrm{grad})V_n = dV_n/dN(\vec{G} \cdot \mathrm{grad})N = dV_n/dN \cdot \mathrm{div}(N\vec{G}) \qquad (5.6)$$

$\mathrm{div}(N\vec{G})d\tau$ is the net transport of the one component by secondary flow out of the volume element $d\tau$. According to the diffusion equation (3.6) in section 3.2, this is equal to the accumulation by turbulent diffusion of the component in the volume element, so that we may write (compare ref. IV, eq. (50) and ref. IVc, eq. (8)).

$$dU/2\pi F = \frac{1}{2\pi}\frac{dV_n}{dN}\left[\frac{\partial}{\partial\eta}\left(\frac{2\eta}{Re_n\sqrt{a}}\left(\frac{\partial N}{\partial\eta} - \frac{\partial N_{eq}}{\partial\eta}\right)\right) + \frac{\partial}{\partial\xi}\left(\frac{\sqrt{a}}{2Re_n}\frac{\partial N}{\partial\xi}\right)\right]d\eta d\xi d\upsilon \tag{5.7}$$

with

$$\partial N_{eq}/\partial\eta \equiv \frac{Co}{l} N(1-N)\,\omega^2 \tag{5.8}$$

Insertion of this expression into (5.5), referred to the whole of region i (fig. 2.5), and partial integration lead to (ref. IV, eq. (51) and ref. IVc eq. (10))

$$\Delta U/2\pi F = d_p + (d_1 - d_o) - \int_o^1\int_o^1 \frac{d^2V_n}{dN^2}\frac{2\eta}{Re_n\sqrt{a}}\frac{\partial N}{\partial\eta}\left(\frac{\partial N}{\partial\eta} - \frac{\partial N_{eq}}{\partial\eta}\right)d\xi d\eta \tag{5.9}$$

$$- \int_o^1\int_o^1 \frac{d^2V_n}{dN^2}\frac{\sqrt{a}}{2Re_n}\left(\frac{\partial N}{\partial\xi}\right)^2 d\eta d\xi$$

(with the integration over the angular co-ordinate carried out).

$(d_1 - d_o)$ is a measure of the value changes caused by diffusion through the axial boundaries of region I (see ref. IVc, eq. (12)); considering the small axial concentration gradients usually encountered, this contribution is unimportant and consequently the term will be neglected. The term d_p measures the contribution from diffusion through the periphery of region I; it is most unlikely to be of any importance in tubes of the usual designs and d_p may therefore be neglected.

The last term on the right side of (5.9) is the contribution from axial diffusion within region I. Since the term is always negative and the value increase, with ordinary boundary conditions, is a quantity greater than zero, it is seen that axial diffusion reduces the amount of useful mass diffusion. The contribution from this term, though important in centrifuges, is negligible in the vortex tube because of the high throughput.

5.1.3. Definition of the Value Function

Eq. (5.9) and the equivalent expression for the total-temperature case, ref. IV, eq. (51), are valid regardless of the form chosen for the functions $V_n(N)$ and $V(T)$. In case of total-enthalpy separation, the simplest choice was made

$$d^2V/dT^2 \equiv 1 \tag{5.10}$$

which, integrated twice and with suitable integration constants, gives

$$V = 1/2\,(T-1)^2 \tag{5.11}$$

(ref. IV eq. (52)).

In the mass separation case, the same choice would be suitable for comparison with the total temperature data, as $N(1-N)$ in $\partial N_{eq}/\partial\eta$ with sufficient accuracy is constant in the present case. The customary definition is, however, to set

$$d^2V_n(N)/dN^2 \equiv \frac{1}{N^2(1-N)^2}, \tag{5.12}$$

since this leads to the desired invariance of ΔU per unit of equipment (i. e. centrifuge or vortex tube) in a larger plant with many units and a major change in mole fraction N up through the plant. This is true because both $\partial N/\partial\eta$ and $\partial N/\partial\xi$, as seen from the mass diffusion eq. (3. 6), must be proportional to $N(1-N)$, since $\partial N_{eq}/\partial\eta$ contains that as a factor. (It is here assumed that the velocity field is independent of N; an approximation which is reasonable at least when the relative molecular mass difference is small). By choosing the following integration constants

$$V_n(0.5) = (dV_n/dN)_{N=0.5} = 0\,, \tag{5.13}$$

the usual value function for mass separation obtains

$$V_n = (2N-1)\ln(N/1-N)). \tag{5.14}$$

The total-temperature equation equivalent to (5. 9) with eq. (5. 11) inserted will be discussed in section 5. 2 (see eq. (5. 34)) on the basis of the work described in ref. IVc. Eq. (5. 9) (with (5. 14) inserted) has had little use since few data exist on concentration distributions within the tubes.

The insertion of (5. 11) into the expression for the value increase of the tube based on total temperature (ref. IV, eq. (45), equivalent to eq. (5. 2)) leads to the simple equation

$$\Delta A/2\pi F = \mu 1/2(T_c-1)^2 + (1-\mu)1/2(T_h-1)^2 \tag{5.15}$$

or

$$\Delta A/2\pi F = 1/2\mu(1-\mu)(T_h-T_c)^2 \tag{5.16}$$

This expression may be compared with the availability of a cooling machine, which is written, when the temperature drop is not too large,

$$a'_c \equiv a_c/(c_p t_o) = 1/2(t_c/t_o-1)^2 \tag{5.17}$$

where t_o and t_c are the temperatures of the gas before entering and after leaving the machine, respectively. As the vortex tube acts both as a cooling machine and as a heating machine, it is appropriate to call the value increase $\Delta A/2\pi F$ in eq. (5.15) the availability of the tube and use it as such for a comparison of vortex tube performance with other refrigerating devices (as done in chapter 6).

The use of eq. (5.14) in (5.2) would appear to lead to a more complex equation than (5.16); however, since the concentration change is small within the tube, a Taylor's expansion of V_n from N_o, carried to second order, provides V_n with sufficient accuracy; thus, after use of the mass balance equation

$$\mu N_c + (1-\mu)N_h = N_o \tag{5.18}$$

and introduction of (5.12), we may write eq. (5.2) as

$$\Delta U/2\pi F = 1/2\mu(1-\mu)\left(\frac{N_h-N_c}{N(1-N)}\right)^2 \tag{5.19}$$

(see ref. 1).

5.1.4. Maximum Value Increases

From eq. (5.9) and the equivalent total-temperature expression (5.34) it is a simple matter to find upper limits to both the separative potential and the availability of a tube with given tangential velocity field. The conditions to be satisfied are (in the first case) that, in all parts of the tube, $(\partial N/\partial \xi)^2$ is equal to zero and $\partial N/\partial \eta$ $(\partial N_{eq}/\partial \eta - \partial N/\partial \eta)$ is at a maximum. The second condition requires (see eqs. (5.8) that

$$\frac{\partial N}{\partial \eta} = 1/2\,\frac{\partial N_{eq}}{\partial \eta} = 1/2\,\frac{Co}{t}\,N(1-N)\omega^2 \tag{5.20}$$

everywhere in the tube. Similarly, in case of the availability the second condition leads to (eq. (4.4))

$$\partial T/\partial\eta = 1/2\ \partial T_{eq}/\partial\eta = 1/2\ Ec[\omega^2 + ((1-Pr)/2\times\eta\partial\omega^2/\partial\eta)] \qquad (5.21)$$

From eqs. (5.9) and (5.20) we obtain

$$\frac{\Delta U_{max}}{2\pi F} = \left(\frac{Co}{t}\right)^2 \frac{1}{2Re_n\sqrt{a}}\, B \qquad (5.22)$$

and from eqs. (5.34) and (5.21), with Pr = 1,

$$\frac{\Delta A_{max}}{2\pi F} = Ec^2\, \frac{1}{2Re_h\sqrt{a}}\, B \qquad (5.23)$$

where $B \equiv \int_0^1\int_0^1 \omega^4\,\eta\,d\eta\,d\xi$ (5.24)

or, introducing dimensional quantities (see section 3.1, eq. (3.3) and section 4.1, eq. (4.2))

$$\Delta U_{max} = \pi\ell\frac{\rho D}{(\rho\varepsilon_n)/(\rho D)}\left[\frac{M_2-M_1}{2R\check{t}}\, v_{po}^2\right]^2 B \qquad (5.25)$$

$$\Delta A_{max} = \pi\ell(\rho\varepsilon_h)\left[\frac{v_{po}^2}{c_p T_\infty}\right]^2 B \qquad (5.26)$$

$\rho\varepsilon_n$ and $\rho\varepsilon_h$ are related through the turbulent Prandtl and Schmidt numbers as follows

$$(\rho\varepsilon_n)/(\rho\varepsilon_h) = Sc \times Pr \qquad (5.27)$$

In the simple case that ω may be considered as constant throughout the tube, we can write

$$B = 1/2 \qquad (5.28)$$

It is useful to introduce the velocity of sound

$$c_\infty = \sqrt{kRT_\infty/M} \qquad (5.29)$$

into the above equations, because v_{po}/c_∞ can be brought into an empirical relation with the Mach number in the inlet jet (see section 2.4). Then eqs. (5.25) and (5.26) read

$$\Delta U_{max} = \pi \ell \frac{\rho D}{(\rho \epsilon_n)/(\rho D)} \left[\frac{M_2 - M_1}{\bar{M}} k \frac{1}{2} \left(\frac{v_{po}}{c_\infty}\right)^2 \right] \left(\frac{T_\infty}{\bar{T}}\right)^2 B \qquad (5.30)$$

and

$$\Delta A_{max} = \pi \rho \epsilon_h \left[(k-1) \left(\frac{v_{po}}{c_\infty}\right)^2 \right]^2 B \qquad (5.31)$$

Eqs. (5.25) and (5.26) (or (5.30) and (5.31)) provide maximum values for the separation potentials of the tube exclusively in terms of the tangential velocity field and pertinent tube parameters.

The actual separation, as measured by the value increase according to eq. (5.9) or (5.34), is necessarily reduced by the influence of the secondary flow. Typically, the experimental value-increases are found to be a factor of about 3 to 5 less than the maximum values (see section 6.1). Since the overall effect of the secondary flow is fairly invariant to changes in certain of the tube parameters, it is often adequate to use the maximum values as guides for evaluation of the tube performance (see section 6.1).

5.2. The Turbulent Diffusivity from Availability Estimations and Comparison with Corresponding Data from the Tangential Velocity Study (Section 2.3)

According to the definition of the approximate availability function in ref. IV (eq. (48)) we may write for the value increase across region I (fig. 1.1)

$$\Delta A/2\pi F = [A(1) - A(0)]/2\pi F \qquad (5.32)$$

with

$$\Delta A(\xi)/2\pi F \equiv \left[-\int_0^1 \frac{\partial \psi}{\partial \eta} \frac{1}{2} (T-1)^2 d\eta \right]_\xi \qquad (5.33)$$

For the same region the availability expression ref. IV eq. (51) equivalent to eq. (5.9) provides the alternative expression

$$\Delta A/2\pi F = -\int_0^1 \int_0^1 \frac{2\eta}{Re_h \bar{a}} \frac{\partial T}{\partial \eta} \left(\frac{\partial T}{\partial \eta} - \frac{\partial T_{eq}}{\partial \eta}\right) d\eta d\xi. \qquad (5.34)$$

Only the latter equation contains Re_h. Thus, in cases where sufficient temperature and velocity data are available, (5.32) and (5.34) combined

may provide estimates of Re_h and thereby of the turbulent thermal diffusivity.

Eq. (5.32) rather than (5.16) should be employed because value changes outside region I may take place. Furthermore, because a test of the quality of the relation between the two availability estimates can be easily made by performing the integration with respect to the axial co-ordinate leading to (5.32) from $\xi = 0$ to a variable ξ. (Ref. IVc, fig. 1 shows the result of a particular successful test of this type).

Estimates of turbulent thermal Reynolds numbers by the method outlined above have been made in five cases as shown in fig. 5.1. Equivalent results

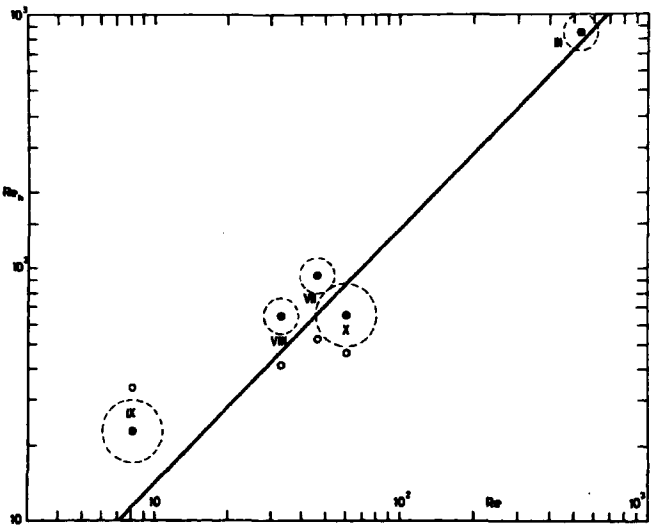

Fig. 5.1. Correlation of thermal Reynolds numbers Re_h from temperature distribution (section 5.2) with Reynolds numbers Re from axial gradient of circulation (section 2.3). Roman numerals refer to data in table 2.1, p. 32, and below.

Case	III	VII	VIII	IX	X
Re	0.26	0.11	0.15	0.10	0.10

Solid points, Re_h based on availability; open points, Re_h based on energy equation. Circles around points indicate range of values obtained. The line drawn is based on a turbulent Prandtl number of 0.7.

obtained on the basis of a quantitative analysis of the energy equation (4.3) (see section 4.2), which must also involve the determination of a most-probable Re_h-value in each case, are also shown in the figure. The two sets of estimates (4 cases) are seen to agree within a factor of two.

The abscissa in fig. 5.1 is the Reynolds number, Re, as obtained in section 2.3 from the axial decay of tangential velocity. The line is drawn on the assumption that the turbulent Prandtl number is 0.7. The quite satisfactory correlation obtained in this way between estimates of turbulent diffusivities by entirely different methods would appear to lend some support to the theories behind, and thereby to the description given in both section 2.3 and section 4.2.

5.3. Comparison of Gas Separation and Temperature Separation Data

Very little has been done experimentally in the way of correlating the mass separation and total-enthalpy separation, the reason being that few papers on the gas separation effect (in the sense meant here, i.e. a net concentration difference between the two gas streams leaving the vortex tube) have been published. The only attempt known to the author is the short discussion in ref. I. There it was found that a large temperature effect in general is associated with a small or negligible concentration effect and vice versa. More specifically it was found that long tubes with weak mean radial inflow, related to the traditional Hilsch type, gave a satisfactory temperature effect but no concentration effect; while short tubes with a strong radial inflow, related to the type investigated for gaseous nuclear rockets, gave hardly any temperature effect but maximum concentration change.

In view of the close similarity between the mathematical expressions for mass and total-enthalpy diffusion as emphasized throughout the present work and in particular in section 5.1 these results would appear rather paradoxical. Certainly, if the ratio of turbulent to laminar diffusivity were constant throughout the tube volume, the theories in sections 3.3 and 4.2 for mass and total-enthalpy separation would fail, since they would then predict proportionality between all equivalent pairs of gradients (neglecting the minor effect of a turbulent Prandtl number different from one, and certain small temperature effects); see also discussion in section 3.3. Thus, in order to reconcile the two sets of results in ref. I it is necessary to show that the variation in turbulence level may account for, in a satisfactory manner, the pronounced lack of correlation found.

5.3.1. The Correlation Found in Special Cases

To start with, it is important to note that a correlation close to proportionality is after all established in special cases, viz. in the very shortest tubes employed in ref. I, as seen in fig. 5.2. As a whole the trend in the curves gives the impression of two independently created temperature effects competing with one another, where the one, correlated with the concentration effect, dominates in short tubes (l/r_p = 2-5). The other contribution, which becomes the dominant one when l/r_p exceeds 10-15, has a dependence on "cold" flow fraction of the same kind as displayed by typical Hilsch vortex tubes. It is therefore a very plausible conclusion that the

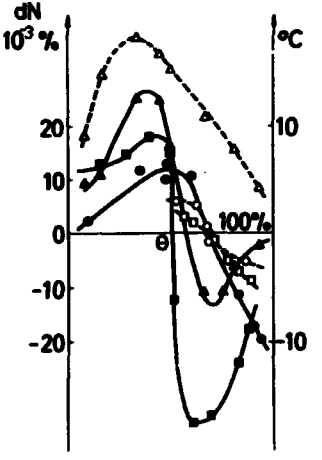

Fig. 5.2. Comparison of gas separation, dN (solid points), with temperature separation (open points). Ordinates, mole fraction difference (left) and temperature difference (right) ("hot" minus "cold" stream (fig. 1.1d)), measured downstream of exit ducts. Abscissa "hot" flow fraction θ(=1 - μ). Ratio of tube radius to length $\sqrt{\delta}$ = (circles) 1/3.3, (squares) 1/11.7, and (triangles) 1/28; r_p = 0.3 cm; $r_c = r_h$ = 0.075 cm. From ref. I (fig. 9).

latter is created in the outer part of the tube, while the concentration-correlated effect has its origin in the core region in agreement with the conclusions, reached in section 3.3, concerning the gas separation results. It was shown there that the symmetry of the secondary flow in the core region, i.e. the independence of the flow on nozzle position, gives rise to the characteristic pattern with both normal and reverse effects, though a peripheral stream, preserving its identity, at the same time finds its way to the "hot" exit at all "cold" flow fractions. The work by Martynovskii and Alekseev, 1957, emphasizes the importance of the symmetry criterion in that a reverse temperature effect was obtained in a Hilsch type tube that was made almost symmetrical about the nozzle plane by the use of a particularly large "cold" orifice; the reverse effect appeared at low "cold" flow fraction, as is the case with the reverse gas separation effects in section 3.3. Dubinskii, 1955, has also, with completely symmetrical tubes, obtained symmetrical temperature effect curves.

5.3.2. The Turbulent Diffusivity

As turbulence supports the total-enthalpy separation but may be detrimental to the mass separation, the discussion in the previous section leads to the conclusion that the effective turbulent diffusivity decreases towards the centre axis, at any rate in tubes with strong radial inflow. This would appear to be a quite likely proposition, and it is in agreement with the view expressed for example by Kendall, 1962, that the turbulence is created mainly at the peripheral wall. On the other hand, it is difficult to find quantitative confirmation of this assertion as few data exist; thus, in the formal definition of the turbulent viscosity ε (ref. IV, eq. (12))

$$\overline{u'v'} \equiv \varepsilon(\tilde{v}/r - \partial\tilde{v}/\partial r) ,$$

$\overline{u'v'}$ appears to have been measured as a function of radius in one case only (Ross, 1964b). In this experiment a porous tube was inserted into the centre and torque balance determinations were made. The measurements show an increase of $\overline{u'v'}$ with decreasing radius, a result which cannot be reconciled with a decrease in ε, since also $(\tilde{v}/r - \partial\tilde{v}/\partial r)$ was found to decrease with decreasing radius. However, the presence of the porous tube, which undoubtedly enhances the axial convection in the vortex tube, as mentioned in section 2.3, and probably at the same time supports the generation of turbulence, makes the results less applicable to the tubes considered here.

Better known are the mean square fluctuations $\overline{u'^2}$, $\overline{w'^2}$, and $\overline{v'^2}$

(Kendall, 1962, Schowalter and Johnston, 1960), which in fact do show a tendency to decrease, in per cent of mean velocity squared, with decreasing radius (Sibulkin, 1962, finds a change from 7% at the periphery to 3% on the axis; see also Kerrebrock and Keyes, 1959, McFarlin, 1955); however, this does not necessarily mean that ε decreases as well, because ε depends on the functional dependence of both the correlation factor and $(\bar{v}/r - \partial\bar{v}/\partial r)/\nu^2$ on radial position. Of these, the correlation factor is unknown; probably it is a function of the history of the flow, because dissipation outweighs production (Kendall) so that conditions cannot be determined by a Prandtl mixing length argument with $\overline{u'v'}$ simply related to $\overline{u'^2}$ and $\overline{v'^2}$. Furthermore, sufficiently accurate tangential velocity data are not available for the determination of the other factor.

In addition to this lack of experimental evidence there is the complication that it seems likely that the turbulent diffusivity does not decrease in a regular manner towards the centre, as is assumed above. Instead, as was concluded in section 3.3 on the basis of flow visualization experiments, this parameter appears to be a more complex function of the radial position, determined by the secondary flow with axial streams at intermediate radii that preserve their identity along the tube but appear well-mixed internally.

5.3.3. An Estimate of the Radial Gradient of the Turbulent Diffusivity

Although direct estimates of ε are not available at present, some indirect experimental evidence for the idea that the effective turbulent diffusivity decreases towards the axis can be obtained from the very data under discussion (ref. 1) by the following argument (where it is taken for granted that both mass and temperature separation may be treated as in section 5.1).

The ratio of maximum separative work to maximum availability may, according to section 5.1, eqs. (5.25) and (5.26), be written (with $Sc \times Pr = 1$)

$$\frac{\Delta U_{max}}{\Delta A_{max}} = \frac{1}{[(\rho\varepsilon_n)/(\rho D)]^2} \left[\frac{M_2 - M_1}{2\bar{M}} \frac{k}{k-1} \frac{T_\omega}{\bar{T}}\right]^2 ; \qquad (5.35)$$

while, according to eqs. (5.19) and (5.16), the ratio of the actual performances is

$$\frac{\Delta U}{\Delta A} = \left(\frac{N_h - N_c}{N(1-N)}\right)^2 / (T_h - T_c)^2. \qquad (5.36)$$

Furthermore, if the crude approximation of section 3.3 that the gradients of N are negligibly small is made and if this idea is extended to the gradients of T (probably permissible in the tubes considered here), the mass diffusion and energy equations give the following ratio for the separation effects

$$\frac{N_h - N_c}{T_h - T_c} = \frac{N(1-N)}{(\rho \varepsilon_n)/(\rho D)} \left[\frac{M_2 - M_1}{2\bar{M}} \frac{k}{k-1} \frac{T_\infty}{\tilde{t}} \right] \qquad (5.37)$$

where Pr = 1 and Sc = 1, as above.

Comparison of eq. (5.35) with eqs. (5.36) and (5.37) (for $\Delta U_{max}/\Delta A_{max} \simeq \Delta U/\Delta A$) shows that the same result is obtained at both extremes; the relations may therefore be used with some confidence. All parameters are experimentally available in these expressions except the ratio of turbulent to laminar diffusivity, which may therefore be calculated from the data; for the 1 cm-tube in fig. 5.2, $(\rho \varepsilon_n)/(\rho D) \simeq 3$ is found. This is a low figure compared with the value of the order of 20 (with $Re_{t,p} \simeq 3\ 10^4$) obtained from fig. 2.2. Since the data in the latter figure are based mainly on conditions in the outer tube region, this result points quite convincingly to the conclusion that a radial gradient of the effective turbulent diffusivity is in fact present in the tubes under consideration.

Additional information on the turbulence in the longer tubes of fig. 5.2 is scarce. From fig. 2.2, one would predict the turbulent diffusivity in the outer part of the tube to increase somewhat with increasing tube length, because the tangential velocity level near the nozzle increases by this change (and approaches the velocity in the inlet jet).

5.3.4. Interpretation of the Experimental Results

For the description of the relation between the two types of separation, mass and total-enthalpy, the following distinct features discussed in section 2.4 are of importance: 1) The tangential velocity in short tubes increases towards the centre in the outer annulus, while at the same time the large pressure gradients at intermediate radii accompanying this distribution tend to produce a well-developed axial flow system near the radius of the exit duct(s); 2) the tangential velocity in longer tubes decreases towards the centre, and the comparatively small pressure gradients necessary for this type of distribution at intermediate radii produce a much more diffuse axial flow system with correspondingly less flow carried in the end wall boundary layer near the nozzle.

Returning to the relation between concentration effects and temperature effects, the picture that emerges is as follows.

In medium-long tubes (ℓ/r_p = 5-10) conditions are somewhere in between the above extremes, 1) and 2). Flows, both directly from the outer region and by way of the intermediate axial streams, find their way to the exits. Total-enthalpy separation takes place in both inner and outer region, in the core owing to high velocity, in the annulus owing to high diffusivity; the first effect varies strongly with "cold" flow fraction while the second effect contributes a fairly constant positive amount to the net temperature effect. On the other hand, the mass separation effect comes almost exclusively from the core region where both high velocity and low turbulence favour its formation.

By a change to long tubes (ℓ/r_p = 15 ref. 1), the centre region separation is destroyed both because the tangential velocity there is reduced in magnitude, and because the axial flow system loses its characteristic counter-current pattern, so that what remains tends to contribute normal effects. A small and fairly constant concentration effect (i. e. one independent of cold flow fraction) results. On the other hand, the temperature effect is enhanced because of the increased contact time in the longer tube, because of the higher peripheral velocity (at least near the nozzle), and, probably, because of the higher turbulent diffusivity.

By a change from medium-long to short tubes the situation is reversed. The tangential velocity in the centre region increases drastically, while that at the periphery drops somewhat. Both the total-enthalpy and the mass separation in the centre region are therefore accentuated; (since the time for contact is reduced, when the length is reduced, it may be the net effect per cm tube length rather than the effect itself that increases). At the periphery, temperature separation tends to drop somewhat. Furthermore a well-defined axial flow at intermediate radii precludes the penetration of a flow of any strength directly from the annulus to the exit, with the result, discussed earlier in this section, that a close correlation between the two types of separation is formed.

6. THE EFFICIENCIES OF THE GAS AND ENERGY SEPARATION

In the present chapter the performance of the vortex tube as a mass and energy separator is discussed on the basis of the separative work and availability functions derived in chapter 5.

In section 6.1 the question of the efficiency as measured by the ratio of the actual performance to the maximum value increase is briefly mentioned, while the remainder of the section is devoted to a discussion of the functional dependence of the maximum performance on pertinent tube parameters, and the prospects of improvement.

In section 6.2, the efficiency of the tube as a mass separator is discussed in relation to that of two other devices for mass separation, the gas ultracentrifuge and the nozzle separator.

In section 6.3, the efficiency of the tube as an energy separator is related to that of ordinary cooling devices.

6.1. The Performance Criteria

It seems likely that the actual performance of the tube as measured by the value increase (eq. (5.19) or (5.16)) bears some quite constant relation to the maximum value increase (eq. (5.22) or (5.23)) under varying conditions, as long as the secondary flow in the tube does not deviate radically from the reference conditions. In the present context, where optimum performance criteria are sought, this requirement is likely to be obeyed at least with respect to the cold flow fraction, which in practice remains within an interval from about 0.3 to 0.7 because of the penalty for exceeding this range expressed by the factor $\mu(1-\mu)$ in eqs, (5.19) and (5.16).

6.1.1. The Relation between Actual and Maximum Value Increase

It was estimated in ref. IV, part 4, that the efficiency, as regards temperature separation was of the order of 1/5 to 1/3 (when measured as the above ratio of actual to maximum availability) in the few but typical cases studied. The corresponding figure for typical mass separation cases can be obtained by use of the result in section 5.3 which says that the turbulent diffusivity is three times the molecular diffusivity at intermediate radii; then, on the basis of the data in refs. I and II, the efficiency in question is found from eqs. (5.19) and (5.25) to be of the order of 1/6 to 1/3. Incidentally the upper limit, 1/3, is so high that the assumption in section 3.3 that the radial concentration gradient remains negligible in the tubes, is somewhat in error; however, this inconsistency is not so large as to

invalidate the discussion in section 3.3.

The above figures should be viewed in relation to the fact that at most 60-70% of the maximum value increase can be obtained in practice even with the most favorable secondary flow. Consequently, it would appear improbable that any marked improvement in performance, of either type of separation, is possible through optimization of the secondary flow.

6.1.2. The Separative Work Potential and the Availability Expressed in Terms of Pertinent Tube Parameters

Thus, the tube performances are quite adequately discussed in terms of the two functions for maximum value-increase, ΔU_{max} and ΔA_{max}. Often the efficiency in relation to energy requirements is of primary importance in which case it is useful to use either eqs. (5.22) and (5.23) or the following two equations (derived from (5.30) and (5.31)) (Pr = 1)

$$\frac{\Delta U_{max}}{2\pi F} \frac{\ell}{2F} \frac{\rho D}{(\varepsilon_n/D)} \left[\frac{M_2-M_1}{\overline{M}} \frac{k}{2}\right]^2 \left(\frac{v_{po}}{v_j}\right)^4 \left(\frac{T_\infty}{t}\right)^2 M_j^4 B \qquad (6.1)$$

$$\frac{\Delta A_{max}}{2\pi F} = \frac{\ell}{2F} \rho \varepsilon_h [k-1]^2 \left(\frac{v_{po}}{v_j}\right)^4 M_j^4 B \qquad (6.2)$$

where M_j is closely related to the jet Mach number.

The parameters in these equations are, 1) the chemical nature of the gas (mixture), 2) the temperature level, 3) the peripheral velocity v_{po}, 4) the tangential velocity distribution (expressed by the factor B), 5) the throughput $2\pi F$, and 7) the length of the tube ℓ; (the factor $(T_\infty/t)^2$ is of order one and may therefore be left out of consideration).

These parameters are not all external or independent of each other, and it is therefore convenient to study them on the basis of the following fundamental set: I) The chemical nature of the gas (mixture), i.e. a) the relative molecular weight difference $(M_1-M_2)/\overline{M}$, b) the ratio of specific heats k, and c) the transport coefficients ν and D, II) the temperature T_∞, III) the pressure of the supply gas p_∞ IV) the overall pressure ratio p_∞/p_s (where p_s is the exhaust pressure), V) the ratio of nozzle diameter to tube diameter r_j/r_p, IV) the ratio of centre exit diameter to tube diameter, r_e/r_p, VII) the ratio of tube radius to tube length $r_p/\ell = \sqrt{\sigma}$, VIII) the fraction of gas exhausted through centre exits, $Q\ell/F$, and IX) a typical length, e.g. the tube radius, r_p.

The functional dependence of the first set of parameters on the second set is extremely complex and a quantitative treatment is out of reach; however, some insight into the problems may be gained by use of the results of chapter 2: First, that, in turbulent tubes, the turbulent diffusivities in the outer tube region are determined by

$$\varepsilon/\nu = C \frac{\rho_{po} v_{po} r_p}{(\rho\nu)} \quad \text{and} \quad Sc = Pr = 1, \tag{6.3}$$

Also, that at intermediate radii, when gas separation takes place there, we may write $\varepsilon_n/D = C_n(\rho_{po} v_{po} r_p/(\rho\nu))$; where $C_n < C$ takes into account the decrease in effective turbulent diffusivity towards the centre axis as was shown in section 5.3 to occur.

Secondly, that the radial tangential velocity distribution may be determined according to the treatment by Rosenzweig, Lewellen and Ross, 1964, as discussed in section 2.2 and qualitatively extended in 2.4 to cover long tubes with peripheral exit. Noting that the throughput may be written

$$2\pi F = \pi r_j^2 \rho_j v_j , \tag{6.4}$$

where the subscript refers to conditions in the nozzle, we may deduce from the expressions in sections 2.2 and 2.4 that, in both laminar and turbulent cases, the free vortex is favoured 1) by a short tube length (large r_p/ℓ), 2) by a large density reduction ρ_j/ρ_{po} (where the gas enters the tube), and 3) by a large velocity reduction, v_j/v_{po} (at the same location); furthermore, in laminar tubes an approach to the free vortex is caused 4) by an increase in the absolute level of ρ_j and v_j expressed by a nozzle Reynolds number Re_j. The effects listed as 2 and 4 are directly related to the effect of a large throughput. The radial distribution of tangential velocity is furthermore a function of the relation between the widths of nozzle and centre exit(s) (see below).

With the introduction of eqs. (6.3) and (6.4), eqs. (6.1) and (6.2) can be written for the turbulent case

$$\frac{\Delta U_{max}}{2\pi F} = \frac{1}{Re_j^2} \frac{1}{C_n} \frac{\rho_j}{\rho_{po}} \frac{\ell}{r_p} \left[\frac{M_2 - M_1}{M} \frac{k}{2}\right]^2 \left(\frac{v_{po}}{v_j}\right)^3 M_j^4 B \tag{6.5}$$

and

$$\frac{\Delta A_{max}}{2\pi F} = \frac{C}{r_j^2/r_p^2} \frac{\rho_{po}}{\rho_j} \frac{\ell}{r_p} [k-1]^2 \left(\frac{v_{po}}{v_j}\right)^5 M_j^4 B \tag{6.6}$$

In the laminar case, which is of interest only for gas separation, introduction of (6.4) into (6.1) with $\varepsilon_n = D$ leads to

$$\frac{\Delta U_{max}}{2\pi F} = \frac{1}{Re_j} \frac{r_p}{r_j} \frac{\ell}{r_p} \left[\frac{M_2 - M_1}{\overline{M}} \frac{k}{2} \right]^2 \left(\frac{v_{po}}{v_j} \right)^4 M_j^4 B. \qquad (6.7)$$

B (eq. 5.24) is a function of the tangential velocity distribution, i.e. of the extent to which the free vortex is approached, and is as such a function of the parameters that governs this distribution, as listed above.

Eqs. (6.5)-(6.7) are expressed, in principle, in terms of basic parameters with the exception of the jet "Mach number" M_j, the (laminar) nozzle Reynolds number Re_j (= $\rho_j v_j r_j / (\rho \nu)$), the velocity reduction v_{po}/v_j and the density reduction ρ_{po}/ρ_j. The latter ratio is related to M_j in such a way that when $M_j < 0.9$ (air) then $\rho_{po}/\rho_j = 1$, while when $\rho_{po}/\rho_j < 1$ then $M_j = 0.9$. These parameters depend in a complex manner on almost all the basic parameters (1-1X), notably the overall pressure ratio.

If a tube is to function properly either as a mass or as an energy separator, it is necessary that a substantial part of the gas is led to the centre region and exhausted through centre exits (as discussed in chapters 3 and 4), thus Q_ℓ/F should not be less than say 0.3 and, of course, in tubes of types d and e (fig. 1.1) it is always one. For this reason the diameter of the centre exit(s) is of decisive importance, as may be seen in the following way. The total pressure ratio can be factored into the number of pressure drops that the flow experiences on its way to and through the centre exit duct:

$$p_\infty/p_s = p_\infty/p_j \times p_j/p_{po} \times p_{po}/p_f \times p_f/p_e \times p_e/p_s \qquad (6.8)$$

Here p_∞/p_j is the (almost) isentropic pressure drop that provides for the acceleration of the gas into the nozzle; p_j/p_o is the irreversible pressure drop (if any) from nozzle to periphery; p_{po}/p_f is the pressure drop from the periphery to the characteristic radius r_f (see below), p_f/p_e is a characteristic pressure drop into the centre exit duct with r_f so chosen that p_f/p_e is a measure of the mean axial flow velocity in the centre exit duct; and p_e/p_s is the pressure drop from the exit duct to the surroundings (or to some reservoir). On the supposition that the aim is to achieve maximum separation potential with minimum waste of energy, it seems plausible that p_j/p_{po} and $p_f/p_e \times p_e/p_s$ should be kept close to one while p_∞/p_j and p_{po}/p_f are made as large as possible. In order to hold p_f/p_s low, the exit

duct must be so wide (r_e so large) that it can easily accommodate the mass flow to the core region. On the other hand, r_e should not be too large either lest the gas is exhausted into the peripheral region of the centre exit duct before it has contributed to the creation of an optimum radial tangential velocity gradient and before its temperature or concentration has had time to change. Thus, on the one hand the object is to match the centre exit diameter to the nozzle diameter allowance being made for the radial pressure drop p_{po}/p_f, and on the other hand, to match the centre exit diameter to the tube diameter. Experience has shown that the best choices, in case of temperature separation, are the following

$$r_j/r_c/r_p = 1/2/4. \tag{6.9}$$

A similar relationship exists for optimum mass separation as was shown in ref. I and further discussed in ref. III (see also section 3.3).

Now, if the overall pressure ratio is so adjusted that the desired sonic conditions exist in the nozzle and the value of p_{∞}/p_j therefore is at a maximum and approximately equal to two, while at the same time allowance is just made for the radial pressure gradient and for the acceleration of the flow into the exit, M_j is at a maximum and ρ_j/ρ_{po} is unity in eqs. (6.5) and (6.6). The following questions may then be asked: What happens if a) the tube length is altered, b) the overall pressure ratio is further increased, c) the pressure level or d) the temperature level is shifted, and if e) another gas (mixture) is substituted?

The influence of the tube length or rather ℓ/r_p has already been discussed in section 5.3, and the criteria developed there are taken to apply here.

6.1.3. The Gas Separation Performance

In case of mass separation at pressures at or above atmospheric pressure the results of section 3.3 apply. By increasing the overall pressure ratio, case b) above, we shall expect B to increase because necessarily the ratio ρ_j/ρ_{po} increases above the reference value, i.e. unity. However, if this is done by increasing p_{∞}, while keeping the exhaust pressure at atmospheric pressure, $1/Re_j^2 \times \rho_j/\rho_{po}$ will decrease at the same time, and the overall effect on the performance (eq. (6.5)) will be uncertain; in fact the effect was found to be small under the conditions of the experiments in ref. I (unpublished results).

increased efficiency should result by a reduction of the pressure level (case c above), since this is a change which increases the factor $1/Re_j^2$ in eq. (6.5); at the same time, laminar conditions are approached (see eq. (6.3)), so that finally eq. (6.7) applies. That an improvement does result has been confirmed experimentally by Mürtz and Nöller, 1961, and by Strnad, Dimic and Kuscer, 1961 (see section 3.2).

The performance might also improve if the temperature was raised (through the positive temperature coefficient of the diffusivity, which appears in the denominator of Re_j).

Finally, improved performance would result if some way was found to make v_{po}/v_j approach unity even in short tubes (cf. section 2.4); this is a problem that has been the subject of numerous fission rocket studies (see e.g. Kerrebrock and Lafyatis, 1958, Rosenzweig, Lewellen and Kerrebrock, 1961, and McFarlin, 1965).

For mass separation in general, a change in the chemical composition of the gas mixture leads to large effects associated with the change in $(M_1 - M_2/\bar{M})^2$, as has indeed been verified experimentally by Mürtz and Nöller, 1961, and in ref. 1.

6.1.4. The Temperature Separation Performance

In case of energy separation, the results of section 4.2 apply. By increasing the overall pressure ratio we shall expect B in eq. (6.6) to increase for the same reason as in the mass separation case; on the other hand the effect of this on the performance will be reduced by the concomitant reduction in ρ_{po}/ρ_j (eq. 6.7)) and thus the overall effect on the performance is again uncertain; here, however, it is a well known fact that an increase of the net temperature effect with increasing overall pressure ratio takes place (as already noted by Hilsch, 1946; see also section 6.3); the results of Lay, 1959, on the velocity and total-temperature distributions at various gauge pressures, provide some, more detailed evidence, though it cannot be said to be conclusive because zero cold flow fraction was employed in the experiments. It is to be noted that the amount of work spent in the system necessarily increases with the pressure ratio so that the efficiency as such may not increase; in fact, Gulyaev, 1966, has found it to be almost constant (section 6.3).

The pressure level would appear to have no effect on the temperature separation (provided eq. (6.3) is valid), while the temperature level enters primarily through the fact that T is a normalized temperature so that the actual temperature effects are proportional to the absolute temperature

level T_{∞}, as indeed found by Gulyaev, 1965. According to Brodyanskii and Martynov, 1964, on the other hand, the prediction is only in qualitative agreement with experiment.

Since v_{po}/v_j apparently reaches its upper limit, i.e. unity (see section 2.4), under the conditions of interest here, and no other factors remain free in eq. (6.6), no further improvement seems possible.

The use of different gases affects the performance through the factor $(k-1)^2$ and, owing to minor pressure adjustments, B. The question has been investigated by various authors (Elser and Hoch, 1950, Martynovskii and Alekseev, 1957) and the impression reached is that $(k-1)^2$ is of primary though not of sole importance.

6.2. The Efficiency of the Gas Separation

A number of investigations on mass separation in the vortex tube (see introduction to chapter 3) has been carried out in order to assess the tube's potential as a separator of heavy isotopes; it is therefore useful to consider its performance in relation to the following two systems, the gas ultra centrifuge and the nozzle separator, both of which are being developed at the present time for industrial use.

The gas centrifuge is a hollow cylinder spinning fast around its axis with special devices inside (scoops) that create a convective flow system. Gas is continuously fed into the cylinder and product streams are withdrawn at the two ends. Flow conditions are thus quite similar to those in the vortex tube except that the feed rate to the centrifuge is orders of magnitude lower than that to the vortex tube. In the nozzle separator, the gas mixture is accelerated along a curved path (see e.g. Becker, 1969, and Zigan, 1962) into a slit nozzle, after which the jet stream is cut into two parts, an outer and an inner stream, by a knife edge placed opposite to the nozzle. The centrifugation of the gas along the curved path and the transverse expansion after the nozzle produce a transverse concentration gradient. The nozzle separator is therefore equivalent in its action to a short concurrent vortex tube.

The gas centrifuge is a complex expensive machine with a rather small power consumption, while the nozzle separator is a rather simple inexpensive device with a large power consumption.

6.2.1. Comparison with the Gas Centrifuge

The equation for maximum separative potential (5.25) is valid unaltered for the gas centrifuge; however, the step from (5.28) to (5.30) is of no

relevance; the reason is that the peripheral velocity in the centrifuge is limited by the strength of the rotor material only. This means, that velocities of the order of at least 400-500 meter per second may be, and apparently have been attained in centrifuges with isotopic uranium hexafluoride (the gaseous uranium compound employed). On the other hand, the corresponding peripheral tangential velocity in the vortex tube, limited as it is to the velocity of sound in uranium hexafluoride, cannot exceed 80-90 m/sec. Thus the efficiency of the tube is for that reason alone a factor of $5^4 = 600$ times poorer than that of the centrifuge.

6.2.2. Comparison with the Nozzle Separator

However, the vortex tube is a very simple inexpensive device and it may therefore be of more interest to see whether its power consumption is exhorbitant in comparison with that of the nozzle separator.

The data of Becker, Bier, Bier and Schütte, 1963, (for a nozzle separator of a somewhat older design than described above) provide a convenient basis for comparison. These data refer to uranium hexafluoride and it is therefore necessary to transform the vortex tube results in ref. I to suit that situation. This may be done on the basis of either the maximum separative potential function, as stated in eq. (6.1), or the simple diffusion equation (3.10), valid if the system remains far from equilibrium. The two procedures are in agreement with one another provided the ratio of turbulent to laminar diffusivity can be written as some constant multiplied by the tangential Reynolds number (as in (6.5)), and provided this constant is invariant to the substitution of uranium hexafluoride for air. It is presumed that the tube and the overall pressure ratio remain unaffected by the transformation and that the pressure gradients and therefore the secondary flow within the tube do not change appreciably; as discussed in ref. I, in connection with the results on different gases, this is indeed largely the case.

The procedure as applied to optimum data from ref. 1 gives the following separative work capacity for the vortex tube as a separator of the uranium isotopes U-235 and U-238 (cf. eq. (5.19))

$$\Delta U/2\pi F = \frac{1}{2} \times 0.23 \times 0.77(6.9 \times 10^{-5})^2 = 4.3 \times 10^{-10} \qquad (6.10)$$

with $2\pi F$ of the order of $7.5\ 10^{-3}$ moles/sec.

The equivalent result for the nozzle separator is

$$\Delta U/2\pi F = \frac{1}{2} \times 0.23 \times 0.77(3 \times 10^{-3})^2 = 8.0 \times 10^{-6} \qquad (6.11)$$

This result, which may seem very high, can be analysed on the basis of an equation equivalent to eq. (3.10) with the modification that the integration over the angular coordinate, which tacitly has been carried out over the 2π-range in eq. (3.10), here covers only the curved path, i. e. an angle less than 2π. The analysis shows that the very high performance of the nozzle separator is due primarily to a low specific throughput helped by laminar conditions in the jet, and to a Mach number greater than one in the active zone (compared with a value of about 2/3 in the vortex tube) (see Zigan, 1962).

These calculations take no account of the fact that the pressure in the nozzle separator used for the comparison has been very low (a factor of about 100 less than in the vortex tube) and that, in order to make the separator attractive from the industrial point of view, it has been necessary to increase the pressure by a factor of about ten or more. A reduction of the efficiency of the order of ten to hundred times by this change may have resulted, unless the specific feed rate has been reduced at the same time and the onset of turbulence has been prevented. Some success in this direction seems to have been achieved in recent years (Becker, 1969) without causing the volume of the equipment to rise excessively; thus it seems clear that the prospects of the vortex tube as a separator of the uranium isotopes are poor. - Unless a considerable increase in tangential velocity level is achieved along the lines suggested in section 6.1, and even then the tube might still be in a difficult position because of its very limited capacity per unit as compared to the nozzle separator.

It should be added that a reduction of the pressure level in the vortex tube, as studied by Mürtz and Nöller and Strnad et al., but with μ at about 0.5 (a situation not investigated), would probably lead to a much improved efficiency; however, the volume of the necessary equipment for large scale separation would rise to prohibitive levels.

It may be appropriate to mention that a considerable improvement in the nozzle separator performance has been achieved by adding a surplus of a light carrier gas to the heavy uranium hexafluoride gas (Becker et al., 1963) whereby the attainable velocity in the nozzle is much increased, and that the same may be done in the vortex tube case and with a similar result (personal communication with Becker).

6.3. The Efficiency of the Energy Separation

Interest in the vortex tube as a cooling device has persisted over the years. Attempts in recent years to establish simple design criteria have

been made, notably by Russian and Japanese investigators (Gulyaev, 1966, Martynov and Brodianskii, 1967, Suzuki, 1960, Takahama, 1965).

Fulton appears to have been the first to present a thorough discussion of the pertinent criteria for the tube efficiency, and to stress that (at the time) the vortex tube performance compared to that of other cooling machines was poor from every point of view. This situation has not changed radically since, as is not surprising in view of the conclusion reached in section 6.1. The best results claimed until now are probably those of Gulyaev shown in fig. 6.2. The ordinate there and in fig. 6.1 is the normalised total temperature T based on T_∞, as used throughout the present work, and the abscissa is a non-dimensional entropy change $(S-S_\infty)/R$, where S_∞ is the entropy per mole of the compressed gas before acceleration into the nozzle.

As argued by Fulton, 1950, and implicit in most studies of recent date, the tube is better viewed as a producer of cold air, than as a machine removing heat from a fixed depressed temperature level (at any rate, as the tube is usually employed; Blatt, 1962, has described the function of a "cold finger" placed along the axis from the cold end in a one-way vortex tube of type b; this design may be of interest in special cases where either a low capacity or a small temperature drop is sufficient).

6.3.1. The Reference Cycle of the Gas in a Cooling Machine

A realistic measure of the efficiency is obtained by comparing the tube performance with that of a cooling machine which employs the following three steps (fig. 6.1): Adiabatic expansion from 1 to 6, with work spent (but not recovered) externally and some gain of entropy owing to irreversible pressure losses. Isobaric heat exchange until the original temperature is reached, 4, where the heat returned to the gas during this step represents the cooling capacity and is given, in normalized form based on RT_∞, by the area under the isobar from 6 to 4. Finally isothermal compression from 4 to 1, where the work spent on the system is equal to the area below the isotherm. Thus, the cooling efficiency (η_1) can be described as the ratio of area (644"6") to area (144"1"). This efficiency definition does not, however, constitute a basic criterion (Fulton, 1950); for that purpose it is useful to define the efficiency in terms of the availability, which is the ability of the system to produce work after the expansion, i.e.

$$a \equiv \int_1^6 (T_\infty - \tilde{t})dS. \qquad (6.12)$$

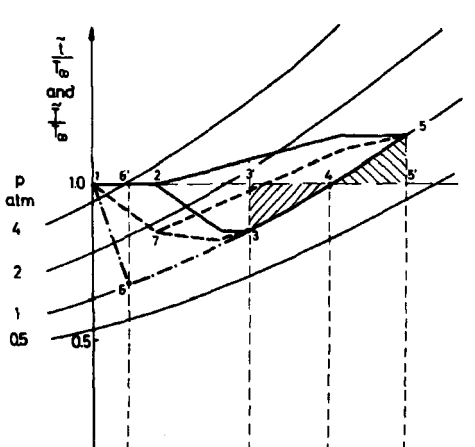

Fig. 6.1. Temperature-entropy diagram of flow processes. Vortex tube; solid lines, total temperature of gas accelerating into nozzle 1 → 2, total temperature changes within tube, in hot stream 2 → 5 and in cold stream 2 → 3, heat exchange with external systems or surroundings 5 → 4 and 3 → 4; dashed lines, corresponding static temperature changes. Reference cooling machine; dot-and-dash line, static temperature change on adiabatic expansion 1 → 6, isobaric heat exchange 6 → 4. $\mu = 0.5$.

If this step is isobaric, we may write

$$a = \int_1^6 (T_\infty - \tilde{T}) \frac{c_p}{\tilde{T}} d\tilde{T} = c_p T_\infty (\ln t_6 - (t_6 - 1)) \qquad (6.13)$$

which for $1 - t_6 \ll 1$ may be written (compare eq. 5.17)

$$a' (\equiv a/T_\infty c_p) = \frac{1}{2} (t_6 - 1)^2 \qquad (6.14)$$

It is seen from inspection of figure 6.2 that the availability a' is the area (6'46) multiplied by the factor $R/(c_p \overline{M}) = (1 - k)$. Thus by dividing this area by area (144''1'') and efficiency η_a is obtained.

6.3.2. The Corresponding Path of the Gas in the Vortex Tube

The path of the gas through the vortex tube, as described in terms of static or total temperature, cannot be traced in detail in fig. 6.1 (because no unique time function can be defined). However, in general terms the path is as follows: Adiabatic, more or less non-isentropic expansion with no change in total-temperature from 1 to 2 until the exit of the nozzle is reached (static temperature 7). Passage through the tube with separation of total enthalpy and necessariiy a loss of stagnation pressure (entropy increase) until both streams are at ambient pressure (one atmosphere in the figure) and their velocities are negligible, from 2 (and 7) to 3 and 5 (the bends on the paths designate entrance into the exits). Then, the useful isobaric heat exchange with the surroundings from 3 to 4 and from 5 to 4 (heat flows in opposite directions). Finally isothermal compression from 4 to 1. The same overall pressure ratio is assumed as applies to the refrigeration machine, so that the expenditure of energy is the same. Thus, area (344"3") or area (455"4") compared to area (644"6") represents the relative goodness of the tube in terms of η_i except for a factor μ or $(1-\mu)$, respectively, which has to be added because the areas are given per unit of gas in a stream regardless of its strength. The two heat flows must necessarily be of equal magnitude and of opposite signs since enthalpy is preserved within the tube.

The availability as defined in section 5.1 is approximately

$$\Delta A/2\pi F \simeq [\mu \times \text{area } (3'43) + (1-\mu) \times \text{area } (455')](1-k) \qquad (6.15)$$

(see eq. (5.19), compared with (5.15) and (5.16)), and thus the goodness of the tube in terms of η_a is represented by the ratio of the weighted area within the brackets to area (6'46).

6.3.3. Discussion of the Tube Efficiency

It is quite obvious from fig. 6.1 why it is impossible to obtain a reasonably high separation efficiency in the vortex tube. For one thing, the acceleration into the tube may be accompanied by quite an appreciable stagnation pressure loss (entropy gain), in particular when the peripheral pressure in the tube is below the critical pressure in the nozzle. Furthermore a loss of stagnation pressure in the tube, especially in the hot stream, is inevitable, though it may be somewhat reduced by use of a diffuser (see Blatt, 1962). Finally the very fact that the gas is divided into two streams of which only one, in most situations, is of practical value makes it most unlikely that

efficiences in terms of η_i much in excess of one tenth of the corresponding figure for a conventional cooling device can be obtained.

This is true even though the vortex tube has one feature which places it in a better position than ordinary cooling machines, namely that the radial equilibrium gradient of total temperature, if it could be utilized, would give twice the isentropic temperature drop (see eqs. (4.1) and (4.4)).

As noted by f. ex. Gulyaev and Takahama, the ratio of the maximum temperature drop in the cold stream (see fig. 4.8) to the isentropic temperature drop based on the overall pressure ratio (i. e. the ratio of area (344"3") to $(644"6")_{max}$ in figs. 6.1 and 6.2) is a parameter which is invariant to various parameter changes. As this ratio multiplied by μ is a measure of the η_i-efficiency, and the cold flow fraction in question apparently is fairly constant, this finding implies that also η_i is fairly invariant. This even applies in cases (fig. 6.2) where the overall pressure ratio appears to

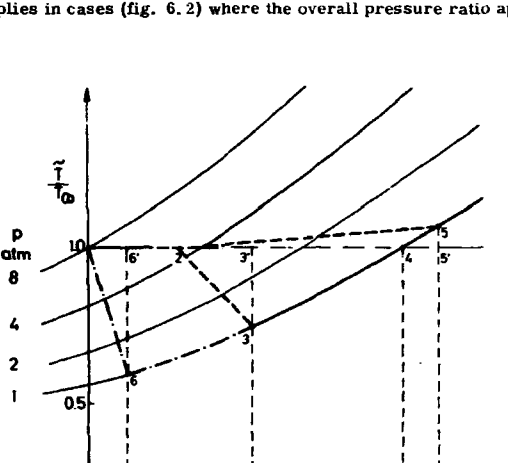

Fig. 6.2. Temperature-entropy diagram of flow processes; data from Gulyaev, 1966. Solid and dashed lines, total-temperature changes (cf. fig. 6.1). Reference cooling machine, dot-and-dash line as in fig. 6.1. $\mu = 0.2$.

be in excess of what is needed for the various steps in the tube, so that an irreversible pressure drop probably takes place on passage from nozzle into tube. Admittedly, the extent to which this has happened in the case shown in the figure cannot be decided on the basis of the data available, because, as discussed in section 6.1, a high pressure ratio favours the creation of a free vortex and with that a comparatively large radial pressure drop; thus the position of point 2 in fig. 6.2 remains uncertain.

In closing the discussion, it may be worth mentioning that the tube is really more of a heating device than a cooling device, provided the interest is simply the attainment of as large a temperature effect as possible. The explanation is that the asymmetry of the tube and the resultant secondary flow pattern, as in a counter-current column, provide for an "unlimited" temperature rise along the tube, if this is made long enough (see eq. 4.21) and if the hot flow fraction, $1-\mu$, is allowed to go towards zero at the same time. The cold temperature drop on the other hand cannot, as mentioned above, exceed twice the adiabatic overall drop. These considerations do not imply of course that the situation met with in practice ever approaches such ideal conditions.

APPENDIX

The Gas Separation Model

The nomenclature of ref. II! does not agree with that used in most chapters of the present work; in order to facilitate reference to ref. III, the old nomenclature, as given in fig. 3.6, is retained here.

According to the approximation leading to eq. (3.10) in chapter 3, the diffusion per cm tube length, u, of heavy component across the boundary between two streams may be written as the product of a constant and the tangential velocity (at the boundary) squared, regardless of the previous history of the streams

$$u \equiv 2\pi\rho D \frac{M_2 - M_1}{R\tilde{t}} N(1-N)\tilde{v}^2 \qquad (A1)$$

or, for a length of tube Δz (in non-dimensional form),

$$\frac{\Delta z \times u}{2\pi F} = \frac{2\,Co}{Re_n \sqrt{at}} N(1-N)\eta u^2 \Delta\xi \; ; \qquad (A2)$$

compare eq. (3.10). On this basis, all transports in fig. 3.6 can in principle be calculated from a knowledge of the radial distribution of tangential velocity (note that fig. 5 in ref. III (except IIIa) is incorrect in that a non-mixing condition between left and right streams is indicated contrary to the stipulation of the model).

The following material balance equations may be written (see fig. 3.6) for the case that $\theta < \theta_o$ (where θ_o is the hot flow fraction with both valves open):

Control volume aets:

$$L'_c N'_c = L^{\mathbf{x}}_c N^{\mathbf{x}}_c + L^{\mathbf{x}}_c N_t + u_c z_c \, , \qquad (A3)$$

control volume fgyx:

$$(L^{\mathbf{x}}_c + L'_h)N'_h + u^{\mathbf{x}} z_h = (L^{\mathbf{x}}_c + L'_h)N_t + u_h z_h \, , \qquad (A4)$$

control volume ebgf:

$$L^{\mathbf{x}}_c N^{\mathbf{x}}_c = L^{\mathbf{x}}_c N'_h + u^{\mathbf{x}} z_h \, , \qquad (A5)$$

control volume abcd:

$$(N'_c - N'_o)L'_c + (N'_h - N'_o)L'_h = 0, \tag{A6}$$

where $N'_o(L'_c + L'_h)$ is total throughput of heavy component minus content in direct end-wall flow; and finally

control surface as:

$$L'_c = L_c + L^{\mathbb{X}}_c. \tag{A7}$$

The following expression for $N'_c - N_o$ with $L^{\mathbb{X}}_c$, N_t, $N^{\mathbb{X}}_c$, and N'_h eliminated can be obtained from (A3)-(A7):

$$L'_c(N'_c - N'_o) = \frac{L'_h}{L'_c + L'_h} u_c z_c - \frac{L'_c}{L'_c + L'_h} u_h z_h + \frac{L^{\mathbb{X}}_c}{L'_h + L^{\mathbb{X}}_c} u_h z_h + \frac{L'_h}{L^{\mathbb{X}}_c + L'_h} u^{\mathbb{X}} z_h \tag{A8}$$

which, introducing $\theta' \equiv L'_h/(L'_h + L'_c)$ and $\theta^{\mathbb{X}} \equiv L^{\mathbb{X}}_c/(L'_h + L^{\mathbb{X}}_c)$, may be written

$$(1-\theta')L'(N'_c - N'_o) = \theta' u_c z_c - (1-\theta')u_h z_h + \theta^{\mathbb{X}} u_h z_h + (1-\theta^{\mathbb{X}})u^{\mathbb{X}} z_h . \tag{A9}$$

The corresponding expression for the case that $\theta > \theta_o$ can be found in an analogous way; it reads

$$(1-\theta')L'(N'_c - N'_o) = \theta' u_c z_c - (1-\theta')u_h z_h - \theta^{\mathbb{X}} u_c z_c - (1-\theta^{\mathbb{X}})u^{\mathbb{X}} z_c . \tag{A10}$$

When both valves of the tube are open (at θ_o) then $\theta^{\mathbb{X}} = 0$ and $u^{\mathbb{X}} = 0$, and both (A9) and (A10) become

$$(1-\theta')L'(N'_c - N'_o) = \theta' u_c z_c - (1-\theta')u_h z_h . \tag{A11}$$

When θ is either reduced below or increased above θ_o, corresponding to the range of validity of eqs. (A9) or (A10), respectively, $\theta^{\mathbb{X}}$ increases from zero and rapidly approaches unity; at the same time $u^{\mathbb{X}}$ increases to either u_h (eq. A9) or u_c (eq. A10). Thus, to a first approximation one may write when θ is low

$$(1-\theta')L'(N'_c-N'_o) \simeq \theta'(u_c z_c + u_h z_h) \qquad (A12)$$

and when θ is high

$$(1-\theta')L'(N'_c-N'_o) \simeq -(1-\theta')(u_c z_c + u_h z_h)\,. \qquad (A13)$$

In order to complete the description the contributions from the end-wall boundary flows must be included, as explained in ref. III; the final equation reads

$$N_c-N_o = \frac{1}{(1-\theta)L}\left[(1-\theta')L'(N'_c-N'_o) + \theta' L_{cw}(N_{wc}-N_o) - (1-\theta')L_{hw}(N_{hw}-N_o)\right] \qquad (A14)$$

where either (A9) or (A10) is, as the case may be, introduced.

ACKNOWLEDGEMENTS

The present work has been carried out in the Chemistry Department of the Research Establishment Risö. The work was initiated by C. F. Jacobsen and the late Th. Rosenberg, whose extensive help and support during the initial phases of the work is acknowledged with deep gratitude.

In later years, C. F. Jacobsen's continued support and interest have been of invaluable importance, as have the always stimulating working conditions of the Chemistry Department. The author is also much indebted to H. Højgaard Jensen for advice and support during a major part of these studies.

REFERENCES

	Cited chapter
Anderson, O.L., 1961, Theoretical Solutions for the Secondary Flow on the End Wall of a Vortex Tube, UAC-Research Lab. R-2494-1.	2p18
Baker, P.S., and W.R. Rothkamp, 1954, Investigation on the Ranque-Hilsch (Vortex) Tube, ORNL-1659.	3p33
Becker, E.W., 1969, Methods for the Separation of Uranium Isotopes, Kerntechnik, 11, 129.	6p93, 95
Becker, E.W., K. Bier, W. Bier and R. Schütte, 1963, Trenndüsenentmischung der Uranisotope bei Verwendung leichter Zusatzgase, Z. f. Naturf. 18a, 246.	6p94, 95
Benjamin, T. Brooke, 1962, Theory of the Vortex Breakdown Phenomenon, J. Fluid Mech. 14, 593.	1p11
Blatt, T.A., R.B. Trusch, 1962, An Experimental Investigation of an Improved Vortex Cooling Device, 1962 ASME Winter Ann. Meet. Paper, 62-WA-200.	6p96, 98
Bornkessel, K., and J. Pilot, 1962, Zur Gas- und Isotopentrennung im Wirbelrohr, Z. phys. Chem. 221, 177.	3p33
Brodyanskii, V.M., and A.V. Martynov, 1964, The Dependence of Ranque-Hilsch Effect on Temperature, Teploenergetika 11, 6, 76.	6p93
Bruun, H.H., 1967, Theoretical and Experimental Investigation of Vortex Tubes (in Danish). Dept. of Fluid Mech. Report No. 67-1. Technical University of Denmark.	2p15, 25, 30; 4p51, 57, 58; table 2.1; figs. 2.2, 5.1
Bruun, H.H., 1969, Experimental Investigation of the Energy Separation in Vortex Tubes, J. Mech. Engng. Sc. 11, 567.	- " -

Cohen, K., 1951, The Theory of Isotope Separation, McGraw-Hill, New York.	3p35, 37; 4p53, 59; 5p72
Deissler, R. G., and M. Perlmutter, 1960, Analysis of the Flow and Energy Separation in a Turbulent Vortex, Int. J. Heat Mass Transfer 1, 173.	2p15, 18, 20, 22; 4p52, 53, 54; fig. 2.1
Dobratz, B. M., 1964, Vortex Tubes, A Bibliography, UCRL-7829.	1p11; 4p51
Donaldson, C. du P., and R. D. Sullivan, 1960, Behavior of Solutions of the Navier-Stokes Equations for a Complete Class of Three-Dimensional Viscous Vortices, Proc. Heat Transfer and Fluid Mech. Inst., Stanford Univ. Press.	2p15
Dubinskii, M. G., 1955, Izv. AN SSSR, Otd. Tekh. Nauk 6, 47.	5p83
Einstein, H. A., and H. Li, 1951, Steady Vortex Flow in a Real Fluid, Heat Transfer and Fluid Mechanics Institute, Stanford Univ. Press.	2p15, 20
Elser, K., M. Hoch, 1951, Das Verhalten verschiedener Gase und die Trennung von Gasgemischen in einem Wirbelrohr, Z. Naturf. 6a, 25.	3p33; 6p93
Fulton, C. D., 1950, Ranque's Tube, Refrig. Engng. 58, 473 (J. of the ASRE).	4p51, 52; 6p96
Gulyaev, A. I., 1965, Ranque's Effect at Low Temperatures, Inzh.-Fiz. Zhurnal, 9, 354.	6p93
Gulyaev, A. I., 1966, Vortex Tubes and the Vortex Effect (Ranque Effect), Soviet Physics, Techn. Physics 10, 1441. (Russ. orig., Zh. Tekh. Fiz. 35 (1965) 1869).	4p52; 6p92, 96, 99; fig. 6.2

Hartnett, J.P. and E.R.G. Eckert, 1957, Experimental Study of the Velocity and Temperature Distribution in a High Velocity Vortex-type Flow, Trans. ASME 79, 751. — 2p15, 25; 4p52, 54, 69; table 2.1; figs. 2.2, 4.1

Hilsch, R., 1946, Die Expansion von Gasen im Zentrifugalfeld als Kälteprozess, Z. Naturforsch. 1, 208. — 4p70; 6p92; fig. 4.8

Hornbeck, R.W., 1969, Viscous Flow in a Short Cylindrical Vortex Chamber with a Finite Swirl Ratio, NASA-TN-D-5132. — 2p18

Kassner, R., and E. Knoernschild, 1948, Friction Laws and Energy Transfer in Circular Flow, Report PB-110936, part I and II. — 4p51, 52

Kendall, J.M. Jr., 1962, Experimental Study of a Compressible Viscous Vortex, Jet Prop. Lab. JPL-TR-32-290 — 2p18; 3p42; 5p83, 84

Kendall, J.S., A.E. Mensing, and B.V. Johnson, 1967, Containment Experiments in Vortex Tubes with Radial Outflow and Large Superimposed Axial Flows, NP-16786, Unit. Aircraft Res. Lab. — 3p33

Kerrebrock, J.L., and J.J. Keyes, Jr., 1959, A Preliminary Experimental Study of Vortex Tubes for Gas-Phase Fission Heating, ORNL-2660. — 2p21; 5p84

Kerrebrock, J.L., and P.G. Lafyatis, 1958, Analytical Study of Some Aspects of Vortex Tubes for Gas-Phase Fission Heating. CF-58-7-4. — 3p33; 6p92

Kerrebrock, J.L., and R.V. Meghreblian, 1958, An Analysis of Vortex Tubes for Combined Gas-Phase Fission-Heating and Separation of the Fissionable Material, CF-57-11-3 (Rev. 1). — 3p33

Keyes, J.J., Jr., 1961, Experimental Study of Flow and Separation in Vortex Tubes with Application to Gaseous Fission Heating, J. Amer. Rocket Soc., 31, 1204. — 2p15, 18, 20; 3p33; table 2.1; fig. 2.2

Lay, J. E., 1959, An Experimental and Analytical Study of Vortex-Flow Temperature Separation by Superposition of Spiral and Axial Flows. Transact. ASME, Sect. C. (J. Heat Transfer) 81, 202. — 2p15; 4p52; 6p92; table 2.1; figs. 2.2, 5.1

Lewellen, W.S., 1962, A Solution for Three-Dimensional Vortex Flows with Strong Circulation, J. Fluid Mech. 14, 420. — 2p20, 21, 23

Lewellen, W.S., 1964, Three-Dimensional Viscous Vortices in Incompressible Flow, Ph.D. thesis, Univ. of California (University Microfilms, Inc., Ann Arbor, Order No. 64-8331). — 1p11; 2p15, 20, 23, 24

Lewellen, W.S., 1965, Linearized Vortex Flows, AIAA J. 3, 91. — 2p15, 18, 31

Linderstrøm-Lang, C.U., 1960, A Differential Oxygen Analyser, Acta Chem. Scand. 14, 1031. — 3p39

Martynov, A.V., and V.M. Brodyanskii, 1967, Investigations of the Parameters of Vortex Flow inside a Ranque-Hilsch Tube, Inzh.-Fiz. Zh. 12, 639. (Eng. Transl. J. Eng. Phys. (USSR) 12, 345). — 6p96

Martynovskii, V.S., and V.P. Alekseev, 1957, Investigation of the Vortex Thermal Separation Effect for Gases and Vapours, Sov. Phys.-Tech.-Phys. 1, 2233. — 5p83; 6p93

McFarlin, D.J., 1965, Experimental Investigation of the Effect of Peripheral-Wall Injection Technique on Turbulence in an Air Vortex Tube, NASA-CR-68867. — 5p84; 6p92

Mürtz, H.J., and H.G. Nöller, 1961, Isotopentrennung in einer Zirkularströmung, Z. Naturforsch. 16a, 569. — 2p27; 3p33, 37, 39; 5p72; 6p92, 95; figs. 2.3, 3.2

Nöller, H.G., and H.J. Mürtz, 1958, Trennung von Gasgemischen in einer Zirkularströmung, Naturwissenschaften 45, 382. — 3p33

Pengelley, C.D., 1957, Flow in a Viscous Vortex, J. Appl. Phys. 28, 86.	2p15
Pivirotto, T.J., 1966, Mass-Retention Measurements in a Binary Compressible Vortex Flow, NASA-CR-75932.	3p33
Ragsdale, R.G., 1960, NASA Research on the Hydrodynamics of the Gaseous Vortex Reactor, NASA-TN-D-288.	3p33, 34; fig. 3.1
Ragsdale, R.G., 1961, Applicability of Mixing Length Theory to a Turbulent Vortex System, NASA TN-D-1051.	2p15, 18; table 2.1; fig. 2.2
Reynolds, A.J., 1961, Energy Flows in a Vortex Tube, J. Appl. Math. Phys. 12, 343.	4p51, 57, 70
Reynolds, A.J., 1962, A Note on Vortex-Tube Flows., J. Fluid Mech. 14, 18.	2p15; 3p44
Rosenzweig, M.L., 1961, Velocity Recovery and Shear Reduction in Jet-Driven Vortex Tubes, Aerospace Corp. Rep. TDR-94.	2p29
Rosenzweig, M.L., W.S. Lewellen and J.L. Kerrebrock, 1961, Feasibility of Turbulent Vortex Containment in the Gaseous Fission Rocket. J. Amer. Rocket Soc. 31, 873.	2p29; 3p33, 34, 35; 6p92
Rosenzweig, M.L., D.H. Ross, and W.S. Lewellen, 1962, On Secondary Flows in Jet-Driven Vortex Tubes, J. Aerospace Sc. 29, 1142.	2p18; 3p42
Rosenzweig, M.L., W.S. Lewellen, and D.H. Ross, 1964, Confined Vortex Flows with Boundary-Layer Interaction, Report No. ATN-64(9227)-2. AD 431844.	2p17, 18, 20, 28, 31; 3p42; 6p89; table 2.1; figs. 2.2, 2.3

Ross, D. H., 1964, a, An Experimental Study of Secondary Flow in Jet-Driven Vortex Chambers, Report No. ATN-64(9227)-1. AD 433052.	2p18; 3p42
Ross, D. H., 1964, b, An Experimental Investigation of Turbulent Shear in Jet-Driven Vortex Chambers, Report No. ATN-64 (9227)-5. AD 445934.	2p15; 5p83
Scheller, W. A., and G. M. Brown, 1957, The Ranque-Hilsch Vortex Tube, Ind. Eng. Chem. 49, 1013.	2p15; 4p69; table 2.1; figs. 2.2, 4.2, 5.1
Scheper, G. W., Jr., 1951, The Vortex Tube; Internal Flow Data and a Heat Transfer Theory, Refrig. Engng. 59, 985 (J. of the ASRE).	4p52
Schowalter, W. R., and H. F. Johnstone, 1960, Characteristics of the Mean Flow Patterns and Structure of Turbulence in Spiral Gas Streams, A. I. Ch. E. J. 6, 648.	2p15; 5p84; table 2.1; fig. 2.2
Sibulkin, M., 1962, Unsteady, Viscous, Circular Flow; Part 3. Application to the Ranque-Hilsch Vortex Tube, J. Fluid Mech. 12, 269.	4p52; 5p84
Stone, W. S., and T. A. Love, 1950, An Experimental Study of the Hilsch Tube and Its Possible Application to Isotope Separation, Report ORNL 282.	3p33
Strnad, J., V. Dimic and I. Kuscer, 1961, Trenneffekt im Gaswirbel, Z. Naturforsch. 16a, 442.	3p33, 39; 6p92, 95
Suzuki, M., 1960, Theoretical and Experimental Studies on the Vortex Tube, Sci. Pap. Inst. Phys. Chem. Research, Tokyo 54, 43.	2p15, 27; 4p52; 6p96; table 2.1; fig. 2.2

Takahama, H., 1965, Studies on Vortex Tubes, Bull. JSME 8, 433.	4p52; 6p96, 99
Takahama, H., and K.-I. Kawashima, 1960, An Experimental Study of Vortex Tubes, Mem. Faculty Engng. Nagoya Univ. 12, 227.	2p15; table 2.1; figs. 2.2, 5.1
Torocheshnikov, N.S., and Zb. A. Koval, 1958, Experimental Study of the Eddy Effect in Small-Diameter Tubes, Nauch. Dokl. Vysshii Shkoly, Khim. Tekhnol., No. 3, 603.	3p33
Vortair Engineering Ltd., London, 1967, Vortex Tubes: Air Cooling Without Moving Parts, Nucl. Eng. March, 207.	1p11
Westley, R., 1954, A Bibliography and Survey of the Vortex Tube, Cranfield Note No. 9.	1p11; 4p51
Wolf, L., Jr., Z. Lavan, and A.A. Fejer, 1968, Study of Swirling Fluid Flows, IIT Res. Inst. Chicago, AD 682529.	2p27
Zigan, F., 1962, Gasdynamische Berechnung der Trenndüsenentmischung, Z. Naturforsch. 17a, 772.	6p93, 95

LIST OF SYMBOLS

Dimensional parameters

u	radial velocity
u_c, u_h, u^x	(in appendix) rate of diffusion per cm tube length across certain cylinder surfaces (fig. 3.6)
w	axial velocity
$\tilde{\psi}$	stream function, defined as in eq. (2.5) or eq. (4.2)
v	tangential velocity
$2\pi\Gamma$	$= 2\pi vr$; circulation
$\tilde{\omega}$	$= \tilde{v}/r$; angular velocity
$\tilde{t}$	static temperature
$\tilde{T}$	total temperature
h	enthalpy
h_o	total enthalpy (enthalpy + kinetic energy)
r	radial coordinate
z	axial coordinate
σ	surface element
$2\pi F$	total flow into tube, defined as volume flow when $\tilde{\psi}$ is defined according to eq. (2.5), and as mass flow with $\tilde{\psi}$ defined as in eq. (4.2)
$2\pi Q\,\ell$	volume or mass flow (see preceeding comment) into core region, i.e. net radial inflow across cylinder $r=r_o$ ($\eta=\eta_o$) where w changes sign, fig. 2.5; or across cylinder $r=r_e$, the exit radius (fig. 1.1)
$v_{po}(v_\infty)$	reference tangential velocity at periphery near nozzle ($r=r_p$, $z=0$) (in ref. IVa and b written v_∞)
Γ_{po}	$= v_{po} r_p$; reference circulation (in ref. IVa and b written Γ_∞)
ω_{po}	$= v_{po}/r_p$; reference angular velocity
T_∞	reference (total) temperature in compressed gas before acceleration into nozzle
r_p	tube radius
r_o	radius at which w changes sign according to model in fig. 2.5
r_c, r_h, and r_e	exit radii, as in fig. 1.1
d_c, d_h, and d_e	corresponding diameters

ℓ	length of region 1 (fig. 2.5); in some cases taken to refer to tube length
z_o	(in section 3.3) length of tube
G	mass flow in a stream of gas
L	(in section 3.3 and appendix) as G
ρ	density
D	diffusion coefficient
$\nu(\nu_{lam})$	kinematic viscosity
ε	combined turbulent and molecular diffusivity for momentum
ε_n	turbulent plus molecular mass diffusivity
ε_h	turbulent (plus molecular) thermal diffusivity
M_2-M_1	molecular weight difference
$\bar{M}$	molecular weight (mean)
R	gas constant per gramme mole
c_p	heat capacity per gramme, at constant pressure
c_∞	$=\sqrt{kRT_\infty/\bar{M}}$; velocity of sound at reference temperature

Non-dimensional parameters

ψ	$=\tilde{\psi}/\psi_s$, where ψ_s is a reference flow rate equal to F unless otherwise specified
f_{oo}	(eq. (2.15)) stream function at $\xi=0$
f_{11}	(eq. (2.15)) radial flow function (see ref. 1Va)
f'_{oo}	$=\frac{-\rho wr^2}{2F}$ or (in section 2.3) $=-\frac{wr^2\rho}{2F}$; axial velocity function at $\xi=0$
v	$=\tilde{v}/v_{po}$; tangential velocity
v_o	v at $\xi=0$
v_{11}	$=\frac{\partial v}{\partial \xi}$; axial gradient of tangential velocity
$2\pi\Gamma$	$=2\pi\tilde{r}/\Gamma_{po}$; circulation
$2\pi\Gamma_o$	(eq. (2.15)) circulation at $\xi=0$
$2\pi\Gamma_{11}$	(eq. (2.15)); axial gradient of circulation
M_j	$=v_j/c_\infty$ (chapter 6)
ω	$=\tilde{\omega}/\omega_{po}$; angular velocity
φ	(eq. (4.8))
N	mole fraction of heavy component in binary gas mixture
dN	(in section 3.3 and fig. 5.2) $=N_h-N_c$
N_o	mole fraction in supply gas

t	$= \tilde{t}/T$; static temperature
T	$= \tilde{T}/T_\infty$; total temperature
$\partial T_{eq}/\partial \eta$	(eq. (4.4)) equilibrium total temperature gradient in absence of secondary flow
η	$= (r/r_p)^2$; radial coordinate
η_i, η_a	(*in section 6.3) separation efficiencies*
z	$= z/\ell$; axial coordinate
η_o	$= (r_o/r_p)^2$
α	$= (r_p/\ell)^2$
θ	angular coordinate, or (in shapter 3 and appendix) hot flow fraction $(1-\mu)$
μ	cold flow fraction
μ_h	$= 1-\mu$; hot flow fraction
Re	$= F/(\varepsilon r_p)$ (eq. (2.14)); turbulent Reynolds number
Re_n	$= F/(\rho\varepsilon_n r_p)$ (eq. (3.4)); turbulent Reynolds number for mass diffusion
Re_h	$= F/(\rho\varepsilon_h r_p)$ (eq. (4.2)); turbulent thermal Reynolds number (Peclé number)
$Re\sqrt{\alpha}$, $Re_n\sqrt{\alpha}$, and $Re_h\sqrt{\alpha}$	Reynolds numbers based on length of region 1 (fig. 2.5)
Re_r and Re_{hr}	corresponding radial parameters defined so that
$Re_r/Re\sqrt{\alpha}$	$= Re_{hr}/Re_h\sqrt{\alpha} = Q\ell/F$; radial flow fraction into core of region I (fig. 2.5) across cylinder surface $r = r_o$; when ℓ is the tube length, $Q\ell/F$ is the fraction of flow through centre exits (equal to μ in tubes of type b (fig. 1.1), equal to one in tubes of type d and e)
$Re_{t,p}$	$= \rho_{po} v_{po} r_p/(\rho\nu)$; tangential Reynolds number; in literature, incl. ref. IVa, $2r_p = d_p$ is used
Re_j	(chapter 6) nozzle Reynolds number
Ro	$= F/(v_{po} r_p^2)$ (eq. (2.14)) Rossby number
Co	(eq. (3.3)) pressure diffusion parameter
Sc	$= \rho\varepsilon_n/(\rho\varepsilon)$; turbulent Schmidt number
Ec	(eq. (4.2)) turbulent Eckert number
Pr	$= \rho\varepsilon/(\rho\varepsilon_h)$; turbulent Prandtl number
k	= ratio of specific heats
E	(eq. (4.9))
$\bar{E}$	(eq. (4.14))

ΔT_h	$= T_p(1)-T_h$; total temperature at periphery and $\xi = 1$ of region I (fig. 2.5) minus temperature (total) of hot stream
B	(eq. (5.24))
V and V_n	(eqs. (5.11) and (5.14)); value functions for energy and gas separation, respectively
$A/2\pi F$	(eq. (5.33)) specific value of a stream
$\Delta A/2\pi F$	(eqs. (5.16) and (5.34)) availability of tube or tube region
$\Delta U/2\pi F$	(eqs. (5.19) and (5.9)) separative work potential of tube or tube region
$\Delta A_{max}/2\pi F$ and $\Delta U_{max}/2\pi F$	(eqs. (5.23) and (5.22)) theoretical maxima of availability and separative work potential, without consideration of secondary flow

Subscripts

s	reference value
p	value at tube periphery
po	value at tube periphery near nozzle ($\xi=0$)
h	value in hot end exit
c	value in cold end exit
e	value in exit
j	value in nozzle
f', f'_{oo} etc	differentiation with respect to radial coordinate η
$\overline{u'v'}$	(in section 5.3) fluctuation term
N' and N''	concentrations in specified streams

DANSK RESUME

Til grund for nærværende arbejde ligger en række tidsskriftsartikler og rapporter om strømningsforholdene i vortexrør af forskellig type. Undersøgelserne, som har været af både eksperimentel og teoretisk art, har alle beskæftiget sig med samspillet mellem den sekundære strømning, der beskriver gassens vej gennem røret, og de diffusionsprocesser, der sættes i gang af gassens rotation.

Til indledning gives i kapitel 1 en beskrivelse af vortexrørets konstruktion samt en oversigt over, hvilke faktorer der bestemmer dannelsen af de karakteristiske temperatur- og koncentrationsforskelle mellem de to produktstrømme fra røret.

For at forstå virkningen af disse faktorer må også samspillet mellem den sekundære strømning og den tangentiale hastighedsfordeling klarlægges; dette er emnet for kapitel 2. Da de aksiale gradienter har vist sig generelt at være mange gange mindre end de radiære, er det ofte tilstrækkeligt at betragte disse sidste; således finder man som diskuteret i kapitel 2 afsnit 1, at et radiært Reynolds tal bestemmer den tangentiale hastighedsfordeling ret eentydigt. Dette simple billede kompliceres dog af, at rørets endevægge ofte trækker en væsentlig del af den radiære strømning til sig, således at disse må inddrages i beskrivelsen; ligeledes finder man i lange rør med indmunding i den ene ende en betydelig reduktion af den tangentiale hastighed langs røret. Disse forhold, samt de faktorer af konstruktionsmæssig art der bestemmer dem, behandles i de tre øvrige afsnit af kapitel 2.

I kapitel 3 og 4 behandles koncentrations- og temperaturfordelingen i røret. Også for disse gælder det, at man under visse forhold kan se bort fra de aksiale gradienter; denne situation er behandlet i afsnit 1 af de to kapitler. Imidlertid er en sådan beskrivelse under forhold, hvorunder røret fungerer optimalt, ikke tilstrækkelig; hovedvægten i de to kapitler er derfor lagt på en tredimensional betragtning af problemerne, og det vises, at man derigennem kan nå til en tolkning af det foreliggende eksperimentelle materiale.

I kapitel 3 afsnit 2 og 3 betragtes vortexrøret som en primitiv centrifuge, der tillader en delvis adskillelse af en gasblanding efter molekylvægt. En sådan funktion er konstateret eksperimentelt i flere tilfælde. I en række forsøg beskrevet i kapitel 3 afsnit 3 fandtes således veldefinerede men små separationseffekter. Da det har vist sig, at den sekundære strømning i disse tilfælde er meget kompliceret, har en detaljeret beskrivelse af koncentrationsfordelingen ikke kunnet gennemføres; dog har det været muligt, som

også beskrevet i afsnit 3, at forklare det eksperimentelle materiale udfra en ret grov men ganske virkningsfuld teori.

I kapitel 4 betragtes temperaturfordelingen i røret. Det vises, at den totale temperatur optræder i energiligningen næsten som koncentrationen i diffusionsligningen. Da den sekundære strømning i den type vortexrør, der har interesse i forbindelse med temperaturseparationen, er betydelig simplere end den, der ligger bag dannelsen af koncentrationseffekterne, har en ret detaljeret løsning af energiligningen vist sig overkommelig; denne er beskrevet i kapitel 4 afsnit 2. En ret tilfredsstillende reproduktion af eksperimentelt bestemte aksiale og radiære gradienter af den totale temperatur under varierende betingelser har herigennem vist sig mulig.

En beregning af den resulterende temperaturforskel mellem de to produktstrømme udfra den teoretiske model giver, som beskrevet i kapitel 4's sidste afsnit, en rimelig overensstemmelse med eksperimenterne.

I kapitel 5 opstilles udtryk for rørets ydeevne, både hvad angår adskillelse af en gasblanding og hvad angår skabelse af en temperaturforskel. Samme principper anvendes som ved bedømmelse af ydeevnen af en gascentrifuge til adskillelse af for eksempel en gasformig blanding af isotoper; dette betyder, at begrebet separativt arbejde anvendes direkte på gasseparationen, medens et dermed analogt begreb udledes for temperaturseparationen.

Det vises, hvorledes disse funktioner tillader en korrelation af gasseparationseffekter og temperatureffekter. Temperaturfunktionen tillader desuden, som vist i kapitel 5 afsnit 2, en kontrol på, at beregningen af temperatureffekterne, hvori indgår en antagelse om turbulensniveauet i røret, er i overensstemmelse med tilsvarende resultater opnået på basis af studiet af den tangentiale hastighedsfordeling (kapitel 2).

I kapitel 6 diskuteres rørets maksimale ydeevne på basis af de to funktioner udledt i kapitel 5, og disse vurderes ved sammenligning med ydeevnen af tilsvarende apparatur henholdsvis til adskillelse af isotoper og til køling.